

**Supercritical assisted processes
for the production of biopolymeric
micro and nanocarriers**

Roberta Campardelli

*Omaggio a:
Pablo Picasso*

“La joie de vivre”



Unione Europea



*Ministero dell'Istruzione,
dell'Università e della Ricerca*



UNIVERSITÀ DEGLI
STUDI DI SALERNO

FONDO SOCIALE EUROPEO

Programma Operativo Nazionale 2007/2013

“Ricerca Scientifica, Sviluppo Tecnologico, Alta Formazione”

Regioni dell'Obiettivo 1 – Misura III.4

“Formazione superiore ed universitaria”

Department of Industrial Engineering

*Ph.D. Scienza e tecnologie per l'industria chimica
farmaceutica ed alimentare
(XI Cycle-New Series)*

SUPERCRITICAL ASSISTED PROCESSES FOR THE PRODUCTION OF BIOPOLYMERIC MICRO AND NANOCARRIERS

Supervisor

Prof. Ernesto Reverchon

Ph.D. student

Roberta Campardelli

Scientific Referees

Dr. Giovanna della Porta

Prof. Libero Sesti Osséo

Prof. Jesus Santamaria

Prof. Silvia Irusta

Ph.D. Course Coordinator

Prof. Paolo Ciambelli

ACKNOWLEDGEMENTS

Here I am, writing acknowledgments. It is the hardest part of a thesis, it is the moment in which every PhD student realizes that a series of events and people made the work special, in a sense that goes beyond the scientific contribution of the research, that is related to individual growth performed during three years of work.

First of all I want to thank my supervisor Prof Ernesto Reverchon, his contribution to this thesis and also to my personal growth is total. It is really difficult to summarize my gratitude for his guidance, support and patience. Following his example I learned how to transform scientific intuition into fruitful results. He is the person who really inspired and promoted my growth as student and as researcher. It was a pleasure and an honor to work with him. Thanks a lot!

I gratefully acknowledge my tutor Dr. Giovanna Della Porta. She followed my growth since I was a student transferring her knowledge and experiences to me, and also leaving me free to experiment and construct my personal method of research. I received from her lots of good ideas and constructive advices and support during the whole course of my PhD.

I wish also to thank Dr. Renata Adami. A long and lucky path of events led us collaborating many times during these three years. She was always present, supporting (with her experiences) and encouraging (with her enthusiasm) my ideas. A great part of my thesis was also made thanks to her support.

Now is the time of my “twin” of PhD, my desk-mate, my “wife” Dr. Sara Liparoti. I think I have no words enough to thank you and I have also a thousand of reasons to do that, I remember each time we spent together and I am sure you too. Our friendship is the biggest results of our PhDs!!!! We are the referees!

My sincere thanks to the “Supercritical Fluids” group at the University of Salerno, for providing me a supportive atmosphere and for friendly discussions, exchanges of knowledge and skills, which helped to enrich my experience. So, thanks to all my Lab-mates, we had great time together in the labs! Special thanks also to Dr. Mariarosa Scognamiglio, you are a collector of special thanks! My cannot miss!

I sincerely acknowledge all the “junior” students that worked with me during these years: Emanuele Trucillo, Ubaldo Fierro, Paolo Trucillo, Marialaura Giodano and Ida Palazzo. Moments and satisfactions shared with you will be forever in my mind and in my heart. Special mention to my “senior” students Massimiliano Morelli e Emilia Orlando for your kind support and help. You have been also sincere friends. Thanks!

Thanks also to my PhD-mates, Lucia Baldino, Islane Esperito Santo, Nunzia Falco “Titti” and Paola Pisanti, We shared many moments that I will never forget. We had fun!

My acknowledgements are also to Prof. Sesti Osséo for his availability to take part in my scientific committee and for his valuable suggestions.

Thinking about the “Spanish period” of my PhD, all my gratitude to Prof Jesus Santamaria for the big opportunity he gave me to work in his research group in Zaragoza. He kindly supported my work, giving me precious advices. His supervision with his expertise and valuable advices were precious for me. I would like also to thank his lovely wife for her kind hospitality. I’m also sincerely grateful to Prof Silvia Irusta for her invaluable support during the last year of my PhD, she was always present, really a nice and sweet person. We are a good team! I would like also to thank all the people of the INA labs, they made me fill “at home” during my stay in Zaragoza. Special mention to my “compañero de trabajo!!” Dr Ramiro Serra, we shared three months of work together; always present to help me, he never gave up! We had a lot of fun together “uno de Enero, dos de Febrero....!” Thank you a lot! In Zaragoza I also found a “Spanish family” that gave me exceptional hospitality, I have no words enough to thank my special friends: Sandra and her husband, little Nicolas, Luis and Maria; you have been my family during those months, I am confident that that period was helpful for my personal growth, also for you!

It is difficult to express my gratitude to my personal “ fun club”: my family! They always believed in me, encouraging and motivating my work in many occasions. Their constant presence in my life made me feel self-confident, their influence during my growth helped me to become a better person. To my family I dedicate this thesis...it is not enough to thank you!

I am heartily thankful to my dear Dario, his love, dedication, patient and confidence in me had inspired all my choices. Your presence in my life gives a sense to everything.

With this I have finished to write my thesis and now I have realized that another important period of my life is ending. The end of something always implies some considerations. My consideration is that I don’t know if I am a good researcher now, I hope, but let the other say it, but I am sure that I love research and this thesis is the results of my efforts, done with constant passion and enthusiasm.

Publications list:

International Journals:

1 G. Della Porta, R. Campardelli, N. Falco, E. Reverchon*, PLGA Microdevices for Retinoids Sustained Release Produced by Supercritical Emulsion Extraction: Continuous Versus Batch Operation Layouts, *J Pharm Sci*, (100) 2011: 4357-4367.

2 R. Campardelli, R. Adami, G. Della Porta, E. Reverchon*, Nanoparticle Precipitation by Supercritical Assisted Injection in a Liquid Antisolvent, *Chem Eng J*. (192) 2012: 246-251.

3 R. Campardelli, G. Della Porta, E. Reverchon* Solvent elimination from polymer nanoparticle suspensions by continuous supercritical extraction, *J Supercrit Fluids* (70) 2012: 100-105.

4 R. Campardelli*, R. Adami, E. Reverchon, Poorly water soluble drug increased bioavailability by supercritical assisted injection in liquid antisolvent, *Procedia Engineering* (42) 2011: 1624-1633.

5 R. Campardelli*, E. Reverchon, G. Della Porta, Biopolymer nanoparticles for proteins and peptides sustained release produced by Supercritical Emulsion Extraction, *Procedia Engineering* (42) 2011: 268-275.

6 G. Della Porta*, R. Campardelli, E. Reverchon, Monodisperse biopolymer nano and micro particles produced by SEE technology, Accepted, *J Supercrit Fluids* 2012.

7 R. Campardelli, G. Della Porta, V. Gomez , S. Irusta, E. Reverchon*, J. Santamaria, Titanium Dioxide nanoparticles encapsulation in PLA by Supercritical Emulsion Extraction to produce photoactivable microspheres, submitted to *J Nanoparticles Res*, 2013

Proceedings of Conferences:

1 R. Campardelli*, G. Della Porta, E. Reverchon, Supercritical extraction of O/W emulsions for the production of biodegradable microcarriers for liposoluble vitamins delivery, 9 th Conference on Supercritical Fluids and their application, Sorrento 2010.

2 R. Campardelli*, G. Della Porta, E. Reverchon, Supercritical fluid extraction of emulsions to produce biopolymers microparticle and nanoparticle, 13 th European Meeting on Supercritical Fluids, The Hague 2011.

3 R. Campardelli, R. Adami, E. Reverchon* Nanoparticle Precipitation by Supercritical Assisted Injection in a Liquid Antisolvent, 13 th International Symposium on Supercritical Fluids, San Francisco 2012

4 I. Espirito Santo* , R. Campardelli , E. Cabral Albuquerque, S.A.B. Vieira de Melo, G. Della Porta, E. Reverchon, Liposomes production by ethanol injection assisted by supercritical CO₂ and solvent elimination, 13 th International Symposium on Supercritical Fluids, San Francisco 2012

5 R. Campardelli*, R. Adami, E. Reverchon Il processo di iniezione assistita da fluidi supercritici in antisolvente liquido per la produzione di sospensioni di nanoparticelle. Convegno GRICU 2012.

Contents

Chapter I	1
Introduction	1
I.1. Nanomaterials	1
Chapter II	5
Biopolymeric Micro & Nanocarriers	5
II.1 Controlled drug delivery	6
II.2 Targeted Drug Delivery	8
II.3 Microsphere-based Tissue Engineering Scaffold	9
Chapter III	11
State of the art: Micro and nanoparticles production	11
III.1 Emulsions for the production of biopolymeric micro and nanoparticles	12
III.1.1 Choice of materials: Disperse phase	13
III.1.2 Choice of materials: Continuous phase	15
III.1.3 Choice of the emulsification technique	16
III.1.4 Solvent Evaporation/extraction of emulsions: advantages and disadvantages	18
III.2 Nanoprecipitation: an alternative method to produce biopolymeric nanoparticles	19
III.2.1 Choice of materials	19
III.2.2 Choice of the nanoprecipitation conditions	20
III.2.3 Mechanism of nanoparticles formation	21
III.2.4 Nanoprecipitation: advantages and disadvantages	22
Chapter IV	23
Supercritical fluid assisted processes	23
IV.1 Supercritical fluids properties	23
IV.2 Nanomaterials production	24
Chapter V	29
Objectives of the work	29
V.1 Objectives of the work	29
Chapter VI	31
Supercritical Emulsion Extraction Continuous Process(SEE)	31
VI.1 SEE-C process	31
Chapter VII	35
Supercritical Emulsion Extraction Continuous Process for Monodisperse Particles Production	35
VII.1 Introduction	35
VII.2 Materials and methods	36
VII.2.1 Materials	36
VII.2.2 Emulsion preparation	36
VII.2.3 Analytical methods	37
VII.2.4 Experimental continuous apparatus description	38

VII.3 Results & discussion	40
VII.3.1 Definition of SEE-C operative conditions	40
VII.3.2 PCL: Effect of sonication	41
VII.3.3 PCL: effect of polymer percentage in oily phase	43
VII.3.4 PCL: effect of surfactant quantity	44
VII.3.5 PLGA and PLA: effect of polymer percentage in the oily phase	46
VII.4 Conclusions	47
Chapter VIII	49
Biopolymer particles for proteins and peptides sustained release produced by Supercritical Emulsion Extraction	49
VIII.1 Introduction	49
VIII.2 Materials and Methods	50
VIII.3 Emulsion preparation and SEE-C operative conditions	50
VIII.4 Droplets and Particles Morphology and Size Distributions	51
VIII.5 Protein loading determination	51
VIII.6 Results and discussion	52
VIII.6.1 BSA encapsulation study	52
VIII.6.2 GF encapsulation study	57
VIII.6.3 PLGA microspheres charged with GF for stem cells differentiation	59
VIII.7 Conclusions & Perspectives	59
Chapter IX	61
Titanium Dioxide nanoparticles encapsulation in PLA by Supercritical Emulsion Extraction to produce photoactivable microspheres	61
IX.1 Introduction	61
IX.2 Materials, apparatus and methods	62
IX.2.1 Materials	62
IX.2.2 Production of TiO ₂ nanoparticles	62
IX.2.3 Emulsion preparation	63
IX.2.4 Supercritical emulsion extraction process	63
IX.2.5 Particle characterizations	64
IX.2.6 Photocatalytic reaction and bacterial viability assay	64
IX.3 Results and discussion	65
IX.3.1 TiO ₂ nanoparticles production	65
IX.3.2 PLA/TiO ₂ nanoparticles production: effect of emulsion formulation and titanium loading	65
IX.3.3 Nanocomposite characterization: TGA, EDX, XPS, TEM	69
IX.3.4 Staphylococcus Aureus loss of viability under TiO ₂ photocatalytic reaction	72
IX.4 Conclusions	73
Chapter X	75

Hollow Gold Nanoshells-PLA nanocomposites for photothermal controlled delivery of Rhodamine	75
X.1 Introduction	75
X.2 Materials, apparatus and methods	76
X.2.1 Materials	76
X.2.2 Hollow Gold nanoparticles production	77
X.2.3 Emulsion preparation	77
X.2.4 Supercritical Emulsion Extraction: apparatus and process conditions	78
X.2.5 Particle characterizations	79
X.2.6 Rhodamine loading and NIR controlled release	80
X.3 Results and discussion	80
X.3.1 Photothermally controlled delivery PLA devices production & characterization	80
X.3.2 Rhodamine loading and NIR controlled release from PLA particles	84
X.4 Conclusions	89
Chapter XI	91
Solvent elimination from polymer nanoparticle suspensions by supercritical continuous extraction processing	91
XI.1 Introduction	91
XI.2 Experimental methods	92
XI.2.1 Materials	92
XI.2.2 Nanoparticles Preparation	92
XI.2.3 Conventional Evaporation and Supercritical Fluids Extraction Process	93
XI.2.4 Nanoparticles morphology, size distributions and zeta potential determination	93
XI.2.5 Solvent Residue Analysis	93
XI.3 Results and discussion	94
XI.3.1 Acetone elimination from PCL water suspensions	94
XI.3.2 Acetone/ethanol elimination from PLGA water suspensions	97
XI.3.3 Influence of the nanoprecipitation parameters on the efficiency of the supercritical post processing	101
XI.4 Conclusions and perspectives	103
Chapter XII	105
Supercritical Assisted Injection in Liquid Antisolvent (SAILA)	105
XII.1 Introduction	105
XII.2 Experimental SAILA apparatus description	111
XII.3 SAILA process description and mechanism of particles formations	113
XII.3.1 Role of the antisolvent	113
XII.3.2 Role of Mixing	114

XII.3.3 Stability of nanoparticle suspensions	115
XII.4 Process parameters	119
Chapter XIII	121
Nanoparticle Precipitation by Supercritical Assisted Injection in a Liquid Antisolvent	121
XIII.1 Introduction	121
XIII.2 Materials & Methods	122
XIII.2.1 Materials	122
XIII.2.2 Nanoparticle morphology, size distributions and solvent residue analysis	122
XIII.3 Results and Discussion	123
XIII.3.1 Feasibility tests	123
XIII.3.2 Temperature effect	127
XIII.3.3 Effect of solvent/non-solvent ratio and polymer concentration	129
XIII.4 Conclusions and perspectives	130
Chapter XIV	131
Preparation of stable aqueous nanodispersions of poorly water soluble drugs by supercritical assisted injection in a liquid antisolvent	131
XIV.1 Introduction	131
XIV.2 Materials & Methods	132
XIV.2.1 Materials	132
XIV.2.2 Nanoparticle morphology, size distributions and solvent residue analysis	132
XIV.3 Results and Discussion	133
XIV.3.1 Feasibility test	133
XIV.3.2 Production of β -carotene nanoparticles suspensions	135
XIV.3.3 Production of ketoprofene nanoparticles suspensions	139
XIV.4 Conclusions	141
Chapter XV	143
Conclusions	143

Figure Index

Figure I. 1 Top-down and bottom-up approaches (Reverchon E. and Adami R., 2006)	2
Figure II. 1 Section of a microsphere.....	7
Figure II. 2 Example of multifunctional pharmaceutical nanocarrier applied to medical or biological field (Salata O., 2004)	9
Figure III 1 Basic steps of microencapsulation by solvent evaporation (Li M. et al., 2008).....	12
Figure III 2 Set-up used for preparation of nanoparticles by the nanoprecipitation method (Mora-Huertas C.E. et al., 2010)	19
Figure VII. 1 Schematic representation of SEE-C process (Della Porta G. et al., 2011a).....	38
Figure VII. 2 Continuous tower diagram: C, CO ₂ supply; E, emulsion supply; PG_1 and PG_2, pressure gauges; SC_P, diaphragm pump used for high pressure SC-CO ₂ ; L_P, piston pump used for the emulsion; TC1...TC8, thermocouples; S, separator; R, rotameter; E_1 and E_2, heat exchangers; V_1...V_8, valves (Falco N. et al., 2012).....	39
Figure VII. 3 Particle size distribution of particles suspensions obtained by SEE-C and by liquid emulsion extraction technology (LEE).....	43
Figure VII. 4 SEM images of PCL nano and micro-particles obtained at different polymer concentration in the oily phase: (a) 1% w/w (b) 10% w/w and processed by SEE-C.	44
Figure VII. 5 Particle size distribution of the PCL suspensions obtained at different PVA concentrations in water phase (% w/w).	45
Figure VII. 6 Mean Diameter of PCL nanoparticles obtained at different PVA concentrations (% w/w), as surfactant of the water phase	45
Figure VII. 7 SEM images of PLGA nanoparticles obtained at different polymer concentrations in the oily phase by SEE-C: (a) PLGA in oily phase of 1% w/w (b) PLGA in oily phase of 5% w/w. Other emulsion data: oil-in-water emulsion, PVA 1% w/w; ultrasounds operating at amplitude of 30% for 1 min.	47
Figure VII. 8 SEM images of PLA nanoparticles obtained at different polymer concentrations in the oily phase by SEE-C: (a) PLA in oily phase of 1% w/w (b) PLA in oily phase of 5% w/w. Other emulsion data: oil-in-water emulsion, PVA 1% w/w; ultrasounds operating at amplitude of 30% for 1 min.	47

Figure VIII. 1 Optical image of the emulsion and SEM image of particles obtained after the SEE process (PLGA 10%, BSA 2.5 mg/gr). DSD and PSD are also reported for comparison.	54
Figure VIII. 2 SEM images and PSD of particles of PLGA microparticles obtained with different BSA loading produced with PLGA 10% w/w in the oil phase.....	55
Figure VIII. 3 Optica images and SEM images of emulsions and particles produced with 10 % of PLA (F9) and PLGA (F10) and BSA loaded at concentration of 5 mg/g.	56
Figure VIII. 4 SEM images of submicroparticles obtained with PLGA (F7) and PLA (F8) at a concetration of 5% w/w in the oil phase and BSA loading of 5 mg/g.	57
Figure VIII. 5 Optical images and SEM images of PLGA particles encapsulating GFs	58
Figure VIII. 6 Cumulative undersize PSD of PLGA microparticles suspensions encapsulating GFs	59
Figure IX. 1 TEM image and XRD diffraction patterns of the microwave synthesized nanoparticles	65
Figure IX. 2 Micro and nanoparticles of PLA+TiO ₂ produced changing emulsion preparation parameters (TiO ₂ 1.2% w/w).	66
Figure IX. 3 PSD of PLA/TiO ₂ particles obtained starting from W ₁ /O/W ₂ emulsion with different W ₁ volume phase.....	68
Figure IX. 4 SEM images of particles produced starting from W ₁ /O/W ₂ (a) and S/O/W (b) emulsion with 1.2 % titanium theoretical loading.	68
Figure IX. 5 PSD of PLA/TiO ₂ particles obtained starting from S/O/W emulsion with different S loading	69
Figure IX. 6 TEM and CrioTEM images of PLA/TiO ₂ particles and EDX spectra of related samples; (a) T4 sample, (b) T7 sample.	70
Figure IX. 7 Thermogravimetric analysis (TGA) results for nanoparticles produced starting from double emulsion and solid in oil emulsion. The effective loading is also reported.	72
Figure IX. 8 The viability of bacteria under various TiO ₂ photocatalitic reaction	73
Figure X. 1 VLE diagram of the system CO ₂ -ethylacetate adapted from Kato et al. 2006.....	79
Figure X. 2 Frequency PSD curves of PLA-HGNs nanoparticles encapsulating Rhodamine with different HGN % in the polymer matrix. Photographs of powders obtained are also reported.....	82
Figure X. 3 SEM images of PLA-HGNs particles encapsulating Rhodamine.....	83
Figure X. 4 TEM mages of PLA/HGN particles encapsulating Rhodamine (a); EDX spectra of related sample (b).	84

Figure X. 5 Rhodamine release from PLA nanoparticles; Sample G1 and G3 results are compared (a); SEM images of particles after one day of release (b) and at the end of the release (c) are also reported.	85
Figure X. 6 Temperature in PLA nanoparticles suspension during NIR irradiation at 80% of the power (a) and 100% of the power (b). NIR irradiation 5 min.	87
Figure X. 7 NIR controlled Rhodamine release from PLA particles loaded with 1% of HGNs in the polymer matrix (sample G3)	88
Figure X. 8 (a) NIR controlled release of PLA particles with different HGN loading and related drug release rate (b) NIR conditions: irradiation at 80% of the power for 5 minutes, each application. (c) and (d) SEM pictures of G4 particles at the end of NIR controlled Rhodamine release release.	89
Figure XI. 1 Acetone residue diagram in PCL nanoparticle suspension for different operating pressures and L/G ratios	97
Figure XI. 2 SEM image of PCL nanoparticles recovered after filtration and drying.....	97
Figure XI. 3 VLE diagram of acetone ■ and ethanol ● with SC-CO ₂ at 38°C adapted from Chiu et al.(Chin H.Y. et al., 2008).....	99
Figure XI. 4 Ethanol and acetone residue in PLGA nanoparticle suspension for different operating pressures and L/G ratios.	100
Figure XI. 5 Macroscopic aspect of nanoparticle suspensions obtained with different PCL content. The polymer percentage in solvent phase is 0.5, 1.0, 2.0 from the left to the right of the image.....	101
Figure XI. 6 SEM images of nanoparticles recovered after filtration and drying. (a): PLGA 0.5%; (b): PLGA 2%.....	102
Figure XII. 1 RESS equipment concept (Jung J. and Perrut M., 2001)	107
Figure XII. 2 Schematic RESOLV experimental apparatus (Turk M. and Lietzow R., 2004)	108
Figure XII. 3 Schematic representation of the SAILA process layout. CO ₂ : Carbon Dioxide reservoir; V1, V2, V3, V4: on-off valves; CB: cooling bath, P1: CO ₂ pump; P2: liquid pump; P3: peristaltic pump SR: solvent reservoir; WR: water reservoir; RV receiving vessel.....	111
Figure XII. 4 Detail of the saturation-injection of the SAILA process apparatus. A: SC-CO ₂ feeding line; B: Liquid Solution feeding line; C: Saturator; D: packing elements; E: heating elements; F: injector; G: non-solvent receiving phase; H: manometer; I: thermocouple.....	111
Figure XII. 5 CAD project of the SAILA plant.....	112
Figure XII. 6 Schematic of particle precipitation process.....	113
Figure XII. 7 Schematic of polymer-particle interaction in aqueous suspension with an increase in polymer concentration	118
Figure XII. 8 The schematic of particle-surfactant interaction in the aqueous solution with an increase in surfactant concentration.	118

Figure XII. 9 Effect of the process parameter on the miscibility hole. The continuous line refers to the binary system Acetone-CO₂..... 120

Table Index

Table III 1 Suggested composition for preparation of nanocapsules by nanoprecipitation 21

Table VII 1 Mean Diameter (MD) and poly-dispersity Index (PDI) of various biopolymers. O/W emulsion ratio 20:80; oily phase: Results obtained by LEE are also reported for comparison*..... 42

Table IX. 1 Mean diameter (MD) and Standard Deviation (SD) of droplets in emulsions and of composite particles produced after SEE processing, shrinkage factor % between droplets and particles mean diameter and TiO₂ theoretical and effective loading. SEE operative conditions were: 80 bar, 38°C, liquid/gas ratio (L/G) 0.1. 67

Table IX. 2 X-ray photoelectron spectroscopy (XPS) results related to PLA/TiO₂ nanoparticles, surface compositions are reported in % 71

Table X. 1 PSD of samples produced after SEE process. Emulsions were obtained: S/O: sonicating at 40% for 1 minute (repeated until stabilization of the suspension); W₁/O sonicating at 40% of the power for 1 minute; W₁/O/W₂ 7000 rpm for 6 min and 60% sonication for 30 seconds, repeated twice. SEE operative conditions were fixed: 80 bar, 38°C, liquid/gas ratio (L/G) 0.1..... 81

Table XI. 1 Acetone residue after continuous supercritical fluid extraction (SFE). CO₂ flow rate=1.4 Kg/h. An example of traditional solvent evaporation is also reported for comparison (SE). All the suspensions were prepared with 0.5% w/w of PCL and at 800 rpm. 96

Table XI. 2 Acetone and ethanol residues after continuous supercritical fluid extraction. CO₂ flow rate=1.4 Kg/h, temperature 38°C. All the suspensions were prepared with 0.5% w/w of PLGA in 25 mL of acetone/ethanol 50/50 and at 400 rpm..... 98

Table XI. 3 Nanoprecipitation conditions of the experiment performed with different stirring rate and with different PCL and PLGA content using acetone and ethanol/ acetone mixtures as solvent phase and 50 mL of water as non-solvent phase. Solvent residue values were measured at the optimized processing conditions: 140 bar, 38°C, L/G 0.05..... 103

Table XIII. 1 Mean diameter (MD), standard deviation (SD) and Polidispersity index (PI) of PCL nanoparticles at 5 mg/mL in acetone. Saturator temperature was set at 80°C. 124

Table XIII. 2 Mean diameter (MD), standard deviation (SD) and Polidispersity index (PI) of PCL nanoparticles produced at different saturator

temperatures and at different GLR. PCL concentration = 5 mg/mL, S/NS = 1/4., P 70 bar	128
Table XIII. 3 Mean diameter (MD), standard deviation (SD) and Polidispersity index (PI) of PCL nanoparticles obtained at different solvent/ non solvent (S/NS) ratios and at PCL concentrations ranging from 1 to 5 mg/mL. GLR=1.8, T=100°C and p=70 bar	129
Table XIV. 1 SAILA feasibility tests for the production of nanosuspensions of different compound poorly water soluble	134
Table XIV. 2 Mean diameter (MD), standard deviation (SD) and Polidispersity index (PI) of β -C nanoparticles obtained from a 0.03 mg/mL β -C solution in acetone. Saturator temperature was set at 80°C	136
Table XIV. 3 Mean diameter (MD), and Polidispersity index (PI) of ketoprofene nanoparticles obtained from a 20 and 30 mg/mL ketoprofene solution in acetone. Saturator temperature was set at 80°C, GLR 0.85.....	140

ABSTRACT

This work provides an innovative point of view on obtaining nanoparticles by supercritical fluids. Supercritical fluids have already been exploited in the production and processing of micro or sub-micro particles, but the production of nanoparticles is still more ambitious, requiring a deep understanding of the thermodynamic of multiphase systems involved and of the fluid dynamics and mass transfer of the process.

This thesis focused on the development of supercritical assisted process for the production of biopolymeric micro and nanocarrier for pharmaceutical and biomedical applications. After a wide study of the state of the, two different processes have been focused on the production of different kind of devices:

- 1) Supercritical Emulsion Extraction process (SEE) for the production of multifunctional nanodevices;
- 2) Supercritical Assisted Injection in Liquid Antisolvent process (SAILA) for the production of stabilized nanoparticle water suspensions.

Supercritical Emulsion Extraction (SEE) has been recently proposed in the literature for the production of drug/polymer microspheres with controlled size and distribution, starting from *oil-in-water (o-w)* and *water-in-oil-in-water (w-o-w)* emulsions. This process uses supercritical carbon dioxide (SC-CO₂) to extract the “oil” phase of emulsions, leading to near solvent-free microparticles. SEE offers the advantage of being a one-step process and is superior to other conventional techniques for the better particle size control, higher product purity and shorter processing times; the SEE process has been proposed in the continuous layout, using a high pressure packed tower. However, monodisperse sub-micro, nanoparticles of biopolymer suitable for pharmaceutical formulations have not been produced until now by SEE.

Therefore, this part of the work was performed on the production of monodisperse biopolymer nanoparticles. Particularly, emulsion formulation parameters have been tested, such as, different surfactant concentrations and biopolymer percentages in the oily phase, and several emulsification techniques (ultrasound or high speed emulsification) and their interactions with SEE processing have been tested to obtain small droplets dimensions from the micro size to the nano size range. *Poly-lactic-co-glycolic acid (PLGA)*, *poly-lactic acid (PLA)* and *poly-caprolactone (PCL)* were the polymers selected to produce micro and nano devices, relative results are shown in Chapter 7.

Then, after the optimization of the process conditions for the production of monodisperse sub-micro and nanoparticles encapsulation of drugs, proteins, peptides and metals has been carried out. For the encapsulation study the SEE technique starting from single or double emulsions was used for the production of nanospheres.

The SEE technology has a great potential regarding the field of protein encapsulation thanks to the mild extraction condition and the short process time, and mainly thanks to the possibility to use multiple emulsions. For this reason, the SEE has been applied to the production of biopolymeric micro and nanoparticles of PLA and PLGA encapsulating peptides and proteins starting from double emulsion. Results are shown in Chapter 8. Bovine serum albumin (BSA) has been selected as protecting protein for growth factor, such as Vascular Endothelial Growth Factor (VEGF) and Bone Morphogenetic Proteins (BMP). Both micro and nanoparticles were produced; the effect of size of particles on protein loading and release has been evaluated. PLGA microspheres loaded with GFs were charged inside a bioactive alginate scaffold to monitor the effect of the local release of these biosignals on cells differentiation. Human Mesenchymal Stem Cells (h-MSC), were used in view of the fact that they are a promising cell source for bone tissue engineering. Good cells differentiation indicates that the SEE process was successful in the encapsulation of proteins and peptides, preserving the functional structure of the proteins, thanks to the mild operating conditions used.

Another important challenge that has been managed is also the production of nanocomposite biopolymeric particles encapsulating metal nanoparticles for the production of light sensitive drug delivery devices. The encapsulation of TiO₂ and Au nanoparticles has been performed for different biomedical applications (Chapter 9 and 10).

In this work PLA/nano-TiO₂ microparticles have been produced using SEE for photodynamic therapy of cells and bacteria. Anatase type nano-TiO₂ ethanol stabilized suspension has been synthesized by precipitation from solutions of titanium alcoxides and directly used as the water internal phase a of double emulsion *water in oil in water* and also TiO₂ fine powder was produced and used for encapsulation experiments using a *solid in oil in water emulsion*. Both micro and sub-microparticles have been produced. High TiO₂ encapsulation efficiencies have been obtained. PLA/nano-TiO₂ particles have been characterized by TEM, TGA and XPS to investigate the dispersion of the metal oxide in the polymeric matrix. Photocatalytic activity of the produced nanostructured microparticles has been also investigated using bacterial killing assay (*StaphylococcusAureus*) under UV light. Pure TiO₂ nanoparticles and PLA/nano-TiO₂ particles showed the same photocatalytic activity.

Stimuli-responsive drug delivery systems were produced dispersing hollow gold nanoshells (HGNS) in PLA particles encapsulating Rhodamine

to obtain the photothermal controlled delivery of the model drug under near infrared irradiation (NIR). HGNs were synthesized via galvanic replacement of Cobalt with Gold using PVP as template stabilizer. HGNs with a mean diameter of 20 nm were produced; the maximum absorption coefficient was located in the optimal NIR region desired for biomedicine, 800 nm wavelength. PLA-HGNs nanocomposite particles encapsulating Rhodamine were produced using the SEE technique. Rhodamine was dissolved in the water internal phase of a double *water-in-oil-in-water* emulsion, whereas HGNs were dispersed in the polymeric solution of the oil phase. Thanks to the fast and efficient extraction of the solvent of the oily phase obtained by supercritical CO₂, non coalescing and spherical PLA-HGNs nanostructured particles were obtained, with a mean dimension around 200 nm. Particles were characterized by SEM, TEM and EDX analysis, HGNs loading was estimated by ICP. Rhodamine release from PLA-HGN nanostructured particles was evaluated under different NIR irradiation conditions demonstrating that release rate is controllable externally, depending of NIR exposures. A pulsatile Rhodamine release was obtained with NIR irradiation.

The SEE plant was also used for the solvent removal from biopolymeric nanoparticles suspensions produced by nanoprecipitation (Chapter 11). Nanoprecipitation is a simple and effective process for the production of biopolymer nanoparticle suspensions. However, until now only a marginal attention has been given to the problem of the solvents elimination from the prepared suspensions. This part of the process is very important in pharmaceutical/medical applications, since even some parts per million (ppm) of these residues can hinder the application of the produced nanoparticles. A new approach to the problem of acetone and acetone/ethanol mixtures removal, from the suspension of nanoparticles has been proposed, using the SEE apparatus for the continuous counter-current extraction of the organic solvent from water based suspensions. The operating parameters (pressure, temperature and liquid to gas ratio) were optimized. Nanoprecipitation process assisted by supercritical solvent elimination has been tested on PLGA and PCL.

Part of this PhD thesis was also focused on the development of a new supercritical assisted technique for the production of nanoparticles stabilized water suspensions, Chapter 12, 13,14. In this part of PhD thesis it has been proposed a novel supercritical assisted process for nanoparticle production, called Supercritical Assisted Injection in a Liquid Antisolvent (SAILA). In this process, an expanded liquid solution formed by supercritical carbon dioxide (SC-CO₂) and an organic, water miscible solvent, is produced, in which a solid solute is solubilised. Then, the solution is depressurized into a water solution in which the solute is not soluble: the water based solution works as a

liquid antisolvent and nanoparticles are produced. In the SAILA process liquid-liquid antisolvent precipitation is obtained when the processed compound is soluble in the solvent and not soluble in the antisolvent; the particles size of the precipitates depends on the efficiency of the micromixing between the two liquids that, in turn, is related to their surface tension. The continuous injection of an expanded liquid solution improves the mixing with the antisolvent thanks to the reduced surface tension of the expanded liquid, thus producing smaller particles.

The process has been proved to be successful in the production of nanoparticles of PCL, selected as model compound. The effect of the process parameters on nanoparticle diameter has been studied; it decreases increasing the gas to liquid ratio, the water to solvent flow rate ratio, the saturator temperature and decreasing the polymer concentration. Nanoparticles with a mean diameter down to 64 nm have been obtained. Nanoparticle formation mechanism seems to be guided by the micromixing between the expanded liquid solution and the receiving water solution, followed by nucleation and growth of nanoparticles. The presence of surfactants in the water receiving solution avoids nanoparticles coalescence. Furthermore the SAILA process has been applied successfully to the production of stabilized nanoparticles suspensions of poorly water soluble drugs, several different compounds have been processed in order to extend the range of applicability of this process not only to the polymer but also active principles.

In conclusion, in this PhD thesis, innovative supercritical assisted processes have been applied successfully to the production of nanoparticles. The SEE process conditions were optimized to produce biopolymeric monodisperse submicro or nanoparticles; the encapsulation of several challenging compounds were carried out using the double emulsion technique. The SEE process reveals to be a powerful and robust technique for the production of multifunctional nanodevices for nanomedicine applications. The nanoprecipitation process assisted by supercritical fluid for the extraction of the organic solvent has also been proved to be a valid alternative to the SEE technique for the production of biopolymeric monodisperse nanoparticles suspensions. A new supercritical assisted process has been developed and proposed in this thesis work named Supercritical Assisted Injection in a Liquid Antisolvent (SAILA). It has been demonstrated that the idea is original and innovative in the field of supercritical fluid processes and successful in the production of nanoparticles stable aqueous suspensions.

Chapter I

Introduction

I.1. Nanomaterials

Scientists are popularly using the term nanotechnology to refer designing, characterization, production and application of structures, devices and systems with at least one dimension in the nanometer range (1 nm=one thousand millionth of a meter, 10^{-9} m). The size range of nanotechnology is often delimited to 100 nm down up to 0.2 nm; this is where materials have significantly different properties (Kaehler T., 1994).

The nanomaterials are known for their unique mechanical, chemical, physical, thermal, electrical, optical, magnetic, biological and also specific surface area properties, which in turn define them as nanostructures, nanoelectronics, nanophotonics, nanobiomaterials, nanobioactivators, nanobiolabels, etc. In the last one decade a large variety of nanomaterials and devices with new capabilities have been generated employing nanoparticles based on metals, metal oxides, ceramics (both oxide and non-oxide), silicates, organics, polymers, etc. One of the most important properties of materials in nano-size regime is the changing physical properties. Nanoparticles possess unique optical and electronic properties not observed for corresponding bulk samples. Owing to a substantial increase in the fraction of surface atoms and to increasing role of the surface effects not only the optical properties but also other characteristics of materials (structure of electronic energy levels and transitions, electron affinity, conductivity, phase transition temperature, magnetic properties, melting points, affinity to biological, polymer and organic molecules, etc.) also become dependent on the nanoparticle size and shape. Such a size dependent properties have been exploited for biological tagging, for example, as fluorescent biological labels.

Hence, it is extremely important to control the size and also shape of the nanoparticles/nanocrystals in order to obtain a desired physical property. For this reason, a major challenge in the nanomaterials science is the accurate

control of the size and shape, which in turn is directly linked with the nanomaterials processing method. On the whole there are only two approaches known for the nanomaterial fabrication: bottom-up and top-down methods (**Figure I. 1**).

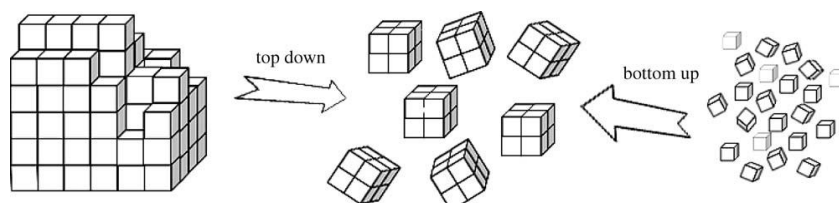


Figure I. 1 *Top-down and bottom-up approaches (Reverchon E. and Adami R., 2006)*

The bottom-up approach deals with the controlled assembly of atomic and molecular aggregates into larger systems (e.g. clusters, organic lattices, supermolecular structures and synthesized macromolecules). This covers the popular synthesis methods like: chemical synthesis, self-assembly, positional assembly, leading to the formation of particles, molecules, cosmetics, fuel additives, crystals, films, tubes, displays, atomic or molecular devices. Whereas the top-down approach deals with the reduction in structure sizes of microscopic elements to the nanometer scale by applying specific machining and etching techniques like: lithography, cutting, etching, grinding, etc., giving rise to electronic devices, chip masks, quantum well lasers, computer chips, precision engineered surfaces, high quality optical mirrors. The present thesis has been restricted to the nanomaterial fabrication for biomedical application, which insists upon the control of size and morphology of drug and drug/polymer powder and its multidimensional structure that is very essential to control the activity and drug delivery.

Nanoparticles can be obtained from a great variety of processes involving the conversion of solid to solid or liquid to solid or gas to solid. The milling, Sol-gel, chemical vapor deposition and colloidal chemistry approaches are the most popularly used techniques for the production of nanomaterials. However, the stringent requirements for the biological applications like the therapeutic, bioimaging, hyperthermia, targeted drug delivery system, biosensors, MRI, etc., insist on the control of the size and shape of nanomaterials. There are several reviews already existing in the literature on the conventional methods of nanomaterial fabrication (Byrappa K. and Yoshimura M., 2001), (Rao B.C.N.R. et al., 2006), and also some occasional reviews on nanomaterial fabrication for pharmaceutical applications using supercritical fluids (SCF) (Vemavarapu C. et al., 2005), (Reverchon E. and Adami R., 2006). The SCF technique of materials processing is playing an important role in nanotechnology. Although a huge amount of literature data concerning SCF techniques, the knowledge on the nucleation, crystallization,

self-assembly, and the growth mechanism of the nanocrystals in the solution media are rather complicated and are still not well understood. Hence, such studies are very essential in order to understand the rational synthesis of high-quality nanoparticles and nanostructures. In following chapter principles for nanoparticle production using the conventional technology have been discussed, before introducing the SCF based techniques used for the synthesis of various nanoparticles for the drug delivery or biomedical applications.

Chapter II

Biopolymeric Micro & Nanocarriers

Biodegradable polymers have significantly influenced the development and rapid growth of various technologies in modern medicine, packaging, textile sector, etc.. Biodegradable polymers are mainly used where the transient existence of materials is required and they find applications as sutures, scaffolds for tissue regeneration, tissue adhesives, and transient barriers for tissue adhesion, as well as drug delivery systems. Each of these applications demands materials with unique physical, chemical, biological, and biomechanical properties to provide efficient therapies (Nair L.S. and Laurencin C.T., 2006).

The incorporation of drugs in polymer particles has numerous advantages, such as controlling the drug release, increasing drug efficacy and reducing dosing frequency, targeting the drug delivery and preventing adverse effects on other organs. All these advantages enhance patient compliance and reduce costs.

These formulations typically employ artificial or natural polymers and/or other excipients that are biocompatible and/or biodegradable. The efficient size control of particles, and particle modifications are essential in enhancing controlled release and target delivery. Biopolymeric microparticles find also application in tissue engineering as building blocks for scaffolds. The microsphere-based tissue engineering scaffold designs offer several benefits, for example, ease of fabrication, control over morphology and physicochemical characteristics, versatility of controlling the release kinetics of the encapsulated factors. The properties of a scaffold, in turn, can be tailored by altering the microsphere design and fabrication method, e.g., to create gradient-based scaffolds (Singh M. et al., 2010)

In spite of the numerous advantages that biodegradable polymer particulates can provide, the development of such systems often poses a serious challenge due to lack of robust manufacturing techniques. Not only

should these manufacturing techniques provide particles having predictable and controllable physical properties such as size distribution, composition, and structure; but, they must also conform to the rigorous requirements of product consistency, purity, and process scalability for pharmaceutical and biomedical applications (Chattopadhyay P. et al., 2006).

II.1 Controlled drug delivery

The basic goal of a controlled drug delivery system is to deliver a biologically active molecule at a desired rate for a desired duration, so as to maintain the drug level in the body within the therapeutic window. Conventionally, drugs are administered into the body via an oral or intravenous route. In these modes of administration, the therapeutic concentration of a drug is maintained in the body by repeated drug administration. The problem with this approach is that during each repeated administration, the concentration of drug in the body peaks and declines rapidly, particularly when the elimination rate of drug is very high. This can lead to an unfavourable situation where at certain times the drug concentration in the body will be too low to provide therapeutic benefit, and at other times the concentration will be too high resulting in adverse side effects. This is particularly of great concern when using very active drugs with narrow therapeutic windows. Moreover, this approach shows low compliance by the patient (Freiberg S. and Zhu X., 2004).

Controlled drug delivery technology has developed into an attractive modality to solve many of the problems of traditional drug administration by regulating the rate as well as the spatial localization of therapeutic agents. In controlled drug delivery, usually the active agent will be entrapped in an insoluble matrix from which the agents will be released in a controlled mode. Furthermore, the release characteristics of the active agents can be effectively controlled by suitably engineering the matrix parameters.

The microencapsulation technology has become one of the principal fields in the area of controlled drug delivery systems. The term “control” includes phenomena such as protection and masking, reduction of dissolution rate, facilitation of handling and spatial targeting of the active ingredient. This approach facilitates the accurate delivery of small quantities of potent drugs; reduces drug concentrations at sites other than the target organ or tissue; protects labile compounds before and after administration and prior to appearance at the site of action (Gouin S., 2004).

In controlled drug delivery, biopolymers are used as approximately spherical particles ranging in size from less than 1 μm up to 1000 μm where the entrapped substance is dispersed throughout the particle matrix (**Figure II. 1**). They are made of polymeric, waxy, or other materials, that is, biodegradable synthetic polymers and modified natural products such as starches, gums, proteins, fats and waxes. The natural polymers include

albumin, chitosan, dextran and gelatine, the synthetic polymers include polylactide acid and polyglycolic acid.

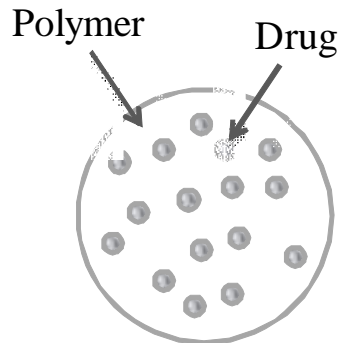


Figure II. 1 Section of a microspheres

Attempts are being made to develop novel delivery systems that can further fine-control the drug release pattern by synthesizing novel polymers as matrix systems, as well as by developing smart systems that can deliver multiple drugs in a controlled manner or under the effect of an external stimulus (Li M. et al., 2008). Furthermore in the controlled drug delivery, polydisperse micro/nanospheres are not desirable as a drug carrier, since they have wide range of surface areas and may have different drug release depending on their sizes (Ito F. and Makino K., 2004). The ability to make dispersions of a known, and controlled size distribution is important for controlled release of drug encapsulated in particles and knowing the exact size of the particles facilitates modelling the drug release and controls aspects such as the initial burst (Gasparini G. et al., 2008).

Nanoparticles offer a number of advantages over microparticles as drug delivery systems. For example, nanoscale particles can travel through the blood stream without sedimentation or blockage of the microvasculature. Small nanoparticles can circulate through the body and penetrate tissues like tumours. In addition, nanoparticles can be taken up by cells through endocytosis. Microparticles do not enable intravenous administration and the size limits the cross of the intestinal lumen into the lymphatic system following oral delivery. The smallest capillaries in the body are 5-6 μm in diameter. The size of particles being distributed into the bloodstream must be significantly smaller than 5 μm , without forming aggregates, to ensure that the particles do not form an embolus.

Nanoencapsulation enhances the transfer across the main hurdle: the brain blood barrier (BBB). An advantageous feature of particles smaller than 220nm is that they could be easily sterilized by filtration, since the sizes of bacteria and viruses are larger. Furthermore, nanoparticles enhance dissolution rates *in vitro* and bioavailabilities *in vivo* of many drugs. For this

reason stabilized nanoparticle suspensions of drugs and Polymer/drug are of great importance in nanomedicine.

Although the definition identifies nanoparticles as having dimensions below 100 nm, especially in the area of drug delivery relatively large (size>100nm) nanoparticles may be needed for loading a sufficient amount of drug onto the particles. In addition for drug delivery not only engineered particles may be used as carriers, but also the drug itself may be formulated at a nanoscale.

II.2 Targeted Drug Delivery

Targeted drug delivery systems are designed to deliver drugs at the proper dosage for the required amount of time to a specific site of the body where it is needed, thereby preventing any adverse effects drugs may have on other organs or tissues. Targeted delivery is relevant particularly in the case of highly toxic drugs such as chemotherapeutic drugs and highly active and fragile biotechnological molecules such as peptides and proteins. Furthermore, targeted drug delivery systems can be employed to deliver drugs to sites that are inaccessible under normal conditions such as the brain (Torchilin V.P., 2006). Depending on the mechanisms of action, targeted drug delivery systems can be classified into:

- passive targeting
- active targeting.

Passive targeting makes use of delivery vehicles such as liposomes or micelles. These structures, due to their optimal size, can target cancer tissues or inflammatory sites with leaky vasculature as well as pass the blood–brain barrier.

Active targeting makes use of the above-mentioned delivery vehicles or polymer–drug conjugates with a targeting agent like an antibody which can target a biomarker such as an antigen on a tissue or organ. Examples of biological coatings may include antibodies, biopolymers like collagen, or monolayers of small molecules that make the nanoparticles biocompatible.

The next step in developing these carriers is an attempt to engineer nanocarriers, which, depending on particular requirements, can demonstrate a combination of various properties/functions, i.e. to construct and use multifunctional pharmaceutical nanocarriers (**Figure II. 2**).

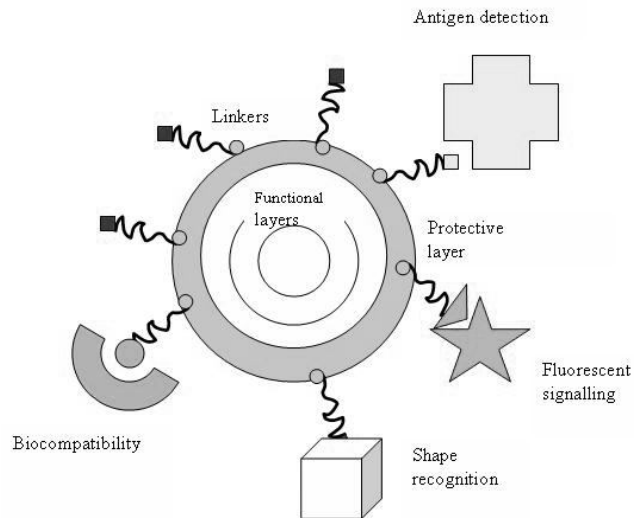


Figure II. 2 Example of multifunctional pharmaceutical nanocarrier applied to medical or biological field (Salata O., 2004)

In a relatively simple case (it is known how to “produce” all individual properties in a reasonably simple way) one may want to have a drug-loaded nanocarrier demonstrating the following set of properties: (a) prolonged circulation in the blood; (b) ability to accumulate – specifically or non-specifically – in the required pathological zone, (c) responsiveness to local stimuli, such as pH and/or temperature changes, resulting, for example, in accelerated drug release, (d) allow for an effective intracellular drug delivery and further to individual cell organelles, and (e) bear a contrast/reporter moiety allowing for the real-time observation of its accumulation inside the target.

Some other properties can be added to the list, such as magnetic sensitivity. Examples of multifunctional matrices for oral and tumoral delivery have been already reviewed (Bernkop-Schnurch A. and Walker G., 2001, Van Vlerken L.E. and Amiji M.M., 2006). Evidently, to prepare such smart multifunctional pharmaceutical nanocarrier, chemical moieties providing certain required individual properties have to be simultaneously assembled on the surface (within the structure) of the same nanoparticle. Moreover, these individual moieties have to function in a certain coordinated way to provide a desired combination of useful properties. However, systems like this still represent a challenge (Salata O., 2004).

II.3 Microsphere-based Tissue Engineering Scaffold

Tissue engineering (TE) is aimed at repairing and restoring damaged tissue employing three fundamental “tools”, namely cells, scaffolds and

growth factors, which, however are not always simultaneously used (Luciani A. et al., 2008). On the other hand, recent experimental and clinical evidences indicates that the success of any TE approach mainly relies on the delicate and dynamic interplay among these three components and that functional tissue integration and regeneration depend upon their integration. Therefore, biomaterial scaffolds have to provide biological signals able to guide and direct cell function through a combination of growth factors sequestration and delivery. Several technologies have been used to make polymer porous scaffolds such as gas foaming (Murphy W.L. et al., 2000), salt leaching (Pamula E. et al., 2005), solvent casting and their combination (Kim S.S. et al., 2006). All these techniques for scaffolds production are classified as top-down methods. However, beside their well-known limitations regarding the control of porosity and interconnectivity along with poor mechanical properties of the resulting scaffold (Mikos A.G. et al., 1993), these techniques are not suitable to include micro- depots in a regulated spatial pattern.

In recent years a large number of investigations about the realization of porous scaffolds by sintering polymeric or ceramic microspheres have been reported. This new approach for scaffolds production is basically a bottom-up approach. Since the first proposal of a microsphere based structures for tissue engineering, 3D scaffolds with a porous interconnected structure, it became evident that this approach could overcome some of the limitations presented by the classical approaches.

The bottom-up approach can realize multifunctional polymer scaffolds with predefined pore dimension and degree of interconnectivity and containing interspersing microdepot for the release of bioactive molecules. Scaffolds were obtained through the thermal fusion of different kinds of biodegradable pharmacologically active microcarriers (PAMs) to obtain scaffolds with controlled porosity, mechanical properties and spatial-temporal distribution of bioactive signals. The pores dimension and the mechanical properties are modulated by the size and formulation of the large microspheres while the rate and the time of release of protein are modulated by the formulation and size of the smaller microspheres. The results obtained are most promising and open the way for the development of microspheres based bioactive sintered scaffolds capable of sequestration and delivery of biological agents.

Chapter III

State of the art: Micro and nanoparticles production

The production of micro and nanocarrier for controlled, targeted delivery and as building block for tissue engineering scaffolds is still a challenge, because good manufacturing techniques for these kinds of products should respect the many basic requirements:

- Production of particles with controlled size distributions;
- Mild operative conditions (which allow the processability of sensible drugs and proteins);
- Continuous, robust and reproducible processing;
- Possibility to process with FDA approved materials;
- Possibility to encapsulate different drugs, proteins and also metal nanoparticles (allowing the production of multifunctional carriers);
- Production of stabilized suspensions.

Microspheres and nanospheres have been prepared by various techniques. Among these, the attention will be focused particularly on the techniques based on the emulsification of homogeneous solutions. The solvent extraction/evaporation of emulsion allows the production of particles with controlled particle sizes both in the nano and in the micrometric range changing accurately the emulsion production process. The nanoprecipitation technique can allow the production of nanoparticles of controlled size and distribution (Sosnik A. et al., 2008). These two techniques of particles production are described in details in the following pages.

III.1 Emulsions for the production of biopolymeric micro and nanoparticles

Solvent evaporation/extraction of emulsions is applied in pharmaceutical industries to obtain microparticles for the controlled release of the drug. The polymer microspheres with drug trapped inside can degrade and release the encapsulated drug slowly with a specific release profile.

There are different methods to produce microspheres by solvent evaporation/extraction technique. The choice of the method that will give rise to an efficient drug encapsulation depends on the hydrophilicity or the hydrophobicity of drug. For insoluble or poorly water-soluble drugs, the oil-in-water (o/w) method is frequently used. This method is the simplest and the other methods derive from this one. It consists of four major steps (**Figure III 1**):

- (1) dissolution of the hydrophobic drug in an organic solvent containing the polymer;
- (2) emulsification of this organic phase, called dispersed phase, in an aqueous phase called continuous phase;
- (3) extraction of the solvent from the dispersed phase by the continuous phase, accompanied by solvent evaporation, transforming droplets of dispersed phase into solid particles; and
- (4) recovery and drying of microspheres to eliminate the residual solvent (Li M. et al., 2008).

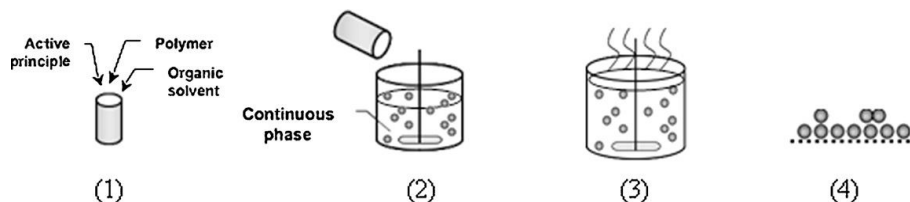


Figure III 1 Basic steps of microencapsulation by solvent evaporation (Li M. et al., 2008)

This method is not suitable for the encapsulation of high hydrophilic drugs. There are two main reasons: (1) the hydrophilic drug may not be dissolved in the organic solvent; (2) the drug will diffuse into the continuous phase during emulsion, leading to loss of drug. The alternative method of the w/o/w double emulsion has been proposed and therefore make it possible to encapsulate the hydrophilic drugs. According to this method, the aqueous solution of hydrophilic drug is emulsified with organic phase (w/o emulsion), this emulsion is then dispersed into a second aqueous solution forming a second emulsion (w/o/w double emulsion). Then, extraction of the

solvent from the dispersed phase by the continuous phase, accompanied by solvent evaporation, transforming droplets of dispersed phase into solid particles.

III.1.1 Choice of materials: Disperse phase

Polymer

The biodegradability or biocompatibility is an essential property for the polymer used for pharmaceutical applications. ‘Biodegradability’ means that the components are degraded into harmless components which are metabolized. ‘Biocompatibility’ means that the component should be physiologically tolerable and should not cause an adverse local or systemic response after administration.

Polymers and copolymers of lactic and glycolic acids are the most commonly used to develop drug delivery systems due to their safe and FDA (Food and Drug Administration) approved applications in humans. They can ultimately degrade by hydrolysis of their constituents, which are usual metabolic products. Other biodegradable polymers such as Polycaprolactone (PCL) and Polyvinylalcohol (PVA) and Polylactic acid (PLA) have been studied for pharmaceutical and medical applications (Amass W. et al., 1998).

Non-biodegradable polymers with good biocompatibility are also used as drug carriers, such as ethyl cellulose (degradable but non-biodegradable) and polymethyl methacrylate (biocompatible but non-degradable). Ethyl cellulose can be administered orally to protect the drug against gastrointestinal tract or administered intraduodenally for a prolonged intestinal absorption (Takishima J. et al., 2002). Polymethyl methacrylate microspheres are extensively used as bone cement material in antibiotics releasing for bone infection (Stallmann H.P. et al., 2006) and bone tumours (Mestiri M. et al., 1993). Surgical removal is required afterwards because the polymethyl methacrylate is not degradable.

The choice of polymer used as drug carrier depends also on the desired drug release rate, which is essentially determined by the polymer’s physical properties. If one polymer cannot offer a satisfying drug release, a single polymer, called co-polymer, can be synthesized from two different polymers. The properties of the co-polymer are improved since it has two segments on the chain.

Solvent

For microencapsulation techniques, a suitable solvent should meet the following criteria:

- ✓ able to dissolve the chosen polymer;
- ✓ poorly soluble in the continuous phase;
- ✓ a high volatility and a low boiling point;

✓ low toxicity.

Chloroform is frequently used, but due to its toxicity and low vapour pressure, it is gradually replaced by methylene chloride. Methylene chloride is the most common solvent for the emulsion formation because of its high volatility, low boiling point and high immiscibility with water. Its high saturated vapour pressure, compared to other solvents, promises a high solvent removal rate, which shortens the duration of fabrication of microspheres. However, this solvent is confirmed carcinogenic according to EPA (Environmental Protection Agency) data and the researchers are making great efforts to find less toxic replacements.

Ethyl acetate shows promising potential as a less toxic substitute of methylene chloride. But due to the partial miscibility of ethyl acetate in water, microspheres cannot form if the dispersed phase is introduced directly into the continuous phase. The sudden extraction of a large quantity of ethyl acetate from the disperse phase makes the polymer precipitate into fibre-like agglomerates (Freytag T. et al., 2000). To resolve the problem created by the miscibility of solvent with water, the aqueous solution can be pre-saturated with solvent (Bahl Y. and Sah H., 2000).

Ethyl formate shows also interesting results. Sah (Sah H., 2000) observed that the evaporation rate of ethyl formate in water is 2.1 times faster than that of methylene chloride although ethyl formate possesses a lower vapour pressure and a higher boiling point. This phenomenon is explained by the fact that more molecules of ethyl formate are exposed at the air-liquid interface because of its higher water solubility.

Recently, some authors reported PLGA microspheres containing vitamin B₁₂ prepared by emulsion extraction using a new emulsion composition formed by acetone, as the solvent for the oily phase and aqueous glycerol, taking advantage of the phase separation between the mixtures. Acetone was then “extracted” with water; indeed, moving the mixture composition in one phase region the PLGA/drug microsphere hardening has been obtained (Matsumoto A. et al., 2008). Although simple, the main disadvantage of this liquid-liquid emulsion extraction method is extremely low yields due to water dilution complications, such as microsphere recovery and drug leakage.

In summary, less toxic solvents have been tested and show a promising future. But, there are not enough results to compare the quality of microspheres prepared by different solvents. Methylene chloride is still the most used solvent because it evaporates fast, shows high drug encapsulation efficiency and produces microspheres with a more uniform shape.

Alternative components

In certain cases, other constituents are added in the disperse phase such as co-solvents and porosity generators. A co-solvent is used to dissolve the

drug that is not totally soluble in the solvent in the disperse phase (Reithmeier H. et al., 2001). Organic solvents miscible with water such as methanol or ethanol are the common choices. A porosity generator, called also porogen, is used to generate the pores inside the microspheres, which consequently increases the degradation rate of polymer and improves drug release rate. Organic solvents such as hexan, which do not dissolve poly(lactic acid) and poly(lactic-co-glycolic acid) can be incorporated into microspheres to form pores (Spenlehauer G. et al., 1988).

III.1.2 Choice of materials: Continuous phase

Surfactants

The surfactant, also called tensioactive agent, is frequently employed for the dispersion of one phase in another immiscible phase and for the stabilization of obtained emulsion. It reduces the surface tension of continuous phase, avoids the coalescence and agglomeration of drops and stabilizes the emulsion. A suitable surfactant should be able to give microspheres a regular size and a small size distribution, guaranteeing a more predictable and stable drug release.

Before choosing the type of surfactant and its concentration, it is important to know the polarity of the two immiscible phases, the desired size of microspheres and the demand on the sphericity of microspheres.

Surfactants for emulsions are amphiphilic. That means one part of the molecule has more affinity to polar solutes such as water (hydrophilic) and the other part has more affinity to non-polar solutes such as hydrocarbons (hydrophobic). When it is present in an emulsion, the surfactant covers the surface of drops with its hydrophobic part in the drop and its hydrophilic part in the water.

There are four different types of surfactant classified by the nature of the hydrophilic part of molecule: anionic, cationic, amphoteric and non-ionic.

The anionic surfactants release a negative charge in the aqueous solution. They have a relatively high HLB (hydrophilic-lipophile balance) level because they have prone to be hydrophilic. The cationic surfactants on the contrary release a positive charge in aqueous solution. The amphoteric surfactants behave an anionic in alkali pH and as cationic in acid pH. Non-ionic surfactants have no charge (Li M. et al., 2008). Among different surfactants, partially hydrolyzed PVA is mostly used because it gives the smallest microspheres (O'hagan D.T. et al., 1994). The increase of surfactant concentration reduces the size of microspheres. The addition of surfactants lowers the surface tension of the continuous phase and the diminution of the latter decreases the particle size. However, due to the critical micelle concentration (CMC), the surface tension cannot decrease infinitely. When surfactants concentration reaches a certain level, the solution surface is

completely loaded. Any further additions of surfactant will arrange as micelles and the surface tension of the aqueous phase will not decrease any more.

Alternative components

Besides the surfactant, the antifoam is sometimes added into aqueous phase in the case of strong agitation because the foaming problem will disturb the formation of microspheres. When the stirring speed increase, more air is entrained and foam forms. So anti-foams of silicon and non-silicon constituents are used to increase the rate at which air bubbles are dissipated (Berchane N.S. et al., 2006).

Recent studies show that it is possible to prepare microspheres without surfactant by replacing it with an amphiphilic biodegradable polymer. The advantage is to avoid the potential harm of surfactant residual on the surface or inside the final microspheres.

III.1.3 Choice of the emulsification technique

Emulsions are usually prepared by the application of mechanical energy produced by a wide range of agitation techniques. The droplet formation step determines the size and size distribution of the resulting microspheres. Microsphere size may affect the rate of drug release, drug encapsulation efficiency, product syringeability, in vivo fate in terms of uptake by phagocytic cells and biodistribution of the particles after subcutaneous injection of intranasal administration.

Particle size are known to have significant influences on the release rate. The effects vary depending on the drug release mechanism. When the drug release is mainly controlled by diffusion, small microparticles tend to release the drug at a relatively high rate due to the large surface area and the short diffusion distance. On the other hand, when the release depends on the polymer degradation, the particle size controls the release rate by affecting additional features such as drug distribution and polymer degradation rate. In this regard, a variety of efforts have been made to obtain microparticles of monodisperse and controllable size.

Stirring

Stirring is the most straightforward method to generate droplets of few microns up to hundred microns of the drug/matrix dispersion in the continuous phase. In the simplest approach, external phase is filled into a vessel and agitated by an impeller. The drug/matrix dispersion is then added, dropwise or all at once, under agitation at a speed sufficient to reach the desired droplet size. Obviously, the impeller speed is the main parameter for controlling the drug/matrix dispersion's droplet size in the continuous phase.

Increasing the mixing speed generally results in decreased microsphere mean size, as it produces smaller emulsion droplets through stronger shear forces and increased turbulence (Yang Y.Y. et al., 2001). The extent of size reduction that is attained depends on the viscosity of the disperse and continuous phases, the interfacial tension between the two phases, their volume ratio, the geometry and number of the impeller(s) and the size ratio of impeller and mixing vessel (Freitas S. et al., 2005).

Ultrasounds emulsification

Often subsequent the stirring, *ultrasound emulsification* consists in sonicating liquids at high intensities (Bilati U. et al., 2003). The sound waves that propagate into the liquid media result in alternating high-pressure (compression) and low-pressure (rarefaction) cycles, with rates depending on the frequency. During the low-pressure cycle, high-intensity ultrasonic waves create small vacuum bubbles or voids in the liquid. When the bubbles attain a volume at which they can no longer absorb energy, they collapse violently during a high-pressure cycle. This phenomenon is termed cavitation. During the implosion very high temperatures and pressures are reached locally. The implosion of the cavitation bubble also results in liquid jets of up to 280m/s velocity. Ultrasound emulsification has been proven to generate very homogenous emulsions of water in oil (w/o) and oil in water (o/w) by the high cavitation shear. As the parameters of ultrasonication are well controllable, the particle size and distribution is well adjustable and repeatable. This method is combined with the stirring emulsification is used in order to obtain very small droplets.

Membrane emulsification

Membrane emulsification (ME) is a new technique of emulsification used to obtain a better control of the PSDs. In conventional direct ME, fine droplets are formed in situ at the membrane/continuous phase interface by pressing a pure disperse phase through the membrane. In order to ensure a regular droplet detachment from the pore outlets, shear stress is generated at the membrane/ continuous phase interface by recirculating the continuous phase using a low shear pump. The rate of mixing should be high enough to provide the required tangential shear on the membrane surface, but not too excessive to induce further droplet break up. Another approach uses systems equipped with a moving membrane, in which the droplet detachment from the pore outlets is stimulated by rotation or vibration of the membrane within a stationary continuous phase. Even in the absence of any tangential shear, droplets can be spontaneously detached from the pore outlets at small disperse phase fluxes, particularly in the presence of fast adsorbing emulsifiers in the continuous phase and for a pronounced noncircular cross section of the pores (Vladislavljevic G.T. and Williams R.A., 2005).

Depending on the membrane hydrophilicity/ hydrophobicity and the compositions of the two liquid phases, O/W, W/O emulsions may be produced. The single emulsion can be subjected to secondary emulsification to form a multiple emulsion or may undergo a process/reaction converting the droplets into solid particles or the continuous liquid phase into a solid phase(Nakashima T. et al., 2000).

Prilling

Another technique of droplet formation is the *prilling*. In this process, the forming droplets were detached from a needle by electrostatic forces. Particle collection and solvent removal occurred in a bath. The electric field was generated by connecting the needle to electric potentials of up to 4 kV and the collection bath to ground. Very large microspheres of 500 to 1500 μm average diameter were obtained, whereby the largest particles formed with voltage-free dripping. It is important to set the appropriate prilling condition to avoid highly polydispersed size distributions(Freitas S. et al., 2005).

III.1.4 Solvent Evaporation/extraction of emulsions: advantages and disadvantages

The solvent evaporation/extraction of emulsions allows the production of both microspheres and microcapsules of FDA approved biopolymers. This technique makes it possible to encapsulate hydrophilic and hydrophobic drugs using double (*water-in-oil-in-water*) and single (*oil-in-water*) emulsions respectively. Despite these potential advantages the solvent evaporation/extraction of emulsion technique suffers of some drawbacks. Indeed, This technology uses a simple vessel/stirrer setup, but may exhibit difficulties in producing large amounts of microspheres in a robust and well-controlled manner. Solvent evaporation may also require elevate temperatures or reduced pressures to eliminate the liquid solvent. Solvent extraction uses relatively large amounts of a second solvent and, then, the mixture of these two solvents has to be recycled. They also require long processing times (several hours) to be completed and, as a consequence, aggregation phenomena occur between the droplets producing microspheres with a larger polydispersity respect to the starting emulsions(Yang Y.Y. et al., 2000).

III.2 Nanoprecipitation: an alternative method to produce biopolymeric nanoparticles

The nanoprecipitation method is also called solvent displacement or interfacial deposition. The nanocapsule synthesis needs both solvent and non-solvent phases (Quintanar-Guerrero D. et al., 1996).

The solvent phase essentially consisting of a solution in a solvent or in a mixture of solvents (i.e. ethanol, acetone, hexane, methylene chloride or dioxane) of a polymer (synthetic, semi-synthetic or naturally occurring polymer), the active substance, and a lipophilic tensioactive.

On the other hand, the non-solvent phase consists of a non-solvent or a mixture of non-solvents for the polymer, supplemented with one or more surfactants. In most cases, the solvent and non-solvent phases are called organic and aqueous phases, respectively. The solvents used for the solvent and non solvent phase are completely miscible. As a general tendency, the solvent is an organic medium, while the non-solvent is mainly water. However, it is possible to use either two organic phases or two aqueous phases as long as solubility, insolubility and miscibility conditions are satisfied. The nanocapsules are obtained as a colloidal suspension formed when the organic phase is added slowly and with moderate stirring to the aqueous phase.

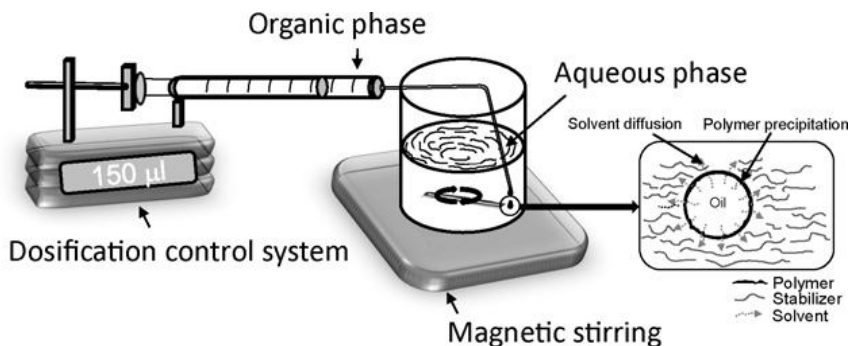


Figure III 2 Set-up used for preparation of nanoparticles by the nanoprecipitation method (Mora-Huertas C.E. et al., 2010)

III.2.1 Choice of materials

Polymers

The polymers commonly used are biodegradable polyesters, especially poly- ϵ -caprolactone (PCL) (Zili Z. et al., 2005), poly(lactide) (PLA) and poly(lactide-co-glicolide) (PLGA) (Murakami H. et al., 1999). Eudragit can

also be used as many other polymers such as poly(alkylcyanoacrylate) (PACA). Synthetic polymers have higher purity and better reproducibility than natural polymers.

Solvent and non solvent

Regarding the polymer solvent, acetone is chosen in most of the cases. Other solvents such as ethanol are used in order for active substance or oil dissolution. Water or buffer solutions can be used as the non-solvent while the stabilizer agent is generally poloxamer 188 or polysorbate 80.

This technique is mostly suitable for compounds having a hydrophobic nature. The presence of alcohol, as cosolvent, in the inner phase, seems to speed up the precipitation of the polymer and increases the phase separation of the polymer during the solvent diffusion (Peltonen L. et al., 2002).

Also the type of non-solvent influence the PSD of the nanoparticles obtained via nanoprecipitation methods, since the higher the rate of diffusion, the smaller the nanoparticles (and the higher the yield of transformed polymer into nanoparticles) (Bilati U. et al., 2005b).

III.2.2 Choice of the nanoprecipitation conditions

In the nanoprecipitation method, the nanocapsules are obtained as a colloidal suspension formed when the organic phase is added to the aqueous phase. The key variables of the procedure seem to be:

- (1) stirring rate of non solvent,
- (2) feed rate of solvent,
- (3) non solvent ratio to the whole solvent,
- (4) temperature of non solvent,
- (5) surfactant concentration in non solvent,
- (6) biopolymer concentration in solvent (Tsukada Y. et al., 2009).

A prototype composition for preparation of nanocapsules at laboratory-scale using the nanoprecipitation method is show in **Table III 1** (nanocapsule size: approximately 150–200 nm).

Table III 1 *Suggested composition for preparation of nanocapsules by nanoprecipitation*

Material	Suggested composition
<i>Active substance</i>	10–50mg
<i>Polymer</i>	1.0–2.0% of inner phase solvent
<i>Inner phase solvent</i>	10 ml
<i>Stabilizer agent</i>	2.0–5.0% of external phase solvent
<i>External phase solvent</i>	40 ml

This technique presents clear advantages over other existing methods such as

- (a) the use of pharmaceutically acceptable organic solvents,
- (b) no need of high-pressure homogenizers or ultrasonication,
- (c) high yields,
- (d) high reproducibility;
- (e) easy to scale up (Quintanar-Guerrero D. et al., 1997)

III.2.3 Mechanism of nanoparticles formation

Disagreement exists regarding the mechanism of nanocapsule formation using this technique, research into polymer precipitation and solvent diffusion have proved useful in this regard. On the basis of Sugimoto's theory on polymer precipitation (Lince F. et al., 2008) indicated that the process of particle formation in the nanoprecipitation method comprises three stages: nucleation, growth and aggregation. The rate of each step determines the particle size and the driving force of these phenomena is supersaturation, which is defined as the ratio of polymer concentration over the solubility of the polymer in the solvent mixture. The separation between the nucleation and the growth stages is the key factor for uniform particle formation. Ideally, operating conditions should allow a high nucleation rate strongly dependent on supersaturation and low growth rate.

On the other hand, in line with the research carried out by Quintanar on mass transfer between two liquids and the Gibbs–Marangoni effect, explained rapid nanoparticle formation as a process due to differences in surface tension (Quintanar-Guerrero D. et al., 1998). Since a liquid with a high surface tension (aqueous phase) pulls more strongly on the surrounding liquid than one with a low surface tension (organic phase solvent). This difference between surface tensions causes interfacial turbulence and thermal inequalities in the system, leading to the continuous formation of eddies of solvent at the interface of both liquids. Consequently, violent spreading is observed due to mutual miscibility between the solvents, the

solvent flows away from regions of low surface tension and the polymer tends to aggregate on the oil surface and forms nanocapsules.

According to this explanation, nanocapsule formation is due to polymer aggregation in stabilized emulsion droplets, while apparently the nucleation and growth steps are not involved. Further experimentations are necessary to try to clarify the mechanism of formation of nanoparticles.

III.2.4 Nanoprecipitation: advantages and disadvantages

The nanoprecipitation technique allows a fast and easy production of biopolymeric nanoparticles, but despite this potential advantages this technique does not allow a reproducible processing because it is fundamentally a batch process. Furthermore, this technique has been extensively used in the literature for the production of nanoparticles, but still a deep understanding of the basic phenomena involved in particle formation is missing. This has led to results that are not easy to explain and difficult to control and predict. A systematic study about nanoparticle production using this technique is required. In addition until now only a marginal attention has been given to the problem of solvent removal from prepared suspensions. This is a very important aspect of the process especially regarding pharmaceutical applications.

Chapter IV

Supercritical fluid assisted processes

IV.1 Supercritical fluids properties

Supercritical fluids (SCFs) are defined as any substance, the temperature and pressure of which are higher than its critical values, and which has a density close to or higher than its critical density. An increasing drive for greener processes in the chemical industry in the 1970s led to the wider exploitation of SCFs as alternative reaction media, and also for extraction and separation processes. The key benefits are perceived as the replacement of traditional solvents which are often hazardous, toxic and contribute strongly to ozone depletion and global warming.

Like gases, SCFs possess high diffusivities, important for reaction kinetics, while also having liquid-like densities that allow them to act as effective solvents for many compounds. Small changes in pressure and temperature, especially near the critical point, can be used to tune the density of a supercritical fluid and therefore its solvating ability, hence giving increased control of reactions. As reagent-carrying media, the intermediate transport properties of SCFs should allow faster rates in diffusion limited reactions compared to liquid systems whilst at the same time providing higher solvation power and increased reactant loadings when compared to gas-phase systems (Fages J. et al., 2004).

Carbon dioxide (CO₂) is probably the most widely used supercritical fluid. CO₂ has relatively easily accessible critical points of 31.06 °C and 7.38 MPa, and tuneable density, as well as a high diffusivity, making it a promising reaction medium for organic compounds. CO₂ is non-combustible and non-toxic as well as being relatively environmentally benign. It is also easily available as it occurs naturally as well as being the by product of many industrial processes. As a consequence of the recent focus on carbon storage approaches for power stations, it is clear that CO₂ will become even more available and cheaper. One more virtue of CO₂ is that it is a gas at

ambient temperatures and pressures so that it can easily be removed after reaction, leaving no solvent residues in the processed material. This contrasts strikingly with the high energy-costs of drying for the removal of conventional solvents and water. In small-scale reactions the CO₂ contribution to global warming is negligible, but for larger scale processes this could be overcome by the ease of recycling back into the reaction system (Mishima K., 2008).

IV.2 Nanomaterials production

A possible general classification of SCF based nanoparticles generation techniques can be proposed according to the role played by the SCF in the process. Indeed, SCFs have been proposed as solvents, solutes, anti-solvents.

Rapid Expansion of Supercritical Solution (RESS)

The rapid expansion of supercritical solutions (RESS) consists of the saturation of the supercritical fluid with a solid substrate; then, the depressurization of the solution through a heated nozzle into a low pressure chamber produces a rapid nucleation of the substrate in form of very small particles that are collected from the gaseous stream. The morphology of the resulting solid material, crystalline or amorphous, depends on the chemical structure of the material and on the RESS parameters (temperature, pressure drop, impact distance of the jet against a surface, nozzle geometry, etc.) (Jung J. and Perrut M., 2001). The very fast release of the solute in the gaseous medium should assure the production of very small particles. This process is particularly attractive due to the absence of organic solvents. The authors that first proposed RESS (Petersen R.C. et al., 1986, Matson D.W. et al., 1987) patented the process with respect to the possibility of producing nanoparticles; but, also microparticles and films formation were claimed. However, only several years later in the scientific literature appeared papers that confirmed this possibility. For example, (Turk M. et al., 2002) used the RESS process to produce β -sitosterol (an anticholesteremic) nanoparticles of about 200 nm mean diameter.

An interesting variation of the RESS process is the rapid expansion of a supercritical solution into a liquid solvent (RESOLV) that consists of spraying the supercritical solution into a liquid. Operating in this manner, it should be possible to quench particles growth in the precipitator, thus improving the RESS process performance. Moreover, by interaction among the nucleating solid particles and the compounds contained in the liquid phase, a chemical reaction step can also be added.

The potential features of RESS, are very interesting from the theoretical point of view; but, the results have not been particularly good in several cases. It is in many cases problematic to control the particle size of the

precipitates. During the expansion, the particles coalesce in the supersonic free jet generated in the precipitation vessel and, therefore, in many cases needlelike particles have been obtained. Sometimes, the formation of oriented needles can be explained by the presence of electrostatic charges on the surface of the particles, induced by the fast relative motion between the particles and the gas contained in the expansion chamber (Reverchon E. et al., 1995). RESOLV configuration has been demonstrated to be more effective in producing nanoparticles, since the liquid that receives the expanding jet, can suppress the particle growth. The addition of a stabilizing agent in the liquid also protects particles from agglomeration.

The major limitation of RESS and RESOLV processes is that they are applicable only to products that show a reasonable solubility in the selected supercritical fluid. Unfortunately, many solid compounds with high molecular weight and polar bonds, that could be candidate to nanoparticles generation, show a very low or negligible solubility in SC-CO₂, that is the most widely SCF used and show a reduced solubility in many other compounds that could be good candidates to act as SCF. RESOLV has also the problem of the recovery of particles from the liquid solution used to improve the process performance: in this configuration, the process is no more solventless.

Supercritical Antisolvent precipitation (SAS)

Supercritical anti-solvent precipitation (SAS) has been proposed using various acronyms; but, the process is substantially the same in all the cases. A liquid solution contains the solute to be micronized; at the process conditions, the supercritical fluid should be completely miscible with the liquid solvent; whereas, the solute should be insoluble in the SCF. Therefore, contacting the liquid solution with the SCF induces the formation of a solution, producing supersaturation and precipitation of the solute. The formation of the liquid mixture is very fast due to the enhanced mass transfer rates that characterize supercritical fluids and, as a result, nanoparticles could be produced. This process has been used by several authors using different process arrangements; however, the most significant differences are related to the way the process operates: in batch or semi-continuous mode (Reverchon E., 1999). In batch operation (GAS: Gas AntiSolvent) the precipitation vessel is loaded with a given quantity of the liquid solution and, then, the supercritical antisolvent is added until the final pressure is obtained. In the semi-continuous operation (SAS), the liquid solution and the supercritical anti-solvent are continuously delivered to the precipitation vessel in co-current or counter-current mode. An important role is also played by the liquid solution injection device (Dehghani F. and Foster N.R., 2003). The injector is designed to produce liquid jet break-up and the formation of small droplets to produce a large mass transfer surface between the liquid and the gaseous phase. Several injector configurations have been

proposed in the literature and patented. High pressure vapor-liquid equilibria (VLEs) and mass transfer between the liquid and the SCF also play a relevant role in SAS. Particularly VLEs the ternary system solute-solvent-SC antisolvent and the position of the operating point in SAS processing with respect to these VLEs, can be decisive for the success of the process. The formation of a single supercritical phase is the key step for the successful production of nanoparticles (Reverchon E. et al., 2002). The washing step with pure supercritical antisolvent at the end of the precipitation process is also fundamental to avoid the condensation of the liquid phase that otherwise rains on the precipitate modifying its characteristics. The mechanism of particles formation with the SAS process is substantially based on nucleation induced by antisolvent effect and consequent particle precipitation. The production of nanospheres is possible, but, instead, the production of nanocapsules is not possible, only coprecipitates can be produced (when the compounds show the same precipitation rate). Furthermore, FDA approved biocompatible polymers suitable for controlled release application did not give good micronization results with this technique.

Supercritical Assisted Atomization

The Supercritical Assisted Atomization (SAA) is a techniques that use CO₂ as co-solute have something in common with the micronization by spray-drying: the SCF and the solution are intimately mixed and then sprayed in a drying atmosphere. This SCF-based micronization technique is very interesting because it can be applied to water-soluble compounds difficult to handle with the other SCF techniques without excluding the possibility of using other organic solvents. Atomization, also assisted by an inert gas, is generally used in the spray drying of solutions. The innovative aspect of the SAA process is the solubilization of SC-CO₂ in the liquid solution formed by the solvent and the (solid) solute, and the subsequent atomization of the gas-solid-liquid mixture using a thin wall nozzle. Indeed, gases are released slowly from the liquid phase and their contribution to a two-step atomization is not relevant (Reverchon E. et al., 2006). Gases at supercritical conditions are released from the liquid phase by a faster process (Reverchon E. and Spada A., 2004); therefore, SC-CO₂ can improve the atomization process, contributing to a two-step atomization. The operating conditions that are characteristic of the SAA process are the formation of a single, expanded liquid, phase in the mixing device. When SAA is properly conducted, two atomization processes take place: the first one is the production of primary droplets at the exit of the nozzle by pneumatic atomization and the second one is the destruction of these droplets by the fast release of CO₂ from the internal of the droplet (decompressive atomization). Depending on the process temperatures and the chemical characteristics of the solid solute, amorphous or crystalline particles have been produced. The SAA process has been successfully performed using

water, organic solvents with relatively low boiling points (EtOH, MeOH, acetone) and mixtures of them. Solvents with high boiling points, typically used e.g. in SAS micronization (i.e. DMSO, NMP, toluene) cannot be used because of the difficulty of removing them during precipitation. The limit of this process is that the smallest particles produced depend on the dimensions of the smallest secondary droplets generated (one droplet-one particle process). The dimensions are connected to the classical parameters that control droplet dimensions during atomization: surface tension, viscosity and quantity of SCF dissolved in the liquid. The SAA process allows the successful production of particles in the range of dimension 1-3 μm . The production of nanoparticles has never been demonstrated until now. Another limitation of the SAA process that reduces the possibility to use this process for the production of devices for biomedical application is the need of elevated temperatures in the precipitation chamber, that can damage thermolabile compounds.

Supercritical Emulsion Extraction (SEE)

The Supercritical Emulsion Extraction technique (SEE) is the innovative version of the conventional solvent evaporation technique for the production of micro and nanoparticles.

This process has been recently proposed by some authors (Kluge J. et al., 2009a, Della Porta G. and Reverchon E., 2008). This process provides a method of producing particles via solvent extraction of emulsion using supercritical fluid. A solute is dissolved in a suitable solvent to form a solution; the solution is then dispersed into an immiscible or partially miscible liquid to form an emulsion. Extracting the solvent from the oil phase of the emulsion, the SEE process produces an aqueous colloidal suspension of particles. Solvent used in the process can be recovered and recycled. In this process, SC-CO₂ selectively extracts the organic solvent from the discontinuous phase resulting in supersaturation of the solute in the solvent. The supersaturation leads to the precipitation of the solute in the form of fine particles into the continuous phase. SC-CO₂ extraction has a relatively faster extraction rate compared to extraction rates of other conventional techniques (processing in minutes instead of several hours), and this allows the formation of relatively smaller particles, with narrow size distributions, and very small solvent residues (Della Porta G. and Reverchon E., 2008).

The solute is preferably a substance that is insoluble or slightly soluble in water. Thus, the method is particularly suitable for producing many pharmaceutical compositions, as many of which are either insoluble or slightly soluble in water, and are delivered to patients as aqueous colloidal suspensions.

The supercritical fluid-soluble liquid or solvent forming the discontinuous phase is preferably an organic solvent or an oil, and thus either

immiscible or only partially miscible with water. Suitable preferred organic solvents that are immiscible in water include, for example, toluene, cyclohexane and higher alkanes. Organic solvents that are partially miscible in water include, for example, ethyl acetate, propyl acetate and 2-butanone. The supercritical fluid-insoluble liquid forming the continuous phase is preferably water.

The PSD can be controlled by controlling the droplet size of the emulsions.

An approach starting from an O/W emulsion and using SC-CO₂ for the extraction of the emulsion organic phase was proposed by Chattopadhyay & co-workers (Chattopadhyay P. et al., 2006, Chattopadhyay P. et al., 2007, Shekunov B. et al., 2006) in the preparation of drug microparticles of megestrol acetate or cholesterol acetate and in the formation of lipid microspheres charged with ketoprofen and indometacin. Della Porta & Reverchon (Della Porta G. and Reverchon E., 2008, Della Porta G. et al., 2010), recently, gave some indications on the mechanism of solvent extraction by SC-CO₂ of an O/W emulsion and a W/O/W for the production of PLGA microspheres loaded with different anti-inflammatory drugs, controlling their size, distribution, and drug loading by varying both emulsion and SC-CO₂ process conditions. These studies confirmed that the SC emulsion processing combines the advantages of traditional emulsion based technology, namely control of particle size and surface properties, with the advantages of supercritical fluid extraction process, such as higher product purity and shorter processing times.

The major limitation of supercritical extraction, shared with traditional evaporation processes, is the fact that these processes are intrinsically discontinuous. Indeed, a batch of emulsion can be treated for each process run. This fact produces some problems: repeatability of the batches and reduction of the process yield due to the material lost on the walls of the precipitation vessel. The problem of batches reproducibility is particularly important for pharmaceutical industry that to obtain the Food and Drug Administration (FDA) approval of a process has to accurately demonstrate that all processed batches produce exactly a product with the same characteristics. For this reason Della Porta and Reverchon (Della Porta G. et al., 2011b) suggested also the possibility of a continuous process layout where the SC-CO₂ is continuously contacted with an O/W emulsion in a column to extract the organic solvent without interacting with dispersant phase. At the bottom of the column, a suspension of microstructured particles can be continuously collected.

The SEE process is particularly suitable for the production of microspheres and microcapsules of biopolymers loaded with drugs for controlled delivery application. The production of multifunctional devices for nanomedicine has never been demonstrated until now, but among the SCF based technique this is, without doubt, the most promising.

Chapter V

Objectives of the work

V.1 Objectives of the work

The aim of this work is to study and optimize supercritical assisted processes for the production of micro and nanoparticles or biopolymeric nanocarriers.

The supercritical emulsion extraction process, recently proposed in the literature, has been successfully applied to the production of biopolymeric microparticles and microspheres for the encapsulation of different drugs. However, submicro and nanoparticles have not yet been produced successfully with this technique. For this reason, a part of the work will be focused on the optimization of the process condition for the production of monodisperse submicro and nanospheres of different biopolymer. In particular, different emulsion formulation will be developed and standardized to enhance the control over particle size distributions.

The SEE technique will also be applied for the production of complex nanodelivery devices. Proteins and growth factor will be encapsulated in PLGA and PLA particles producing the so called PAMs, which will be next charged in alginate scaffolds and tested for regenerative medicine. Light sensitive drug delivery devices will be also produced with this technique. Titanium oxide (activated by UV light) and Gold (activated by NIR irradiation) nanoparticles will be loaded in PLA nanocomposite devices for photodynamic therapy of cells and photothermally controlled drug delivery respectively.

The SEE apparatus will be also applied for the extraction of the solvents from nanoparticles suspensions produced by nanoprecipitation technique. This technique allows a fast and reproducible production of biopolymer nanoparticles, but solvent removal from aqueous suspensions requires complicated post-processing operations that may damage particles size distribution. We propose a supercritical solvent extraction from water based suspensions using the continuous counter-current apparatus used for the SEE technique. Different nanoprecipitation formulations will be tested leading to different final composition of the nanoparticle suspensions. Solvent used to obtain particles precipitation will be extracted using SC-CO₂ solvent power.

Supercritical solvent extraction operating conditions will be optimized to reduce solvent residue well below the limits for pharmaceutical applications.

In addition a new supercritical assisted process will be proposed for the production of nanoparticles.

The basic idea of the new process, named Supercritical Assisted Injection in Liquid Antisolvent (SAILA) comes from the general principle according to which particles can be formed thanks to liquid-liquid antisolvent, when the processed compound is soluble in the solvent and not soluble in the antisolvent. An expanded liquid solution formed by supercritical carbon dioxide (SC-CO₂) and an organic, water miscible solvent, is produced, in which a solid solute is solubilised. Then, the solution is depressurized into a water solution in which the solute is not soluble: the water based solution works as a liquid antisolvent and nanoparticles are produced.

The particles size of the precipitates depends on the efficiency of the micromixing between the two liquids that, in turn, is related to their surface tension. The continuous injection of an expanded liquid solution improves the mixing with the antisolvent thanks to the reduced surface tension of the expanded liquid, thus producing smaller particles. The SAILA process will be validated and feasibility tests will be conducted for the production of polymeric nanoparticles. A systematic study of the operating parameters will be done with the attempt of postulating a possible mechanism of particle formation. Furthermore, the applicability of this process to several different compound will be tested in order to find the field of application of this technique.

Chapter VI

Supercritical Emulsion Extraction Continuous Process(SEE)

VI.1 SEE-C process

The increasing interest in advanced controlled release formulations and the combination of their characteristics provide the increasing potential of supercritical fluids technology in the pharmaceutical industry. The preparation of controlled release formulations using supercritical fluid-assisted techniques offers several unique features such as the ability to perform the process in a single stage without any exposure of the products to the external environment, the ease solvent removal, the use of high-grade stainless steel equipment and the inherent sterilizing effects, low handling and disposal expenses (York P., 1999). Furthermore, the supercritical fluid technology may facilitate the development of significant improvements in the efficiency of both currently marketed drugs and new therapeutic entities.

Recently, Supercritical Emulsion Extraction (SEE) has been proposed in literature for the production of particles with controlled size and distribution, starting from *oil-in-water (o-w)* and *water-in-oil-in-water (w-o-w)* emulsions. In this process, SC-CO₂ has been proposed for the selective extraction of the oily phase of emulsions, obtaining the polymer hardening and microspheres formation. The use of supercritical fluids as extraction media is a promising alternative for the formation of microparticles of active principles and pharmaceutical excipients. There are two main reasons for using this technique. Firstly, the selective solvating power of supercritical fluids makes it possible to extract the organic solvent from emulsions and produce microspheres. Secondly, the favorable mass transfer properties and high solubility of solvents in the supercritical fluid make the solvent removal rapid and efficient with low level of residual solvent as requested by the authorities. The process layout of SEE has been first proposed by Chattopadhyay et al.(Chattopadhyay P. and Gupta R.B., 2003, Chattopadhyay P. et al., 2006, Chattopadhyay P. et al., 2007) , obtaining

particles of nanometric and micrometric size with narrow particle size distribution. Particularly, they used SC-CO₂ to eliminate the organic solvent from *o-w emulsions* for the preparation of drug microparticles of megestrol acetate, griseofulvin and cholesterol acetate, or for the formation of biopolymer particles charged with ketoprofen and indometacin. It has been reported that the mean diameter of the particles ranged between 0.1 and 2 μm and the residual solvent was less than 50 ppm.

In the apparatus used by Chattopadhyay et al. for the precipitation of particles the extraction of the solvent from emulsions was carried out in an electrically heated stainless-steel extraction column. The SCF fluid delivery system consisted of a liquid CO₂ pump which provided SC-CO₂ to the bottom of the extraction column through a frit. The emulsion was delivered from the top countercurrently, using an HPLC pump, and was injected through a capillary nozzle, which broke the emulsion into droplets, thereby increasing its surface area of contact with SC-CO₂. After the contact with SC-CO₂, an aqueous particles suspension was formed at the bottom of the column and removed through a needle valve. The effluent SC-CO₂ was vented from the top of the column. The pressure inside the column was maintained constant using a backpressure regulator valve.

A different process layout for the extraction of the emulsion organic phase using SC-CO₂ was also proposed by Della Porta and Reverchon (Della Porta G. et al., 2010, Della Porta G. and Reverchon E., 2008). The apparatus proposed by Della Porta and Reverchon for the precipitation of particles in the supercritical fluid extraction operated in batch mode. The emulsion was placed into a cylindrical stainless steel vessel. SC-CO₂, delivered using a high pressure diaphragm pump, was bubbled into the extraction vessel, through a cylindrical stainless steel porous dispenser located at the bottom of the extractor. The dispenser maximizes the contact between the two phases during the extraction. Temperature was controlled using an air-heated thermostated oven. The pressure inside the reactor was controlled by a micrometric valve located downstream the extractor. A separator located downstream the extractor was used to recover the liquid solvent extracted and the pressure in the separator was regulated by a backpressure valve. At the exit of the separator, a rotameter and a dry test meter were used to measure the CO₂ flow rate and the total quantity of CO₂ delivered, respectively. When the extraction process was complete, the microspheres suspension produced was removed from the bottom of the extractor vessel for analysis and further processing.

Mazzotti and co-workers (Kluge J. et al., 2009a, Kluge J. et al., 2009b) also proposed the use of SC-CO₂ for the production of particles of pure PLGA and PLGA loaded with lysozyme or ketoprofen through supercritical fluid extraction of emulsions. Particles with average sizes ranging between 0.1 μm and a few μm with very narrow size distributions were produced. In the layout proposed by Mazzotti and co-workers for supercritical fluid

extraction of emulsions CO₂ was drawn from a dip tube cylinder and pre-cooled in a pressure module before being delivered to the reactor by a piston pump. The stream then passed a backpressure regulator above the desired reactor pressure, to reduce stream fluctuations generated by the piston pump. The emulsion was delivered to the reactor by an HPLC pump. Both streams were mixed at the inlet of the reactor in a two substance nozzle. The reactor was kept at the operating temperature by a thermostat. The particles were formed by solvent extraction from the organic emulsion droplets and remained suspended in the continuous water phase throughout the whole process. The product suspension accumulated at the bottom of the reactor was withdrawn through an outlet at the bottom of the reactor. The off-gas stream left the reactor through an outlet at the top. The pressure inside the reactor was controlled by a backpressure regulator located downstream, through which the off-gas stream was expanded to atmospheric pressure and was vented.

It has been shown that the average size of particles is clearly related to the average size of droplets in the original emulsion. The size of the emulsion droplets mainly depends on the mixing rate or the degree of homogenization and the concentration of surfactant or polymer. Generally, a high degree of homogenization, higher concentrations of surfactant and lower concentrations of polymer tend to produce smaller droplets. Therefore, precipitation of particles with different sizes can be accomplished by varying the emulsion formulations and by optimization of the solvent-surfactant system.

The SCF-based emulsion extraction is beneficial compared to the traditional emulsion evaporation/extraction. Indeed, SEE process combines the advantages of traditional emulsion based technology, namely control of particle size and surface properties, with the advantages of supercritical fluid extraction process, such as higher product purity and shorter processing times. Due to the enhanced mass transfer of SC-CO₂, this process has a relatively faster extraction rate compared to other conventional techniques (processing in minutes instead of several hours) and, thus, adds to the formation of relatively smaller particles with narrow size distributions. In the SEE process, microparticles aggregation phenomena are not observed, due to the presence of the external water phase, immiscible with SC-CO₂, which prevents their aggregation. High product purity and low content of residual solvents may be achieved at the same time, at moderate operating temperatures and with reasonable CO₂ consumption. One of the major limitation of the SEE process, in these discussed configuration, is that the process remains intrinsically discontinuous, sharing this inconvenient with traditional solvent evaporation/extraction processes. Indeed, a batch of emulsion can be treated for each run with problems of repeatability of the batches and reduction of the process yield, due to the material lost. For this reason Della Porta and Reverchon (Della Porta G. et al., 2011b) suggested

also the possibility of a continuous process layout (SEE-C) where the SC-CO₂ is continuously contacted with an O/W emulsion in a column to extract the organic solvent without interacting with dispersant phase. At the bottom of the column, a suspension of microstructured particles can be continuously collected. The SEE-C continuous layout has been used during this thesis.

Chapter VII

Supercritical Emulsion Extraction Continuous Process for Monodisperse Particles Production

VII.1 Introduction

In biomedical and pharmaceutical field, particles ranging between 100-500 nm are generally indicated as nanoparticles (De Jong W.H. and Borm P.J.A., 2008) though more restrictive definitions assume smaller dimensions as the limit for nanoparticles production (Reverchon E. and Adami R., 2006). The development of such microdevices poses a serious challenge, due to the lack of robust manufacturing techniques, that can provide particles with predictable and controllable size distribution, composition and structure. They have also to conform to rigorous requirements of product consistency, purity and process scalability (Chattopadhyay P. et al., 2006). It is particularly relevant to produce submicro or nanoparticles with very narrow particle size distributions (PSD) since, in that case, fluid dynamic and therapeutic behavior of all the particles would be similar to those having the mean diameter of the distribution and an ideal performance will be obtained. The polydispersity index (PDI) is a parameter that measures the dispersion of particles around the mean diameter, it is the ratio between the standard deviation (SD) and the mean diameter (MD) of the distribution of particles; the lower is the PDI, the sharper is the distribution. An optimum condition is reached when PDI is lower or equal to 0.1; in this case the system is defined as monodisperse; i.e., all the particulate system can be treated as formed by particles of the same dimensions.

Different conventional methods have been reported for the preparation of micro and nanoparticles with different PDI, including dispersion

polymerization (Zhang X. et al., 2008), nanoprecipitation (Barichello J.M. et al., 1999), solvent evaporation of emulsions (Feng S.S. and Huang G.F., 2001), spray drying (Vehring R., 2008). These techniques show some drawbacks, such as the difficulty in the removal of toxic solvents (Freitas S. et al., 2005, Odonnell P.B. and McGinity J.W., 1997) and low encapsulation efficiency (Li M. et al., 2008), batch processing.

The SEE process has been successfully used for the production of microspheres, overcoming most of the common drawbacks of the conventional techniques. However, monodisperse sub-micro, nanoparticles of biopolymer suitable for pharmaceutical formulations have not been produced until now.

Therefore, the aim of this part of the work is to demonstrate that SEE-C technology can produce very sharp or even monodisperse biopolymer submicro or nanoparticles. To obtain this result emulsion formulation parameters are tested, such as, surfactant concentration and biopolymer percentage in the oily phase, and different emulsification techniques (ultrasound or high speed emulsification) and their interactions with SEE-C processing are tested to obtain small droplets dimensions from the microsize to the nanosize range. *Poly-lactic-co-glycolic acid* (PLGA), *poly-lactic acid* (PLA) and *poly-caprolactone* (PCL) are the polymers tested to produce these micro and nano devices. SEE-C operative conditions are optimized to control the micro and nanodevice sizes and distributions, as well as, the solvent residue. The produced particles are characterized by morphology, size and poly-dispersity index.

VII.2 Materials and methods

VII.2.1 Materials

CO₂ (99.9%, SON, Naples, Italy), polyvinyl alcohol (PVA, MW: 30.000–55.000), acetone (Ac, purity 99.9%), glycerol (GLY, purity 99%) and poly-caprolactone (PCL, MW: 14.000), were purchased from Aldrich Chemical Co.. Poly-lactic acid (PLA, MW: 28.000, Resomer R 203H), PLGA (PLGA, 75:25 MW: 20000, Resomer RG 752S) were provided by Boehringer and used as received.

VII.2.2 Emulsion preparation

To obtain a stable emulsion using acetone as the oily phase, glycerol was added in the external water phase. Indeed, it is known from the literature that when acetone, water, and glycerol are mixed, two phases can be formed due to phase separation in an appropriate (and relatively narrow) composition range; for an emulsion formulation, the ternary mixture composition should lie in this region. In a previous work (Della Porta G. et al., 2011a) we

verified that the optimal emulsion composition was O:W ratio 20:80 with the water phase formed by a solution of aqueous glycerol (20:80 of water:glycerol); this emulsion ratio was used also in this work. A known amount of polymer (from 1 to 10% w/w) was dissolved into 20 g of acetone to form an organic solution. Then, the solution was added into 80 g of aqueous glycerol (20/80 w/w) PVA solution to form an emulsion using a high-speed stirrer (mod. L4RT, Silverson Machines Ltd. Waterside, Chesham Bucks, UK) and in some experiments the emulsion obtained in this way was, then, sonicated to reduce the size of the droplets (Digital Sonifier Branson mod. 450, ½" diameter micro-tip, 20 kHz, nominal power 400 Watt).

80 gr of the prepared emulsion were processed using the SEE-C apparatus described in the previous chapter. Conventional Liquid Emulsion Extraction (LEE) of the oily solvent was performed for comparison purposes. Typically, the remaining 20 g of emulsion was charged in a beaker and the solvent was extracted adding dropwise 60 g of aqueous-glycerol (ratio 50:50 water/glycerol), the resulting solution was stirred for 80 min at 400 rpm; subsequently, 40 g of pure water were added dropwise and the extraction was performed at the same stirring conditions for other 100 min.

Particles were recovered from the suspension by centrifugation at 6500 rpm for 45 minutes and washed with distilled water. They were then recovered by membrane filtration (porosity: 0.1 or 0.4 μm).

VII.2.3 Analytical methods

The morphology of the produced particles were studied using a Field Emission-Scanning Electron Microscope (FE-SEM mod. LEO 1525; Carl Zeiss SMT AG, Oberkochen, Germany). A sample of powder was dispersed on a carbon tab previously stuck to an aluminum stub. Samples were coated with gold (layer thickness 250Å) using a sputter coater (mod.108 A, Agar Scientific, Stansted, UK). Particles size distributions (PSD) were measured by dynamic light scattering by using a Malver Zeta Sizer instrument (mod. Zetasizer Nano S, Worcestershire, UK). 1 mL of the produced suspension was used for each test without any further dilution step.

Acetone residues in the suspensions were measured to determine the efficiency of the SEE process in solvent removal. Solvent residues were measured using a head space sampler (mod. 50 Scan, Hewlett & Packard) coupled to a gas chromatograph interfaced with a flame ionization detector (GC-FID, mod. 6890 Agilent Series, Agilent Technologies Inc). The solvent was separated using a fused-silica capillary column 30 m length, 0.55 mm internal diameter, 0.1 μm film thickness (mod. DB-WAX). Oven temperature in the GC was set to 45°C for 10 min, then 15°C/min until 150°C. The inlet temperature was set at 250°C, detector at 270°C. Helium was used as carrier gas (5mL/min), split mode ratio 1:10. Head space

conditions were: vial temperature 95°C, loop temperature 95°C, transfer line temperature 105°C. Head space samples were prepared in 10 mL vials filled with 1 mL of suspension. All measurements were performed in triplicates.

VII.2.4 Experimental continuous apparatus description

Process equipment consists of a high pressure packed column where gas and liquid phases (SC-CO₂ and emulsion) are contacted counter currently and mass transfer between the two phases is improved by the internal packing elements.

A schematic representation of SEE-C process is illustrated in **Figure VII. 1**.

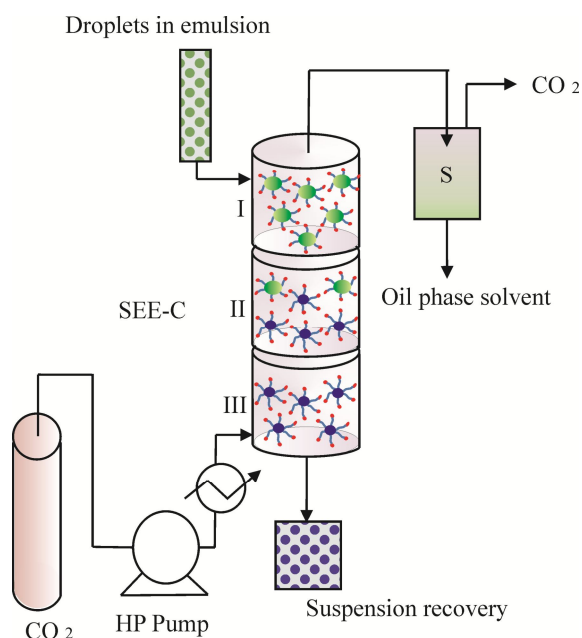


Figure VII. 1 Schematic representation of SEE-C process (Della Porta G. et al., 2011a).

The SEE-C apparatus mainly consists of a 1680 mm long column with an internal diameter of 13.11 mm. The column is packed with stainless steel packings 4 mm nominal size with 1889 m⁻¹ specific surface and 0.94 voidage (0.16-inch Pro-Pak, Scientific Development Company, State College, PA, USA), and is formed by five AISI 316 cylindrical sections connected by 4-port elements. The extraction stages are three. The apparatus is thermally insulated by ceramic cloths and its temperature is controlled by six controllers (Series 93, Watlow, Milan, Italy) inserted at different heights of the column. SC-CO₂ is fed at the bottom of the column by a high-pressure diaphragm pump (mod. Milroyal B, Milton Roy, Pont Saint-Pierre, France)

at a constant flow rate. The emulsion is taken from a reservoir and delivered from the top of the column, using a high pressure piston pump (mod. 305; Gilson, Villiers-le-Bel, France), at a constant flow rate. Particles formation in emulsion is achieved by removal of the internal organic oil phase from the emulsion droplets by extraction using SC-CO₂. A separator located downstream the top of the column is used to recover the extracted “oily” solvent and the pressure in the separator is regulated by a backpressure valve (26-1700 Series, Tescom, Selmsdorf, Germany). At the exit of the separator, a rotameter (mod. N5-2500, ASA, Sesto San Giovanni, Italy) and a dry test meter (mod. LPN/S80AL class G2.5, Sacofgas, Milan, Italy) are used to measure the CO₂ flow rate and the total amount of CO₂ delivered, respectively. The microspheres suspension is continuously removed from the bottom of the extraction column by decompression, using a needle valve (mod. SS-31RS4, Swagelok, Brescia, Italy). A detailed representation of the SEE-C process layout is reported in **Figure VII. 2**:

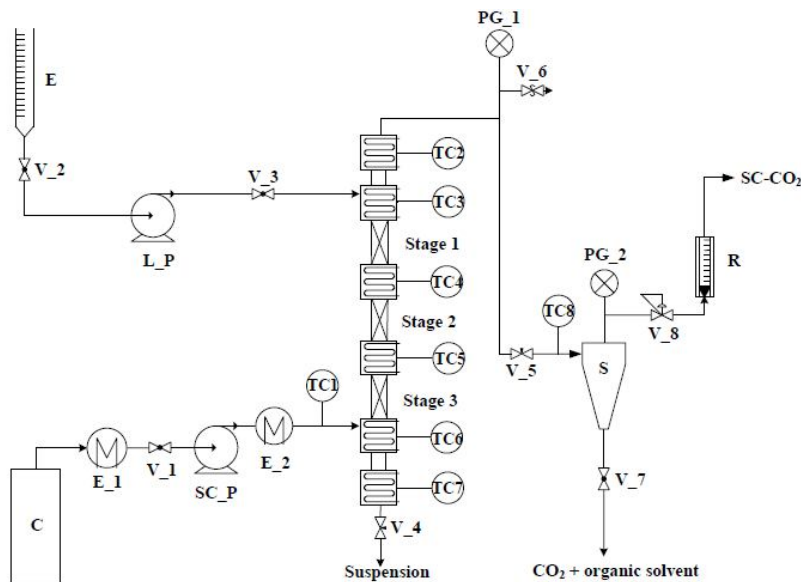


Figure VII. 2 Continuous tower diagram: C, CO₂ supply; E, emulsion supply; PG₁ and PG₂, pressure gauges; SC_P, diaphragm pump used for high pressure SC-CO₂; L_P, piston pump used for the emulsion; TC1...TC8, thermocouples; S, separator; R, rotameter; E₁ and E₂, heat exchangers; V₁...V₈, valves (Falco N. et al., 2012)

The start-up of the extraction process begins delivering SC-CO₂ from the bottom of the column until the operating pressure is reached. Then, the emulsion delivery is started at the top of the column. At the end of each run, the column is washed with distilled water to eliminate any processing

residue from the packing surface. After the SEE-C experiment, particles are recovered from the suspension and separated from the surfactant by centrifugation with a large volume of distilled water at a rotation speed of 4500 rpm for 45 min. Then, the supernatant is discharged and particles are re-suspended in pure water, recovered by membrane filtration and dried at air for further processing.

VII.3 Results & discussion

VII.3.1 Definition of SEE-C operative conditions

SEE-C operating conditions of pressure and temperature were chosen to allow the selective extraction of acetone from the oily phase of the emulsion. Considering the high pressure vapor-liquid equilibrium diagram (VLE) of the system acetone/CO₂ (Sato Y. et al., 2010), that reports the equilibrium pressure/composition values at given temperature, the operating point was selected above the mixture critical point (MCP); i.e., at a pressure of 80 bar for a temperature of 38°C. This temperature is also compatible with the glass transition temperatures of the selected polymers. At these operative conditions the solubility of the glycerol-water external phase in SC-CO₂ is extremely small (Sabirzyanov A.N. et al., 2002, Sovova H. et al., 1997) and a selective extraction of the oily phase of the emulsions can be obtained. The counter-current operation in the packed column is also favored by large density differences between the two phases (liquid and SC-CO₂) involved in the process, since it allows the counter-current flow inside the column. In the case of a supercritical fluid, the lower is the pressure the lower is the fluid phase density and the larger is the density difference at a fixed temperature. At 38°C and at 80 bar, a large difference in density between the emulsion and SC-CO₂ is obtained, because densities are about 1 g/cm³ and 0.31 g/cm³, respectively. Another important operating parameter, to be taken into account when operating with a continuous extraction tower, is the liquid to gas ratio (L/G). Difficult separations are characterized by a very low L/G ratios; it means that high quantities of SC-CO₂ are necessary per unit of liquid treated to obtain the desired extraction efficiency (Brunner G., 2009). However, it is not possible to decrease freely the L/G ratio since, when very large flow rates of the gas stream are used, the liquid is entrained by the gas and flooding occurs determining the failure of the process. In our case, L/G ratio was fixed at 0.1, as a consequence of a previous optimization of the tower fluid dynamics (Falco N. et al., 2012). A CO₂ flow rate of 1.2 kg/h and an emulsion flow rate of 2.3 mL/min were used according to the previous discussion.

Another relevant process parameter in the continuous operation is the time required to obtain steady state conditions in the column. Indeed, during the continuous operation, mass transfer between the two phases is activated,

but, variations in the top and bottom product composition can be observed until steady state conditions have been obtained. Therefore, the SEE-C performance evaluations were always performed after reaching the steady state conditions. This initial phase of the process is also important to wet the column packing with the surfactant, that favors particles slipping on the packing surface. Indeed, the use of packed towers is commonly not suggested for processes involving the presence of a solid phase that could cover the packing surface, producing a reduction of the mass transfer and, then, the blockage of the column. However the dimensions of the microparticles produced in this work are always in the micronic or submicronic range; therefore, tend to remain suspended in the falling liquid film inside the column.

Operating in this manner, also very low solvent residues (less than 500 ppm) were measured in the recovered suspension, that are significantly lower than those that can be found after the conventional liquid emulsion extraction (LEE) (Della Porta G. et al., 2011a). Since the scope of this part of the thesis work is to produce submicro and nanoparticles of controlled size and distribution, some different emulsification procedures were also tested such as high speed emulsification coupled to ultrasonication steps, varying surfactant concentration and type and biopolymer content in the oily phase.

VII.3.2 PCL: Effect of sonication

The first emulsion parameter tested was the addition of a sonication step to the preliminary high speed emulsification. A synthesis of the results obtained is reported in the top part of **Table VII 1**. Since the preliminary stirring was very intense, when the emulsion with no sonication was processed by SEE-C, near monodisperse PCL particles were obtained (PDI \approx 0.1); but, the mean size of the particles dispersion was too large for the target of this study (MD = 619). Therefore, experiments with different sonication amplitudes and duration were performed. The mean diameter of the PCL particles was rapidly reduced to about one half with respect to the previous tests: 342 nm, operating at an amplitude of 30% for 1 min; but, the PDI increased to 0.16. A possible explanation is that the mechanical energy dissipated in the O/W system contributed to the breakage of the droplets, but gave also a contribution to the entropy of the system that was not counter balanced by a larger stability of the surfactant layer on the surface of the droplets. When, sonication amplitude and duration were furtherly increased, the mean size of the resulting particles was very similar to the one of the previous experiment (around 330 nm); but the PDI decreased to 0.11 for two minutes and to 0.10 for 60% amplitude sonication and 1 minute emulsification. It means that the length of the emulsification and the larger quantity of energy put in the starting emulsion, did not give a further

contribution to droplet diameters reduction, but contribute instead to surfactant layer stabilization. The best results in this series of experiments is obviously the one that give the smaller PDI producing monodisperse nanoparticles (60% amplitude sonication and 1 minute emulsification).

In this part of the work some liquid extraction (classical) tests (LEE) were also performed on the PCL emulsions previously discussed. The comparison between SEE-C and conventional results is reported in **Figure VII. 3** and, as expected, the PSD obtained by LEE is moved to larger particles and the particle size distribution is enlarged, when compared to the corresponding results obtained by SEE-C.

Table VII 1 Mean Diameter (MD) and poly-dispersity Index (PDI) of various biopolymers. O/W emulsion ratio 20:80; oily phase: Results obtained by LEE are also reported for comparison*.

	Polymer (%, w/w)	PVA (%, w/w)	Sonication %	sonication (min)	MD (nm)	PDI
PCL	1	1	---	----	619	0.10
	1	1	30	1	342	0.16
	1	1	30	2	332	0.11
	1	1	60	1	328	0.10
	5	1	30	1	342	0.19
	10	1	30	1	761	0.25
	1	0.6	30	1	864	0.15
	1	1	30	1	360	0.16
	1	2	30	1	263	0.12
	1	3	30	1	292	0.10
	1	4	30	1	294	0.12
PLGA	1	1	30	1	212	0.10
	5	1	30	1	761	0.25
PLA	1	1	30	1	233	0.07
	5	1	30	1	241	0.07
PCL*	1	1	30	1	710	0.30

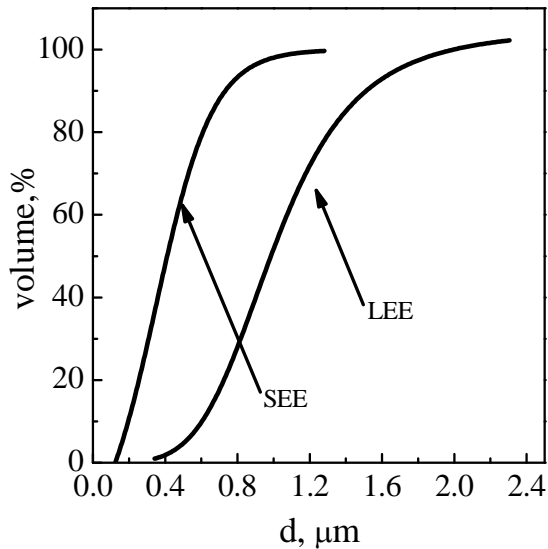


Figure VII. 3 Particle size distribution of particles suspensions obtained by SEE-C and by liquid emulsion extraction technology (LEE).

VII.3.3 PCL: effect of polymer percentage in oily phase

Another parameter that can influence the size of the droplet/particle dimensions of an emulsion is the content of solute in the disperse (oily) phase. Therefore, some experiments of emulsification plus continuous supercritical drying were performed using the base emulsion conditions and increasing the percentage of PCL from 1 to 10% w/w in acetone. Examples of the results obtained are reported in **Figure VII. 4**, where PCL microparticles from 1 and 10% w/w emulsions are shown. In both cases, non coalescing spherical particles were obtained; but, while at 1 % w/w PCL nanoparticles with a sharp PSD were obtained, operating at 10% w/w PCL submicro particles with MD of 761 nm were produced. It is clear that the increase of PCL percentage adversely affect either the diameter, either the PDI of the produced particles; the variation of this second relevant property of the particles is evident in **Figure VII. 4** and the PDI in Table 2 increases to 0.25.

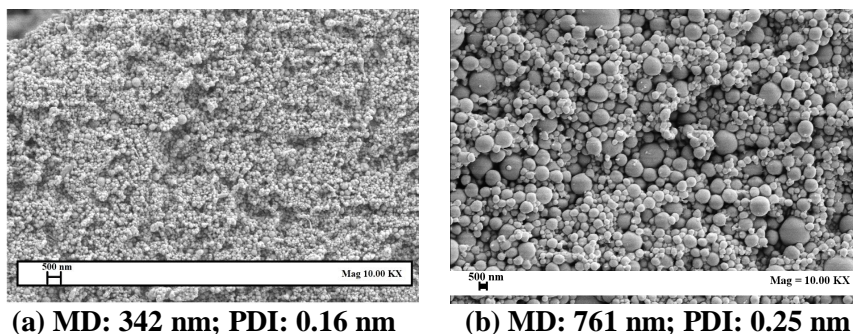


Figure VII. 4 SEM images of PCL nano and micro-particles obtained at different polymer concentration in the oily phase: (a) 1% w/w (b) 10% w/w and processed by SEE-C.

VII.3.4 PCL: effect of surfactant quantity

A series of experiments were performed, starting again from the base case, and modifying the surfactant (PVA) content from 0.6 to 4% w/w in the continuous water based phase. The results shown in **Table VII 1** demonstrate that up to a 2% w/w content, PVA largely reduces the mean size of the PCL particles; then, (up to 4% w/w) an asymptotic value of both MD and PDI is obtained. These results are reported in **Figure VII. 5** and **Figure VII. 6**. **Figure VII. 5** shows the comparison, not only in terms of MD, but reporting the whole quasi-Gaussian distributions obtained in these experiments. **Figure VII. 6** reports the MD against the PVA% in water and the asymptotic behaviour that originates at PVA% between 1 and 2% is evidenced. However, PDI in presence only of a large % of PVA, remains near the borderline of monodispersity ($PDI \approx 0.1$); i.e., the increase of PVA content does not induce a larger/uniform stabilization of the emulsion droplets around the mean value of the distribution. This effect is somewhat unexpected since it should be attended that a larger quantity of surfactant could allow the disperse phase to organize more uniformly: the larger availability of surfactant molecules should produce very similar droplets characterized by the same number of surfactant molecules around the oily droplet.

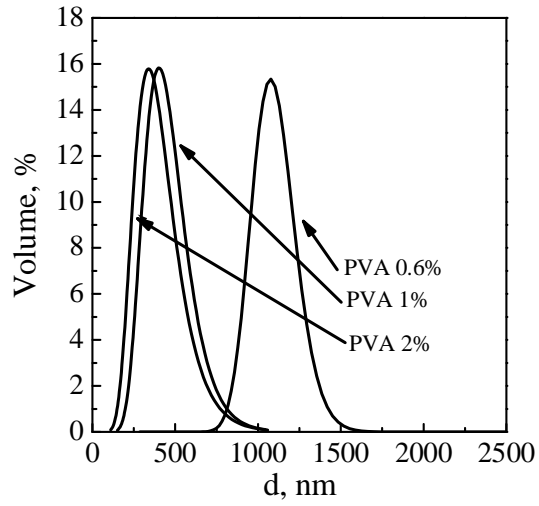


Figure VII. 5 Particle size distribution of the PCL suspensions obtained at different PVA concentrations in water phase (% w/w).

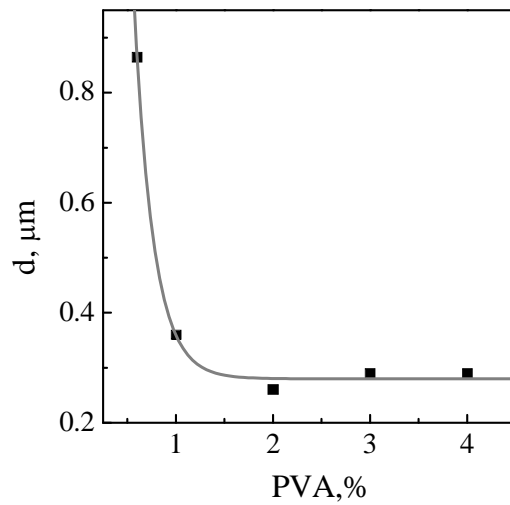
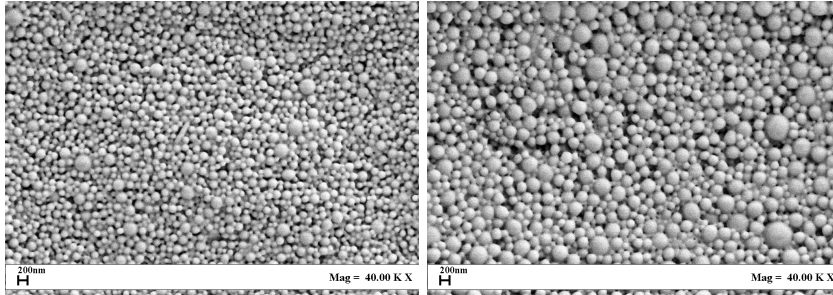


Figure VII. 6 Mean Diameter of PCL nanoparticles obtained at different PVA concentrations (% w/w), as surfactant of the water phase

VII.3.5 PLGA and PLA: effect of polymer percentage in the oily phase

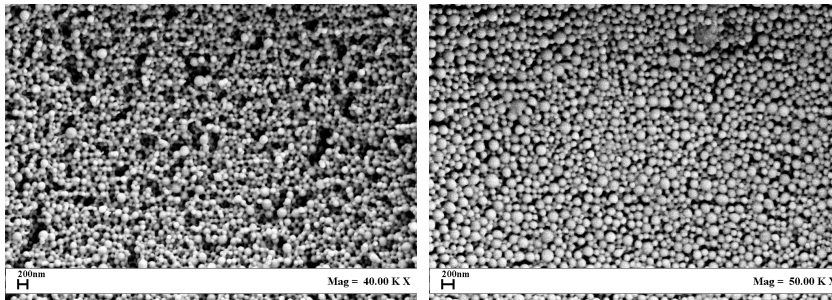
PLGA and PLA nanoparticles were also prepared. Different emulsion formulations were tested and processed by SEE-C fixing the biopolymer concentrations percentage at 1 and 5% w/w, in oily phase, respectively and the PVA concentration in the external water phase at 1% w/w; the sonication amplitude used was of 30% for 1 min. The results of this part of the study are also summarized in **Table VII 1**, in terms of MDs and PDIs of the produced nanoparticles. PLGA showed a very large increase of MD and PDI, with a MD variation from 212 nm (PDI 0.10 nm) to 761 nm (PDI of 0.25 nm) varying the PLGA content from 1 to 5% w/w, respectively. On the contrary, PLA was practically insensitive to this parameter, in the same range explored. Indeed, PLA particles with mean diameters of 240 nm and PDI of 0.07 nm were produced in both cases. This effect is well evidenced in **Figure VII. 7 a-b** and **Figure VII. 8 a-b** where, SEM images of the PLGA and PLA, nanoparticles are reported, respectively, with the same enlargement. From **Figure VII. 7 a-b**, it is possible a qualitative evaluation of the increase of the MD and PDI, when the PLGA concentration was varied from 1 to 5% w/w; whereas, the two images reported in **Figure VII. 8 a-b** confirmed the absence of an evident size difference between the PLA nanoparticles, produced at different polymer concentration. Moreover, in the case of PLA, a PDI values of 0.07 was always obtained. Why PLGA and PLA based emulsions shown this different behaviour with the polymer percentage variation and, particularly, why PLA was insensitive to this parameter? We excluded an effect of the molecular weight of the two polymers because the weights used are very close (see methods section). A possible explanation can be the different (equilibrium) solubility of the two polymers in acetone; therefore, if PLA is largely more soluble than PLGA (and PCL), its percentage variation used in the present work could not influence the droplet formation and could justify also the smallest PDI observed. As a consequence, we may also conclude that, fixed the others parameters of emulsion formulation, when the oily phase is prepared as a diluted system, the polymer concentration will not more influence the droplet dimension and monodispersed nanoparticles can easily be obtained.



(a) MS: 212 nm; PDI: 0.13

(b) MS: 761 nm; PDI: 0.25

Figure VII. 7 SEM images of PLGA nanoparticles obtained at different polymer concentrations in the oily phase by SEE-C: (a) PLGA in oily phase of 1% w/w (b) PLGA in oily phase of 5% w/w. Other emulsion data: oil-in-water emulsion, PVA 1% w/w; ultrasounds operating at amplitude of 30% for 1 min.



(a) MS: 233 nm; PDI: 0.07

(b) MS: 241 nm; PDI: 0.07

Figure VII. 8 SEM images of PLA nanoparticles obtained at different polymer concentrations in the oily phase by SEE-C: (a) PLA in oily phase of 1% w/w (b) PLA in oily phase of 5% w/w. Other emulsion data: oil-in-water emulsion, PVA 1% w/w; ultrasounds operating at amplitude of 30% for 1 min.

VII.4 Conclusions

SEE-C technology confirmed the possibility of the continuous fast processing of emulsions, eliminating the problems of droplets coalescence and solvent residues. As a consequence, the nanoparticles obtained showed diameters and distributions very near to that of the corresponding droplets in emulsion and it was possible to work directly to the optimization of the

droplets size and distribution to produce nanoparticles with a strictly control of their PDI. This target was not simple to be obtained and only the optimization of several emulsion processing parameters together with SEE-C operative conditions allowed the production of monodisperse or near monodisperse nanoparticles of the various polymers processed. Different polymers also shown different behaviors to the emulsion formulation parameters; indeed, different PLGA concentrations in the oil phase generated very different MDs and PDIs of the particle; whereas, in the case of PLA processing, the size of the nanoparticles obtained was not really sensitive to this parameter. The observed phenomenon could be only slightly related to the polymers molecular weight (that were almost similar), but could be connected to the different polymer solubility in acetone.

Chapter VIII

Biopolymer particles for proteins and peptides sustained release produced by Supercritical Emulsion Extraction

VIII.1 Introduction

Proteins possess small half-lives and are not capable to diffuse through biological membranes. Their instability in the stomach and intestine makes oral delivery of these drugs difficult. Alternative administration by frequent injections is also tedious and expensive. Therefore, the development of biodegradable polymeric microspheres has been seen as a promising way to overcome the administering problems of these macromolecules (Yang Y.Y. et al., 2000). A vehicle is needed capable of encapsulating proteins, minimizing the mechanisms of degradation and maximizing the in vivo activity, and providing controlled release that can be delivered via parental administration is needed.

Proteins and GFs controlled release from particulate devices has been widely reported in the literature (Determan A.S. et al., 2004). Frequently, these delivery systems were based on natural polymers, such as gelatin and alginate (Park H. et al., 2005, Gu F. et al., 2004). Particulate systems based on these polymers are able to encapsulate GFs with minimum loss of bioactivity of the encapsulated molecule. However, they lack the capacity to provide long-term release, particularly when formed as nanoparticles. These limitations can be overcome by particulate systems based on biodegradable polyesters (i.e., PLA, PLGA) (Slager J. and Domb A.J., 2002).

Protein and GFs encapsulation in biodegradable polyesters microspheres is still a challenging task due to stability issues occurring during microsphere-processing, shelf-life and protein release. Techniques to entrap

protein in biopolymeric microspheres are all joined by the common aim of realizing experimental conditions as mild as possible (Freitas S. et al., 2005, Sinha V.R. and Trehan A., 2003). Indeed, few sustained release therapeutic protein products based on biodegradable polymers have received FDA approval due to the inherent instability of proteins when they are exposed to the conditions normally encountered during microparticle fabrication using conventional techniques. Other problems encountered are low encapsulation efficiencies and high burst release of the drug. For many therapeutic proteins achieving an acceptable dose volume (i.e., high drug content) while maintaining satisfactory release kinetics (i.e., minimal burst, acceptable duration) represents a very significant formulation challenge (Zheng C.-H. et al., 2004).

The SEE-C technology has a great potential regarding the field of protein encapsulation thanks to the mild extraction condition and the short process time.

For these reasons, the objective is to demonstrate that it is possible to apply the SEE-C to the production of biopolymeric micro and nanoparticles encapsulating peptides and proteins starting from double emulsion. Bovine serum albumin (BSA) has been selected as model protein while Vascular Endothelial Growth Factor (VEGF) and Bone Morphogenetic Proteins BMP has been used as peptide.

VIII.2 Materials and Methods

CO₂ (99.9%, SON, Naples, Italy), polysorbate (Tween 80, Aldrich Chemical Co.), Ethylacetate (EA, purity 99.9%, Aldrich Chemical Co.), distillate water, PLGA (50:50 MW: 38,000 Da, Resomer RG 504H; Boehringer, Firence, Italy), PLA, (MW: 28.000 Da, Resomer R 203H, Boehringer, Firence, Italy) were used as received. Bovine pancreas albumin (BSA, purity 99.9%) was obtained by Sigma-Aldrich Co. (Milan, Italy), h-VEGF (recombinant) and h-BMP-2 were supplied from PeproTech.

VIII.3 Emulsion preparation and SEE-C operative conditions

w-o-w emulsions for the encapsulation of BSA (w-o-w ratio: 1.5:28.5:170 w/o/w) were prepared using 1mL of water/PVA solution (0.04% w/w of PVA), as internal water phase, in which BSA was dispersed at 0.5% w/w, that was added into polymer/EA solutions (1-10% w/w of PLGA or PLA) and sonicated using the Digital Sonifier Branson (mod. 450, ½” diameter micro-tip, 20 kHz). The primary w-o emulsion was, then, added into water Tween80 (0.6% w/w Tween80) solution to form the secondary emulsion using a high-speed stirrer (mod. L4RT, Silverson Machines Ltd., Waterside, Chesham Bucks, UK). w-o-w emulsions for the encapsulation of VEGF and BMP were produced following the same procedure described

above, adding in the water internal solution of BSA and PVA the VEGF and BMP at a concentration of 10 μ g/mL. 200 mL of emulsions were prepared each times and processed with the SEE-C technique.

The extraction condition were 80 bar 38°C, liquid to gas ratio L/G 0.1. Before feeding the emulsion, the tower was conditioned with 30 mL of Tween80 aqueous solution, then was fed the emulsion. The bottom products recovered at different times were collected and mixed together. At the end of each run, particles suspension was washed several times by centrifugation with distilled water, recovered by membrane filtration, and dried at air

VIII.4 Droplets and Particles Morphology and Size Distributions

Field Emission-Scanning Electron Microscope (FE-SEM, mod. LEO 1525; Carl Zeiss SMT AG, Oberkochen, Germany) was used to study the morphology of the produced microspheres. A sample of powder was dispersed on a carbon tab previously stuck to an aluminum stub. Samples were coated with gold (layer thickness 250Å) using a sputter coater (mod.108 A, Agar Scientific, Stansted, UK). Droplet size distributions (DSD) and particle size distributions (PSD) of microparticles were measured by dynamic light scattering (DLS, mod. Mastersizer S, Malvern Instruments Ltd., Worcesterstershire, UK). PSD and DSD of nanoparticles were measured by DLS using a Malver Zeta Sizer instrument (mod. Zetasizer Nano S, Worcesterstershire, UK).

VIII.5 Protein loading determination

The amount of BSA loaded into the microspheres was monitored using the procedure described by Bilati et al.(Bilati U. et al., 2005a). Briefly, 10 mg of dried microspheres were dissolved in 600 μ L of acetonitrile in centrifuge tubes and sonicated until the complete transparency of the solution. Then, 1400 μ L of water containing 0.1% TFA (0.1% aqueous TFA solution) were added dropwise to the corresponding centrifuge tube to dissolve BSA. The remaining undissolved polymer was separated by centrifugation at 2000 rpm for 2 minutes. The resulting clear supernatant solution was directly analyzed at room temperature by HPLC (model 1200 series; Agilent Technologies Inc.) equipped with a LiCrosphere C18 column (250 \times 4.6 mm), packed with 5 μ m particles size of 100 Å pore size. The mobile phase was composed of acetonitrile/water mixture (32:68 v/v) containing 0.1% v/v TFA. The flow rate was 0.9 mL/min, the injection volume of the test sampled was 40 μ L and the detecting wavelength was 214 nm. The amount of BSA in solution was calculated by means of a calibration curve and then converted in the effective BSA loading as the amount (mg) of

BSA charged in microspheres (g). Encapsulation efficiency (EE) is the ratio of the final BSA loading to the nominal one.

VIII.6 Results and discussion

VIII.6.1 BSA encapsulation study

Micro and nanoparticles of PLGA and PLA loaded with BSA were produced using a double emulsion w/o/w with a water internal phase with different BSA (2.5-5 mg/mL) and PVA (0.04% w/w). All the data related to experiments shown in this chapter are reported in **Table VIII. 1**. In the case of microparticle production, the oily dispersed phase was formed by a polymer solution in ethyl acetate at 10% w/w. The water external phase was formed by water saturated with ethylacetate plus Tween80 as surfactant (0.6% w/w). The primary emulsion w/o was obtained by ultrasonication. Then the primary emulsion was added to the external water by a rotative system at 3300 rpm for 6 minutes. The emulsion prepared was processed with the SEE technique. Optical image of the emulsion prepared with 10% PLA and BSA loading 2.5 mgr/gr of polymer is reported in **Figure VIII. 1**, where also SEM image of particles obtained after the supercritical extraction is reported. The emulsion is stable with well defined droplets. Particles obtained after the solvent removal are spherical and non coalescing. DSD and PSD are compared in the same graph in **Figure VIII. 1**. After the SEE process it is typical a shrinkage of the DSD due to the removal of the solvent, thus final PSD is always smaller and narrower than DSD, as also shown in the figure for this specific case.

Table VIII. 1 *Sample description of experiment discussed in this chapter. PSD data and efficiency of recovery (%) are also reported. SEE opetarive conditions: 80 bar, 38°C, L/G 0.1*

Sample	Description	D₁₀; D₅₀; D₉₀ (µm)	Recovery%
F2	PLGA 10% BSA 2.5 mg/g	D ₁₀ 1.4; D ₅₀ 2.6; D ₉₀ 4.8	90%
F3	PLGA 10% BSA 2.5 mg/g VEGF 10 µg/g	D ₁₀ 1.6; D ₅₀ 2.7; D ₉₀ 4.1	90%
F4	PLGA 10% BSA 2.5 mg/g BMP 10 µg/g	D ₁₀ 1.4; D ₅₀ 2.6; D ₉₀ 4.6	90%
F5	PLGA 10% BSA 2.5 mg/g VEGF 10 µg/g BMP 10 µg/g	D ₁₀ 1.3; D ₅₀ 2.7; D ₉₀ 4.9	90%
F7	PLGA 5% BSA 5 mg/g	D ₁₀ 0.1; D ₅₀ 0.4; D ₉₀ 1.1	95%
F8	PLA 5% BSA 5 mg/g	D ₁₀ 0.2; D ₅₀ 0.3; D ₉₀ 0.8	90%
F9	PLA 10% BSA 5 mg/g	D ₁₀ 0.8; D ₅₀ 1.9; D ₉₀ 4.1	90%
F10	PLGA 10% BSA 5 mg/g	D ₁₀ 1.3; D ₅₀ 2.5; D ₉₀ 4.9	91%

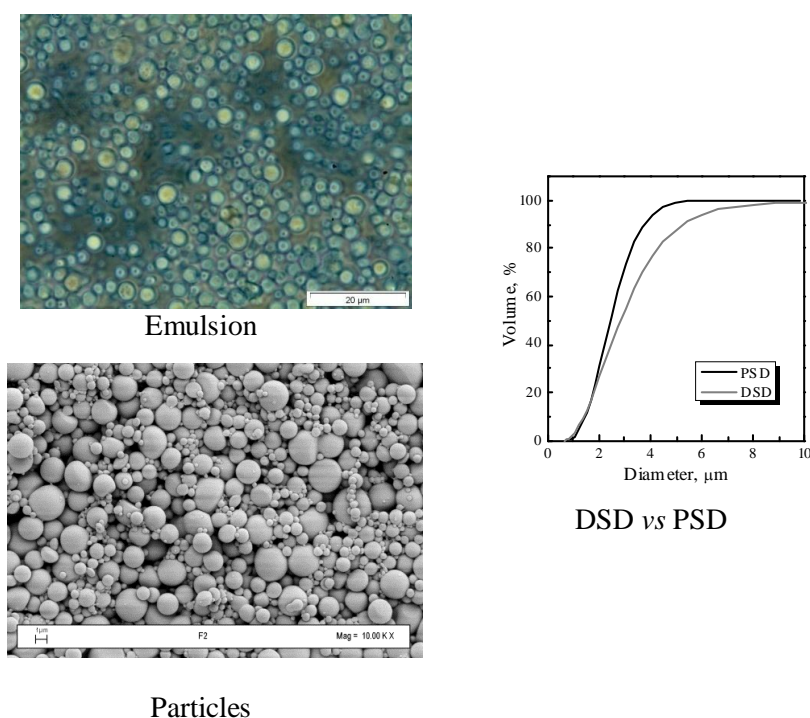


Figure VIII. 1 Optical image of the emulsion and SEM image of particles obtained after the SEE process (PLGA 10%, BSA 2.5 mg/gr). DSD and PSD are also reported for comparison.

PLGA microparticles were charged with different BSA loading to study the effect on the encapsulation efficiency. BSA 2.5 mg/g and 5 mg/g was charged with respect to the polymer. SEM images of particles obtained after the SEE process are reported in **Figure VIII. 2** where also cumulative PSD are plotted together for comparison. Particles with a mean size around 2.5 μm are obtained independently from the BSA loading. In both cases spherical and not aggregated particles are obtained after the SEE process. Furthermore, high recovery of particles has been obtained, as shown in **Table VIII. 1**.

Microparticles of PLA were also produced for the encapsulation of BSA, to investigate the behaviour of another important biopolymer commonly used for controlled drug delivery. Results are shown in **Figure VIII. 3**, for the case of BSA loading of 5 mg/g of polymer. Emulsions produced were both stable with non coalescing droplets, no great changes in DSD were observed when the two different polymers were used, as also shown in the

optical microscope images of the emulsion of sample F9 (PLA 10% in the oil phase) and F10 (PLGA 10% in the oil phase). Smaller particles has been produced in the case of PLA (MD 1.88 μm) see **Table VIII. 1** and **Figure VIII. 3**, thus a larger shrinkage effect has been reported in the case of sample F9. This result can be explained considering the different molecular weights of the polymer tested. PLA used has a lower molecular weight of PLGA, thus smaller particles can be expected due to the reduced viscosity of the oil phase obtained using this polymer.

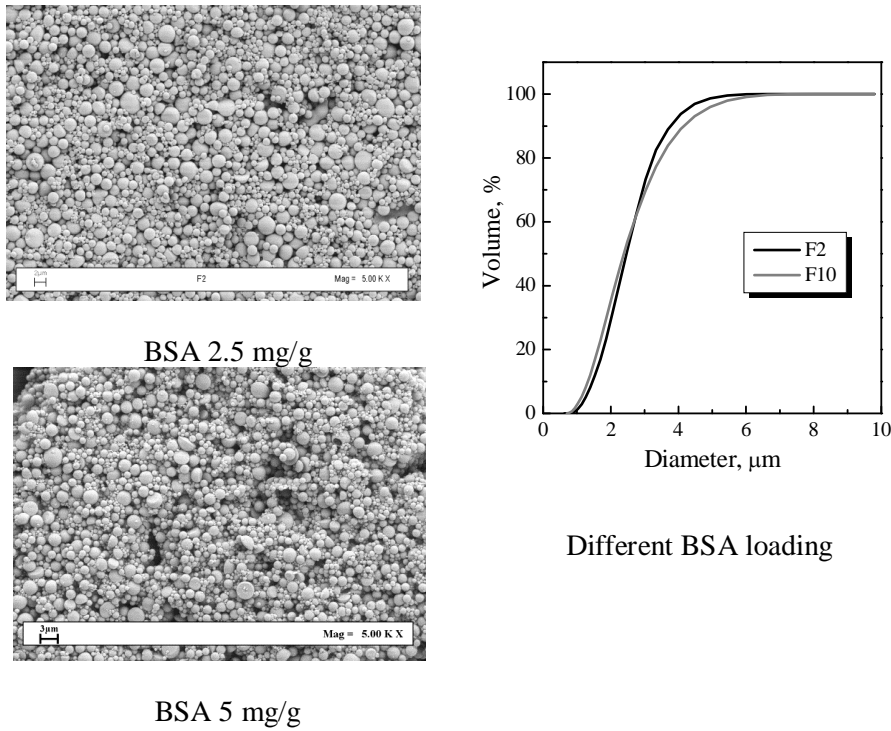


Figure VIII. 2 SEM images and PSD of particles of PLGA microparticles obtained with different BSA loading produced with PLGA 10% w/w in the oil phase.

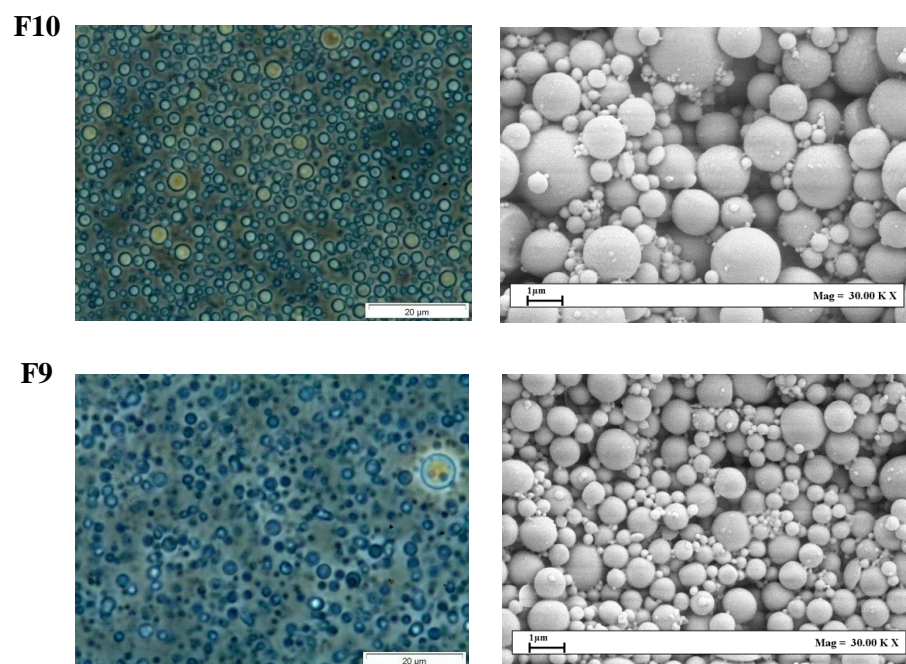


Figure VIII. 3 *Optica images and SEM images of emulsions and particles produced with 10 % of PLA (F9) and PLGA (F10) and BSA loaded at concentration of 5 mg/g.*

Also submicro particles of PLA and PLGA were produced; the oily phase was formed by a polymer solution in ethyl acetate at 5% w/w. The primary w/o emulsion was obtained again by ultrasonication. Then, it was added to the external water phase by a rotative system operating at 6000 rpm for 6 minutes. At the end the final emulsion was sonicated again at 30% amplitude for 2 minutes. Examples of FE-SEM images of nanoparticles of PLGA and PLA with BSA loading of 5 mg/gr of polymer obtained after SEE-C processing are reported in *Figure VIII. 4*, respectively.

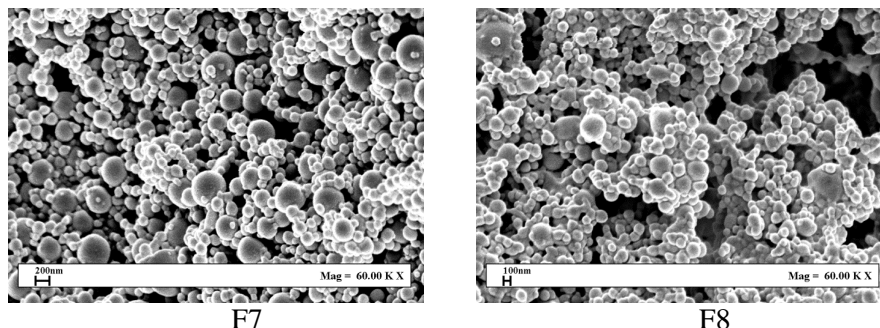


Figure VIII. 4 SEM images of submicroparticles obtained with PLGA (F7) and PLA (F8) at a concentration of 5% w/w in the oil phase and BSA loading of 5 mg/g.

Submicroparticles with a MD around 350 nm were obtained using a lower amount of polymer and different emulsification conditions (i.e. speed and ultrasonication). All the samples prepared with this technique

VIII.6.2 GF encapsulation study

Microparticles of PLGA loaded with GFs were produced using the same emulsion described in the case of BSA encapsulation in PLGA microparticles; a double emulsion w/o/w was used in which in the internal water phase at the aqueous solution of BSA (2.5 mg/mL) was added 20 ug/mL of VEGF (F3), or BMP (F4) and BMP/VEGF in the ratio 1/1. BSA also acts as stabilizing and protecting agent for the growth factor. The oil phase was composed of a polymeric solution in ethyl acetate at 10% w/w of PLGA. The water external phase was formed by water saturated with ethylacetate plus Tween80 as surfactant (0.6% w/w). The primary emulsion w/o was obtained again by ultrasonication. Then the primary emulsion was added to the external water phase and the emulsion was obtained agitating the system at 3300 rpm for 6 minutes.

Figure VIII. 5 shows optical images of the emulsions obtained and corresponding SEM images of particles obtained after SEE process. Samples with only BSA loaded (F2) is also reported for comparison. The process is very reproducible, very similar emulsions were obtained in all the cases and consequently particles with an omogeneuos and reproducible PSD were produced as shown also in **Figure VIII. 6**. Particles with mean diameters in the range 2.4-2.7 μm were obtained as also shown on **Table VIII. 1**. in conclusion the different GF loading did not affect the PSD of microspheres obtained.

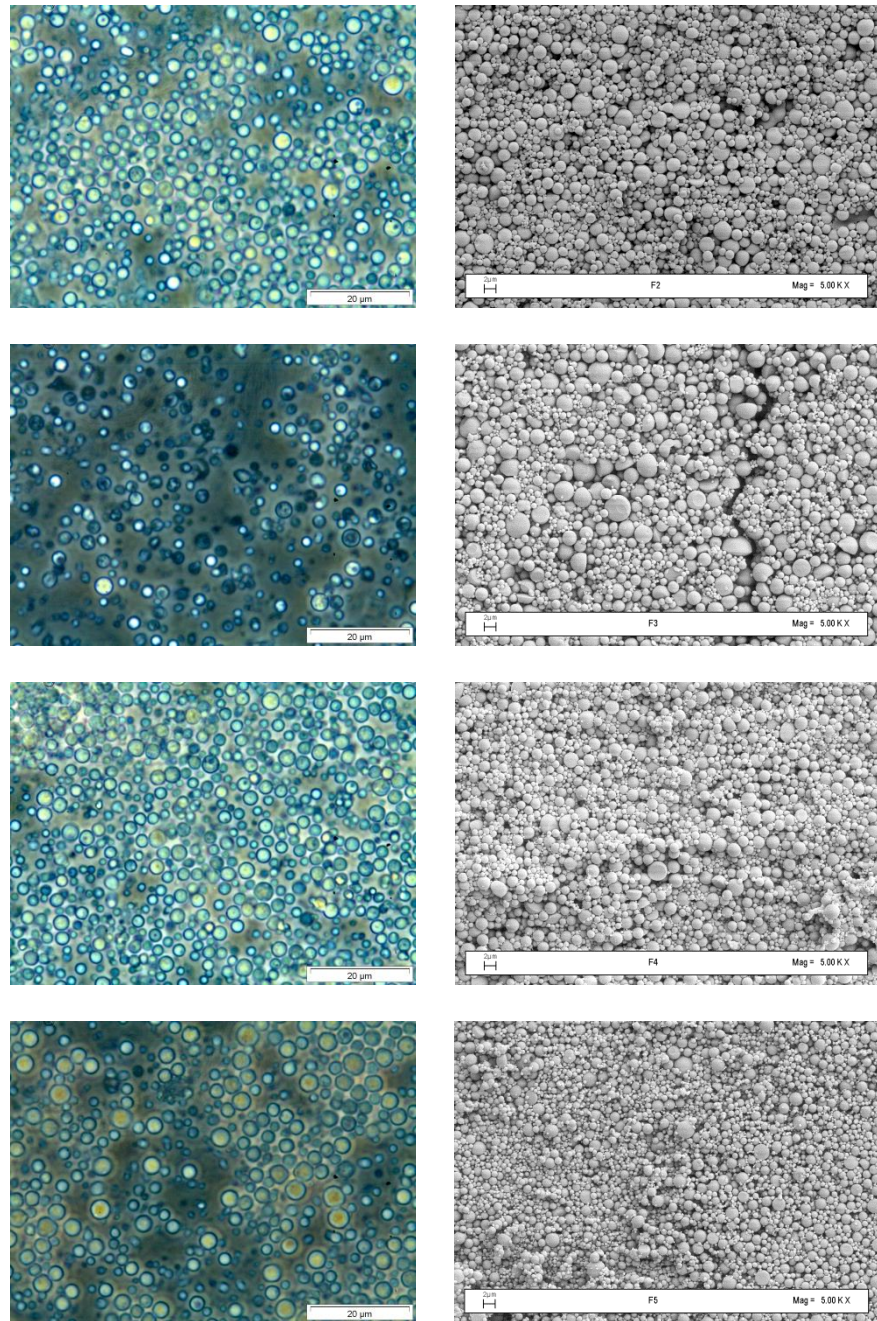


Figure VIII. 5 *Optical images and SEM images of PLGA particles encapsulating GFs*

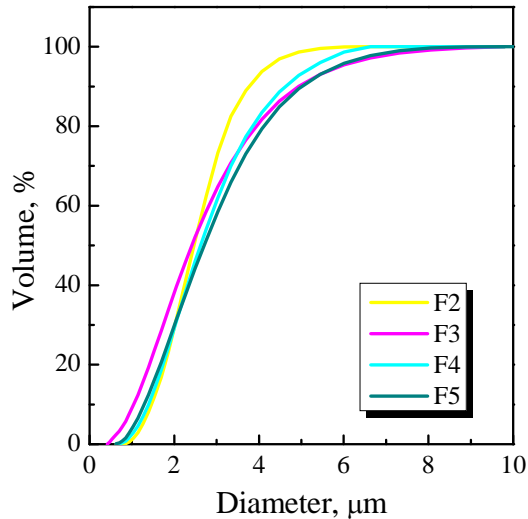


Figure VIII. 6 Cumulative undersize PSD of PLGA microparticles suspensions encapsulating GFs

VIII.6.3 PLGA microspheres charged with GF for stem cells

differentiation

PLGA microspheres loaded with GFs were charged inside a bioactive alginate scaffold to monitor the effect of the local release of these biosignals on cells differentiation. This part of the thesis was developed in collaboration with the University of Meriland where samples were sent for cell differentiation study. Human Mesenchymal Stem Cells (h-MSC), were used in view of the fact that they are a promising cell source for bone tissue engineering. Alginate beads were recovered from dynamic and static culture at different time points (1st, 7th, 21st and 28th days). The immunoassay analyses confirmed always a better cells differentiation in the bioreactor with respect to the static culture and revealed a greater influence of the BMP-2 released in the scaffold on cell differentiation.

VIII.7 Conclusions & Perspectives

SEE was successfully applied for the production of micro and nanospheres of PLGA and PLA PAMs encapsulating protein and peptides. Thanks to the mild SEE operating conditions the functionality of the

encapsulated bioactive molecules was preserved. Indeed, PLGA-PAMs loaded with GFs were charged in bioactive alginate scaffolds. The ability of a bioactive living scaffold with a locally controlled release of GFs to enhance the growth and differentiation of h-MSCs cultivated in a dynamic system by a tubular perfusion bioreactor system bioreactor was demonstrated, confirming that the SEE technique does not compromise GFs integrity.

Chapter IX

Titanium Dioxide nanoparticles encapsulation in PLA by Supercritical Emulsion Extraction to produce photoactivable microspheres

IX.1 Introduction

Titanium oxide (TiO₂), in form of nanoparticles, is one of the most important pigments and fillers used in painting, coating, packaging, biological and medical applications. Nano-TiO₂ particles are chemically stable, relatively nontoxic and environment friendly. It is well known that using UV illumination on TiO₂ nanoparticles in aqueous solution it is possible to generate reactive oxygen species (ROS), such as hydroxyl radical, hydrogen peroxide, that allow the decomposition of some organic compounds (Chowdhury D. et al., 2005) Therefore, nano-TiO₂ based suspensions, attracted a large interest for biomedical applications (Song M. et al., 2006), in the so called photodynamic therapy (PDT) of cells and bacteria, that is one of the most promising anticancer therapies under investigation (Harada Y. et al., 2011, Szacilowski K. et al., 2005, Cai R.X. et al., 1992).

In terms of photocatalytic applications, the anatase crystalline form of titania has been reported to present the best combination of photoactivity and photostability and, consequently, it has been preferred for this kind of processes.

Titania powders generally are obtained directly from titanium-bearing minerals or by precipitation from solutions of titanium salts or alcoxides (Mahshid S. et al., 2006). However due to high density and surface

properties of TiO₂ nanoparticles, there are some drawbacks in their colloidal stability, such as particles agglomeration and sedimentation². Thereby, to enhance the dispersion stability of TiO₂ nanoparticles, several methods of polymer encapsulation have been proposed to resolve this problem. However, encapsulation should maintain the photoactivity of the produced microspheres; therefore, the selection of the preparation process and of the polymer are relevant parameters for a successful application.

Traditional techniques have been until now not particularly successful in the efficient production of TiO₂ loaded polymeric microspheres (De Oliveira A.M. et al., 2005, Park J.H. et al., 2007, Rong Y. et al., 2005a, Rong Y. et al., 2005b). SCFs based processes applied in this field, have been not particularly satisfactory in the case of RESS (Kongsombut B. et al., 2009); whereas, SEE has never been applied to TiO₂ encapsulation (Furlan M. et al., 2010).

Therefore, the aim of this part of the work is to try the production of photoactivable, biodegradable and nanostructured PLA/TiO₂ sub-microparticles using SEE-C process. Anatase type nano-TiO₂ has been synthesized by precipitation from solutions of titanium alcoxides. Two different kind of emulsions were tested: *water in oil in water* emulsion W/O/W and *solid in oil in water* emulsion S/O/W. In the first case, a nano-TiO₂ ethanolic stable suspension was used as the water internal phase of the emulsion; whereas, in the second case TiO₂ fine powder was directly dispersed in the oil phase. Particles produced were characterized in terms of morphologies, TiO₂ loading and dispersion in polymer matrix. Furthermore, the photocatalytic activity of pure TiO₂ and nanostructured PLA/TiO₂ particles were tested using bacterial killing assay under UV irradiation.

IX.2 Materials, apparatus and methods

IX.2.1 Materials

CO₂ (99.9%, SON, Naples, Italy), polysorbate (Tween 80, Aldrich Chemical Co.), ethyl acetate (EA, purity 99.9%, Aldrich Chemical Co.) poly-(lactic) acid (PLA, MW: 28.000, Resomer R 203H) were used as received.

IX.2.2 Production of TiO₂ nanoparticles

TiO₂ nanoparticles were prepared using a microwave process. Briefly, 2 mL titanium (IV) propoxide (Sigma-Aldrich, 97%) and 30 ml of absolute ethanol (Panreac, analytical grade) were mixed under magnetic stirring; then, 3 mL of acetic acid (Panreac) were added. After 5 min under magnetic stirring, 5 mL of deionised water were added and at the end the mixture was poured into an autoclave that was sealed and heated up in a microwave oven

(Ethos Plus) up to 120°C for 15 min. The final solid was isolated by centrifugation and thoroughly washed with ethanol several times. The washed particles were diluted with ethanol to a final concentration of 12 mg/mL, whereas for the production of dry powder, washed particles were dried at 80°C.

IX.2.3 Emulsion preparation

Two different kind of emulsions were prepared: double emulsion *water in oil in water* (W/O/W) and *solid in oil in water* (S/O/W). For the preparation of the double emulsion, an ethanolic stabilized suspension of TiO₂ nanoparticles (12 mg/mL) was used as the water internal phase W₁. The suspension was sonicated at 40% (Digital Sonifier Branson mod. 450, ½" diameter micro-tip, 20 kHz, nominal power 400 Watt) of the power for 1 min, immediately before its utilization, to allow the complete dispersion of TiO₂. The oil phase was prepared dissolving 1 gr of PLA in 20 gr of ethyl acetate. The primary emulsion W₁/O was obtained adding 1 mL of W₁ in the oil phase and sonicating at 40% of the power for 30 seconds. The sonication was repeated twice. Then the primary emulsion was added to 80 gr of the water external phase W₂ (1% Tween 80 solution in water saturated with ethylacetate). The secondary emulsion was obtained by high speed stirring at 7000 rpm for 6 min (mod. L4RT, Silverson Machines Ltd. Waterside, Chesham Bucks, UK). The W₁/O/W₂ emulsion obtained was furtherly sonicated to reduce droplets mean size (60% for 30 seconds, repeated twice). When the S/O/W emulsion was prepared a known amount of TiO₂ powder was directly dispersed in to the oil phase, prepared as previously described. The dispersion (S/O) of the powder in the oil phase was obtained with sonication at 60% for 60 sec. The S/O/W emulsion was prepared adding the S/O suspension in to 80 gr of water external phase, prepared as previously described and emulsifying at the same condition described above.

IX.2.4 Supercritical emulsion extraction process

The emulsions prepared where processed using the SEE process. The detailed description of the experimental apparatus is reported elsewhere. The operative condition in terms of pressure and temperature are selected considering the vapor-liquid equilibrium diagram of solvent-CO₂ system. In the case of ethyl acetate-CO₂ the condition were fixed at 80 bar 38°C to operate above the mixture critical point (MCP). Another operative condition is the ration between the liquid and the gas (L/G ratio). This value is generally selected taking in to consideration the flooding phenomana. In this work the L/G ratio was fixed at 0.1, as optimized in previous works (Della Porta G. et al., 2011b).

IX.2.5 Particle characterizations

Emulsions and corresponding suspensions obtained after the SEE process were characterized by particle size distribution (PSD) dynamic laser scattering (DLS) using a Nanosizer (NanoZS Malvern Instrument, UK) equipped with a He–Ne laser operating at 4.0 mW and 633 nm, to measure the hydrodynamic diameter of the particles. Particles were recovered from suspensions by membrane filtration (membrane porosity 0.1 μm) and dried at air. Particles morphology and approximate composition was observed using field emission-scanning electron microscope (FESEM, mod. LEO 1525, Carl Zeiss SMT AG, Germany), coupled with an energy dispersive X-ray spectroscopy (EDX, INCA Energy 350, UK). Transmission electron microscopy (TEM) was also used to characterize PLA/ TiO₂ nanoparticle composites. X-ray photoelectron spectroscopy (XPS...) was used to obtain a surface chemical analysis of the nanoparticles obtained. Encapsulation efficiency was obtained with thermogravimetric analysis (TGA), as the residue remaining after the total combustion of the polymeric component of the particles. The sample was placed in alumina crucibles and heated up to 600 °C at a rate of 10 °C/min, under a constant air flow of 5 N cm³/min).

IX.2.6 Photocatalytic reaction and bacterial viability assay

A colony of *Staphylococcus Aureus* was suspended in 50 mL of tris-buffered saline (TBS) solution and incubated for 24 h at 37°C. A 10⁹ CFU/mL bacterial suspension was obtained and further diluted to obtain 10⁷ CFU/mL bacterial concentration.

In the photocatalytic experiments, the protocol reported by Tsuang et al. 2008 (Tsuang Y.H. et al., 2008) was used. Briefly, stock aqueous PLA/TiO₂ suspensions (10 mg/mL) in deionized water were prepared immediately prior to the photocatalytic reaction and kept in the dark. Washed bacteria (approximately 10⁷ CFU/mL) were resuspended in deionized water. Aliquots of 1 mL stock aqueous PLA/ TiO₂ suspension were added in a 50 mL glass beaker containing 8 mL of sterilized deionized water and 1 mL of washed cells. The PLA/TiO₂ slurry was placed on a magnetic stir plate with continuous stirring and was illuminated with 40 W black light bulb. The peak wavelength of the bulb was 365 nm. Samples were exposed to UV light for 5 hours.

Loss of viability was determined by viable count procedure. The PLA/TiO₂ bacterial slurry was exposed to UV light with continuous stirring. A *Staphylococcus Aureus* suspension without TiO₂/PLA particles was illuminated as a control, and the reaction of PLA/TiO₂ -bacteria slurry in the dark was also carried out. Samples were taken and the viable count was performed on agar plates after serial dilutions of the samples in sterilized PBS. All plates were incubated at 37°C for 24 h.

IX.3 Results and discussion

IX.3.1 TiO₂ nanoparticles production

The XRD spectrum of the synthesized nanoparticles (**Figure IX. 1**) shows that microwave synthesis produce material with good crystallinity and all the characteristic lines attributed to the anatase phase (JCPDS B° 2000) even at 110 °C. The strongest peak was observed for the (1 0 1) reflection at 25.2 °. Prominents peaks were also observed for (0 0 4), (2 0 0) and (2 1 1) reflections. No extra peaks were detected indicating the absence of rutile or brookite phases. The crystallite size of the obtained material calculated by Scherrer equation was estimated of 7 nm

The morphology and particle size distribution of the synthesized nanoparticles was studied by electronic microscopy. TEM images revealed the formation of prismatic particles with mean size of 15±5 nm and narrow particle size distribution. The difference between TEM and XRD obtained sizes would indicate that each nanoparticle is formed by several crystallites.

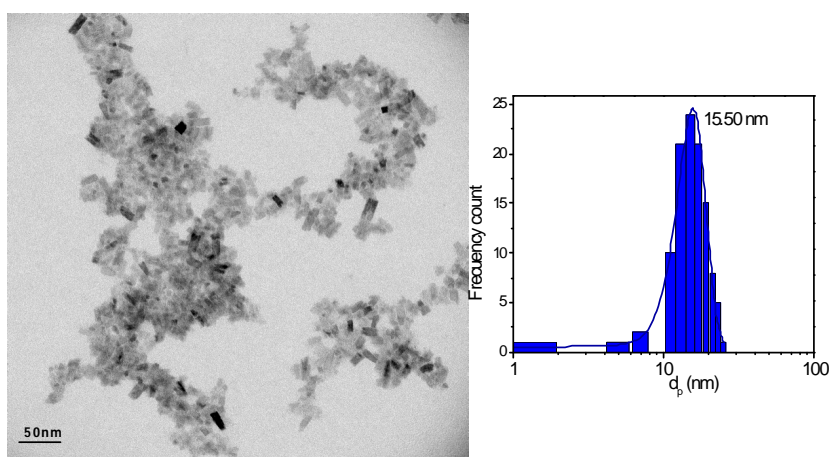


Figure IX. 1 TEM image and XRD diffraction patterns of the microwave synthesized nanoparticles

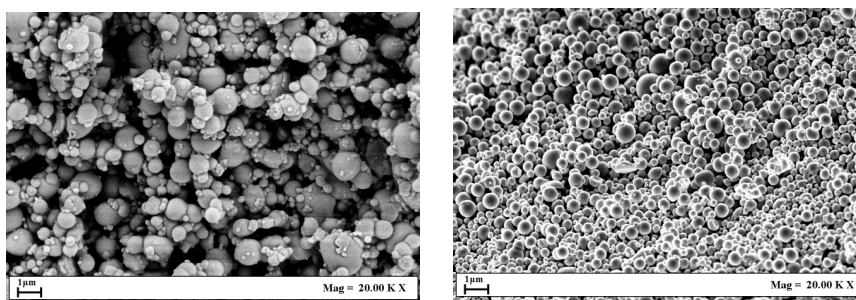
IX.3.2 PLA/TiO₂ nanoparticles production: effect of emulsion

formulation and titanium loading

Composites nanoparticles PLA/TiO₂ were prepared using the SEE-C technique. W₁/O/W₂ and S/O/W emulsions where used for the preparation of biopolymeric sub-micro particles encapsulating TiO₂, as described in the previous section.

In the SEE processing the dimension of particles is directly connected with the dimension of the droplets in the emulsion. For this reason a direct control over droplet size distribution (DSD) in the emulsion is preliminary required.

In the case of the double emulsion, emulsification parameters were changed to find the best condition for the production of droplets, and consequently of the particles, in the range 100-300 nm. In details, the ethanolic TiO_2 suspension was sonicated at 40% of the power for 1 min, immediately before the preparation of the emulsion to allow the complete dispersion of TiO_2 . The primary emulsion W_1/O was obtained adding 1 mL of W_1 in the oil phase and sonicating at 40% of the power for 30 seconds. The sonication was repeated twice. Then, the primary emulsion was added to 80 g of the water external phase W_2 (1% Tween 80 solution in water saturated with ethylacetate). The secondary emulsion was obtained by high speed stirring at 7000 rpm for 6 min. In the attempt to produce smaller particles, the $W_1/O/W_2$ emulsion was furtherly sonicated to reduce droplets mean size (60% for 30 seconds, repeated twice). In **Figure IX. 2** SEM images of particles produced with and without the final sonication step are reported. It is possible to note that particles are spherical and not aggregated in both cases; this result can be attributed to the fast and efficient extraction obtained operating with the continuous counter-current high pressure column. Microparticles with a mean diameter (MD) of $0.9 \mu\text{m}$ (**Figure IX. 2 (a)**) were obtained when weaker emulsification process was used; i.e., when the final sonication step was not applied; whereas sub-microparticles with MD of 265 nm (**Figure IX. 2 (b)**) with a narrower PSD were produced applying the final emulsification using the sonication probe. For this reason the final sonication was always applied for all the other experiments reported in this work.



(a) $0.9 \mu\text{m} \pm 0.5$

(b) $265 \text{ nm} \pm 69$

Figure IX. 2 Micro and nanoparticles of PLA+ TiO_2 produced changing emulsion preparation parameters (TiO_2 1.2% w/w).

Once fixed the emulsification conditions, W₁ volume was changed (1, 2 and 3 mL) to produce different TiO₂ theoretical loadings, respectively 1.2, 2.4 and 3.6% w/w of TiO₂ with respect to the polymer content. **Table IX. 1** reports all the particle size data of emulsions and particles discussed in the following.

Table IX. 1 Mean diameter (MD) and Standard Deviation (SD) of droplets in emulsions and of composite particles produced after SEE processing, shrinkage factor % between droplets and particles mean diameter and TiO₂ theoretical and effective loading. SEE operative conditions were: 80 bar, 38°C, liquid/gas ratio (L/G) 0.1.

	Theoretical TiO ₂ loading (%)	Effective TiO ₂ loading (%)	Emulsion MD±SD (nm)	Particles MD±SD (nm)	Shrinkage Factor (%)
W₁/O/W₂					
T1*	1.2	85.42	1241±558	909±499	26
T2	1.2	85.00	450±139	203±40	55
T3	2.4	90.42	498±129	265±69	47
T4	3.6	97.22	1214±582	559±263	54
S/O/W					
T5	1.2	91.67	320±58	205±33	36
T6	2.4	90.21	315±108	179±34	43
T7	3.6	86.67	296±100	193±60	35

* Produced without final sonication step.

Increasing the volume of the W₁ phase and, consequently, TiO₂ % a significant increase of particle mean diameters and of PSD has been observed, as shown in **Table IX. 1** and **Figure IX. 3** where PSD expressed in terms of volume% are reported. In conclusion, increasing the volume of the water internal phase, larger water droplets are obtained in the primary W-O emulsion, that results in the production of larger particles and in the enlargement of the PSD. The smallest particles were obtained in the case of 1.2% TiO₂ theoretical loading, in this case nanoparticles with a MS of 203±40 nm were obtained.

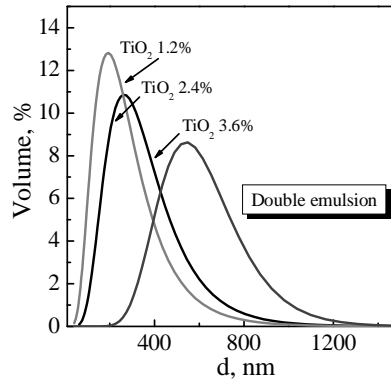


Figure IX. 3 PSD of PLA/TiO₂ particles obtained starting from W₁/O/W₂ emulsion with different W₁ volume phase.

The same TiO₂ theoretical loading with respect to the polymer (1.2, 2.4 and 3.6% w/w) was obtained directly suspending titanium powder in the oil phase. Results are shown in **Table IX. 1** (lower part) and in **Figure IX. 4** where SEM image of particles produced with the S-O-W(b) is compared with that of particles produced with the W-O-W emulsion (a). The figure proposes SEM images of PLA particles with 1.2% w/w of TiO₂ at the same enlargement; it is evident that both the emulsions led to the production of spherical non coalescing particles; no relevant changes in the morphologies of the PLA particles produced can be noted. Furthermore very small particles were obtained in both cases, with MD around 200 nm, as also reported in **Table IX. 1**.

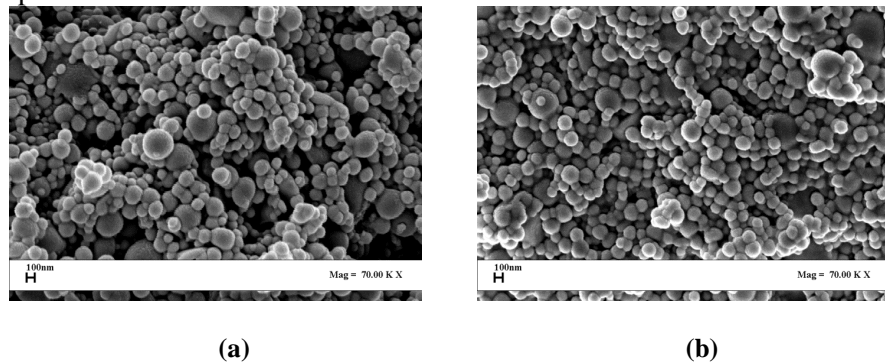


Figure IX. 4 SEM images of particles produced starting from W₁/O/W₂ (a) and S/O/W (b) emulsion with 1.2 % titanium theoretical loading.

Figure IX. 5 reports the PSDs of the experiment obtained starting from S-O-W emulsions, with different TiO₂ theoretical loading; data are also reported **Table IX. 1**. From **Figure IX. 5** it is possible to note that there is a

weak effect of TiO₂ loading on the mean diameter of the particles obtained, that is always around 200 nm. But, increasing TiO₂ content there is a more evident enlargement of the PSD. Also in this case, the increase of the TiO₂ theoretical loading produce higher polydispersity.

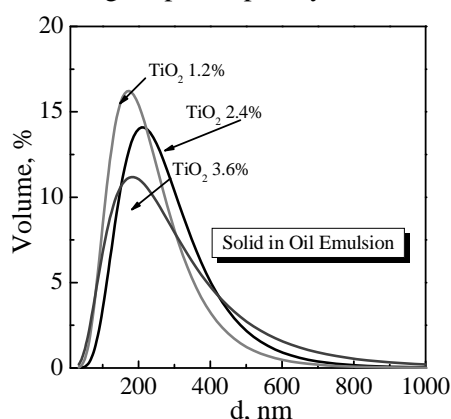


Figure IX. 5 PSD of PLA/TiO₂ particles obtained starting from S/O/W emulsion with different S loading

Comparing the particles obtained using the two different emulsions, S-O-W emulsions produce particles with smaller diameters and narrower PSD. In the case of W-O-W emulsion the increase of nano-TiO₂ theoretical loading implies the consequent increase of the water internal phase, that has a larger effect on MD, then the increase of powder content used in the S-O-W to increase the nano-TiO₂ loading.

IX.3.3 Nanocomposite characterization: TGA, EDX, XPS, TEM

PLA particles were further characterized to evaluate the efficiency of TiO₂ encapsulation inside polymeric particles and to verify if an homogeneous dispersion of the nanoparticles in to the polymeric matrix was obtained. For this reason a first EDX analysis was performed, to evaluate if TiO₂ was encapsulated in nanospheres. Results are reported in **Figure IX. 6**, for the experiments with 3.6% theoretical TiO₂ loading obtained starting from a W₁/O/W₂ emulsion (**Figure IX. 6 (a)**) and from a S/O/W emulsion (**Figure IX. 6 (b)**). TEM and CrioTEM images of the related samples are also reported in the same image. EDX spectra show that TiO₂ is present in the samples, in both cases proposed. TEM micrographs also show that TiO₂ nanoparticles are inside the particles. Furthermore the TEM images show another important results: in the case of particles produced starting from the double emulsion, TiO₂ nanoparticles are encapsulated in the polymeric matrix and also well dispersed inside it; whereas, particles obtained starting from the S/O/W emulsion show a non homogeneous distribution of TiO₂ in

the polymer matrix and it is sometimes possible to see particles formed only by the polymer. Therefore, $W_1/O/W_2$ emulsion gives the better results in terms of distribution of metal oxide nanoparticles in the polymeric nanospheres. Therefore, the use of nano-TiO₂ directly as ethanolic stabilized suspension as water internal phase gives the best results; in the S-O-W emulsion TiO₂ tends to aggregate probably due to the low viscosity of the polymeric oil phase (PLA used has low molecular weight and apparent viscosity). Another important information that has been obtained from XPS analysis, is reported in **Table IX. 2**. X-ray photoelectron spectroscopy (XPS) is a quantitative spectroscopic technique that measures the elemental composition by irradiating a material with a X-rays beam while simultaneously measuring the kinetic energy and number of electrons that escape from the top 1 to 10 nm of the material analyzed; the result is a sort of map of the elements that form the surface of the material. Analyzing results of **Table IX. 2**, it is possible to note that nanoparticles produced starting from double emulsion behave completely different from those obtained starting from S/O/W emulsion. Indeed, particles produced starting from $W_1/O/W_2$ emulsion show TiO₂ dispersed also on the surface, and the content of TiO₂ on the surface increases with the increase of the theoretical loading; whereas, particles produced starting from S/O/W emulsion have low TiO₂ content on the surface, as also confirmed by TEM images.

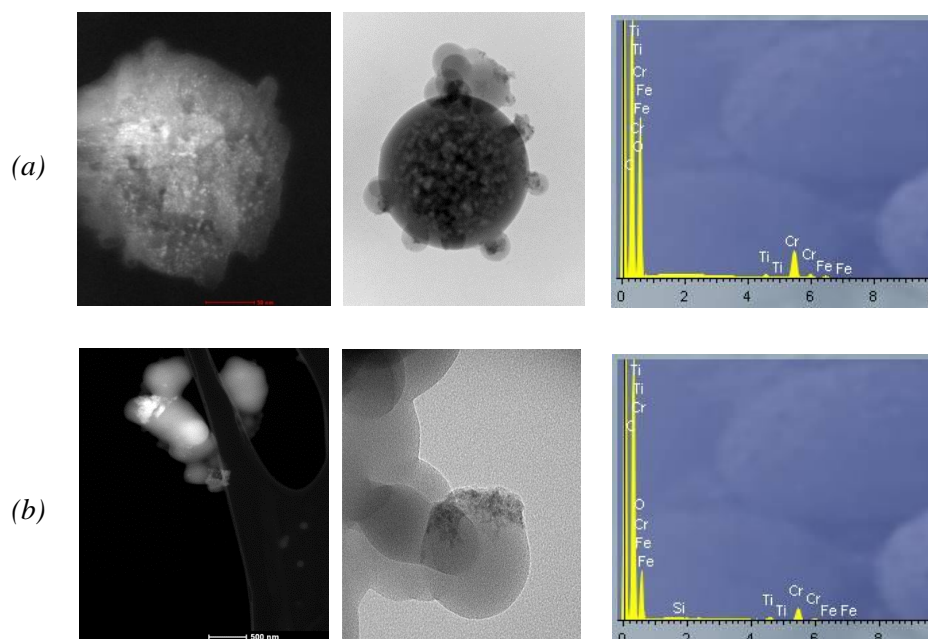


Figure IX. 6 TEM and CrioTEM images of PLA/TiO₂ particles and EDX spectra of related samples; (a) T4 sample, (b) T7 sample.

Table IX. 2 X-ray photoelectron spectroscopy (XPS) results related to PLA/TiO₂ nanoparticles, surface compositions are reported in %

	Sample	C (%)	O (%)	TiO ₂ (%)
W₁/O/W₂				
	T1	65.86	33.87	0.27
	T2	68.74	30.95	0.31
	T3	68.61	30.92	0.47
	T4	68.57	30.70	0.73
S/O/W				
	T5	69.23	30.59	0.18
	T6	68.09	31.71	0.20
	T7	68.82	30.01	0.17

A possible explanation is that the tendency of water internal phase to migrate towards the water external phase allows a better radial distribution of nano-TiO₂ in the polymeric spheres in the case of W/O/W emulsion. The effective loading was also calculated for all the samples by TGA.

Figure IX. 7 reports the corresponding thermogravimetric curves and the effective loading, corresponding encapsulation efficiency are reported in **Table IX. 1**. Looking at the results reported in

Figure IX. 7 it is possible to conclude that the encapsulation efficiency (defined as effective loading/theoretical loading ratio) is always high $\approx 90\%$; better results are obtained using the double emulsion. The explanation can be that the viscosity of the oil phase used in this work is not high enough to avoid TiO₂ settling and aggregation. For this reason S-O-W emulsions give particles with lower encapsulation efficiency and less homogeneous TiO₂ distributions.

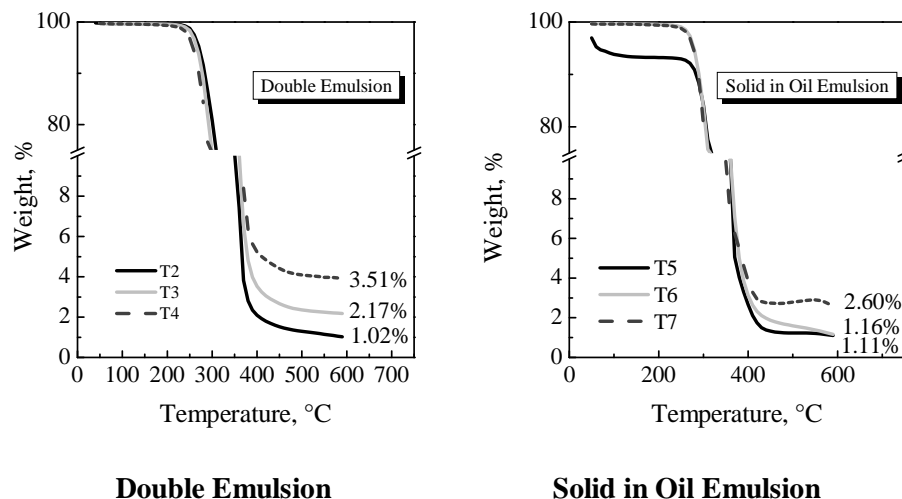


Figure IX. 7 Thermogravimetric analysis (TGA) results for nanoparticles produced starting from double emulsion and solid in oil emulsion. The effective loading is also reported.

From **Table IX. 1** and

Figure IX. 7 it is evident that an increase of encapsulation efficiency is obtained increasing the TiO_2 theoretical loading in the case of double emulsion, whereas a practically constant encapsulation efficiency is obtained increasing the TiO_2 theoretical loading in the case of S/O/W emulsions; in this case the increase of the TiO_2 content does not produce an improvement of the encapsulation efficiency due to problems of suspension instability in the oil phase.

IX.3.4 *Staphylococcus Aureus* loss of viability under TiO_2

photocatalytic reaction

Until now we have seen that TiO_2 has been efficiently dispersed in PLA particles using the SEE technique, but the key characterization is related to the photoactivity of the produced materials.

Photocatalytic activation of PLA/ TiO_2 nanoparticles was tested under UV light and quantified with the determination of *Staphylococcus Aureus* loss of viability. First TiO_2 nanoparticles alone were tested following the protocol previously described in Materials and Methods section. When *S. Aureus* was treated with TiO_2 powder under UV light, a considerable loss of viability was

observed, as reported in **Figure IX. 8**; about 98% of the cells were killed, with respect to the initial concentration, after 5 hours of UV irradiation. A control was always performed (the sample without TiO₂ particles was exposed to the same UV irradiation) and no relevant change in survivor cell number was observed.

When PLA/TiO₂ particles were tested (results for sample T2 and T5 are reported in the same Figure), the same loss of viability was obtained as in the case of pure TiO₂, indicating that the encapsulation of the metal oxide nanoparticles in the biopolymeric matrix does not affect photocatalytic activation of TiO₂ particles; but, however increase their biocompatibility; therefore, devices that are in situ activated and biocompatible are obtained. At the concentration of the powder tested, no relevant changes in results were noted in the case of particles produced starting from W₁/O/W₂ or S/O/W.

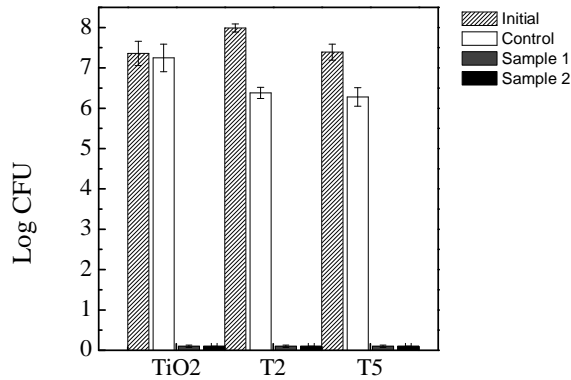


Figure IX. 8 The viability of bacteria under various TiO₂ photocatalytic reaction

IX.4 Conclusions

It has been demonstrated that SEE-C can be successfully used to produce PLA/TiO₂ nanostructured particles. Higher encapsulation efficiencies were obtained with the respect to the related literature, thanks to the fast and efficient extraction of the oily phase of the emulsions. The double emulsion W/O/W gave the most promising results, allowing the production PLA particles with a homogeneous TiO₂ dispersion in the polymeric matrix.

The photocatalytic activity of the nanostructured carriers was not reduced by the polymeric shell, allowing the production of in situ activable and biocompatible devices.

Chapter X

Hollow Gold Nanoshells-PLA nanocomposites for photothermal controlled delivery of Rhodamine

X.1 Introduction

Light-sensitive drug delivery systems (DDS) are receiving increasing attention owing to the possibility of developing materials sensitive to innocuous radiation (mainly UV, visible, or near infrared region) which can be applied on demand at well delimited sites of the body (Barrett C. and Mermut O., 2005, Jiang H.Y. et al., 2006). Near infrared (NIR) resonant materials are receiving increasing interest in this field because NIR light, with the range of wavelengths from 650 to 900 nm, has a deep light penetration into living tissues and, in this region, hemoglobin, lipids and water have the lowest absorption coefficient. Furthermore, NIR is innocuous and does not cause a significant heating in the area of its application (Donnelly R.F. et al., 2005, McCoy C.P. et al., 2007, Klohs J. et al., 2008). Hollow Gold nanoshells (HGNs) have attracted increasing interest as NIR resonant metal nanostructure for biomedical applications; they are Gold shells filled with the imbedding medium (Xia Y. et al., 2000). In HGNs the ratio of shell diameter and thickness (defined as aspect ratio of the nanostructure) determines the peak position of the surface plasmon resonance and their uniformity determines its bandwidth (Zhang J. and Noguez C., 2008, Schwartzberg A.M. et al., 2006).

The application of HGNs in photothermal therapy has been reported by Hirsh et al. (Hirsch L.R. et al., 2003); the authors demonstrated that Silica/Au nanoshell particles could be used to deliver a therapeutic dose of

heat to kill targeted cell without damaging normal cells because of local heating. Poly(N-isopropylacrylamine-co-acrylamide)-Au nanoshell composites containing methylene blue, ovalbumine or bovine serum albumine (BSA) were synthesized and the drug release from these composites was reported to be enhanced by NIR irradiation (Sershen S.R. et al., 2000). However, these DDS are not appropriate for drug delivery because of their toxicity. Biodegradable multilayer polymer/metal nanoparticles have been also proposed in the literature. Rhodamine is encapsulated within PLGA and metal multilayers are deposited on these nanoparticles. The authors reported that the drug release from PLGA matrix is accelerated by increasing the temperature during NIR irradiation. However the physical deposition method yields half-shell of metal layer and the drug is released from the remaining non coated surface. This leads to the generation of temperature and concentration gradients inside PLGA nanoparticles and considerable reduction of the total surface area available for drug release (Park H. et al., 2008). HGNs were also used to initiate release from liposomes. Indeed, liposomes have been evaluated as drug nanocarriers for decades, but their clinical applications are often limited by slow release or poor availability of the encapsulated drugs. Irradiating with NIR pulsed laser HGNs near complete release have been obtained within seconds. These DDS do not allow the control of the release rate, because when NIR is absorbed and converted into heat the drug is instantaneously released from the disrupted lipid membrane. In conclusion light based approach applied on DDS have been demonstrated to be promising but, unfortunately, these studies are still in a primordial research stage (Wu G.H. et al., 2008).

For these reasons the aim of this study is the production of biocompatible and biodegradable PLA-HGNs composite devices for photothermal induced delivery of Rhodamine, used as model compound. HGNs were synthesized by galvanic replacement of Cobalt with Gold using PVP as template stabilizing agent. PLA-HGNs-Rhodamine composite delivery devices were produced using the Supercritical Emulsion Extraction technique (SEE). Rhodamine was dissolved in the aqueous phase of a W/O/W emulsion, whereas HGNs were dispersed uniformly in the polymeric organic phase. PLA was used as polymer matrix. DDS were characterized in terms of morphologies, Rhodamine loading, HGNs loading and dispersion in PLA matrix. Rhodamine release from DDS produced was tested under different NIR irradiation conditions.

X.2 Materials, apparatus and methods

X.2.1 Materials

CO₂ (99.9%, SON, Naples, Italy), polysorbate (Tween 80, Aldrich Chemical Co.), ethyl acetate (EA, purity 99.9%, Aldrich Chemical Co.)

poly- (lactic) acid (PLA, MW: 28.000, Resomer R 203H), Rhodamine B (purity 99.9%) were used as received.

X.2.2 Hollow Gold nanoparticles production

Hollow Gold nanospheres (HGNs) were synthesized following protocol reported by Preciado-Flores et al. (Preciado-Flores S. et al., 2011) with some modifications. The synthesis was carried out using air free methods to reduce premature oxidation of the cobalt particles. Additionally, all glassware that was used was cleaned thoroughly with Alconox®, aqua regia, and ultrapure water. In a 500 mL two-necked round-bottom flask, 100 mL of ultrapure (18 MU) water was combined with 100 mL of 0.4 M cobalt chloride hexahydrate ($\text{CoCl}_2 \cdot 6\text{H}_2\text{O}$) and 400 mL of 0.1 M sodium citrate trihydrate ($\text{Na}_3\text{C}_6\text{H}_5\text{O}_7 \cdot 3\text{H}_2\text{O}$). The solution was deaerated by bubbling with argon gas for 40 minutes with no magnetic stirring. To that solution, 100 mL of 1.0 M sodium borohydride (NaBH_4) was injected, and the solution turned from a pale pink color to brown over the course of a few seconds indicating the formation of cobalt nanoparticles. Simultaneously, 100–900 mL of a 1 wt% solution of poly (vinylpyrrolidone) ($\text{C}_6\text{H}_9\text{NO}$)_n, with an average Mw of 55 000, was injected. The as-formed cobalt nanoparticle solution was further deaerated by passing argon through the reaction flask for a further 40 minutes until the evolution of H_2 bubbles ceased, indicating the complete hydrolysis of borohydride. Subsequently, 30 mL of the cobalt nanoparticles were transferred to a 100 mL beaker and immediately added to a stirring solution of 10 mL of ultrapure water and 15 mL of 0.1 M chloroauric acid trihydrate ($\text{HAuCl}_4 \cdot 3\text{H}_2\text{O}$), allowing the formation of CoCl_2 and the reduction of Au^{3+} . The solution was allowed to stir for another five minutes under ambient conditions to allow the complete oxidation of any unreacted cobalt and a slow change in color from brown to green indicates that the formation of hollow Gold spheres was completed. HGNs obtained were centrifuged several times and concentrated with liofilization.

X.2.3 Emulsion preparation

Double emulsion *w-o-w* were prepared for the production of PLA nanoparticles encapsulating Rhodamine (used as a model drug) and HGNs. *w-o-w* emulsion ratio was selected at *1-19-80*. The water internal phase (1 ml) was prepared dissolving Rhodamine in water to a final concentration of 5 mg/mL. The oil phase was prepared dissolving 1 gr of PLA in to 19 gr of ethylacetate. HGNs were dispersed in the oil phase (from 5 to 15 mg) using an ultrasound probe at 40% of the power for 1 minute, (Digital Sonifier Branson mod. 450, ½” diameter micro-tip, 20 kHz, nominal power 400 Watt). The ultrasound dispersion was repeated until the suspension became stable and homogeneous. The primary emulsion *w-o* was obtained dispersing

1 mL of the water internal phase in the oil phase, the HGNs dispersion in PLA solution, using ultrasound emulsification at 40% for 1 minute. Then the primary emulsion was added to 80 gr of the water external phase (1% Tween 80 solution in water saturated with ethylacetate). The secondary emulsion was obtained with high speed stirring at 7000 rpm for 6 min (mod. L4RT, Silverson Machines Ltd. Waterside, Chesham Bucks, UK). The *w-o-w* emulsion obtained was furtherly sonicated to reduce droplets mean size (60% for 30 seconds, repeated twice).

X.2.4 Supercritical Emulsion Extraction: apparatus and process

conditions

The SEE process allows the production of microparticles and nanoparticles extracting the oily solvent of an emulsion. The first step for microparticles formations is the production of an emulsion; it can be single *oil-in-water* emulsion *o/w* and double *water-in-oil- water* emulsion *w/o/w*. The polymer is generally dissolved in the oil phase, whereas the drug could be dissolvent in the oil phase (lipophilic compounds) or in the water internal phase (hydrophilic compounds). The emulsion is stabilized by a surfactant. In the supercritical conditions CO₂ shows good solvent power for the majority of organic solvent, and low affinity with water. Thus, selecting opportunely the operative conditions it is possible to extract selectively the organic solvent of the oil phase, allowing the production of micro and nanoparticles.

The supercritical extraction of the solvent is obtained using a continuous counter-current tower, described in details elsewhere (Della Porta G. et al., 2011a). Looking at the binary vapor-liquid equilibrium diagram (VLE), **Figure X. 1** (Kato M. et al., 2006), the mixture critical point for the system CO₂-ethylacetate is at 80 bar and 40°C. In this condition ethyl acetate is completely miscible in SC-CO₂ and it can be extracted.

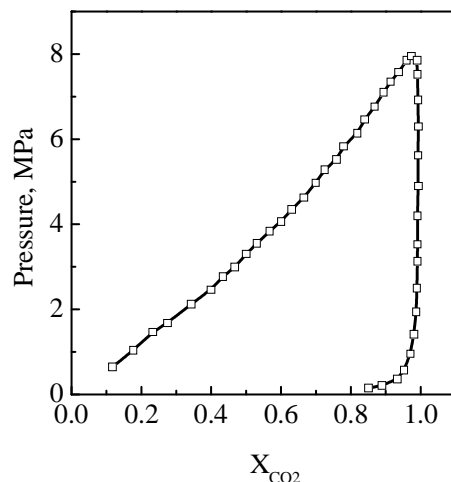


Figure X. 1 VLE diagram of the system CO₂-ethylacetate adapted from Kato et al. 2006.

When operating with continuous counter-current tower with dense gases, pressure and temperature conditions are selected from thermodynamic considerations (VLE diagram) as previously discussed; instead flow rate ratio (the liquid to gas ratio (L/G)) is selected from fluid dynamic considerations. In general increasing the gas flow rate there is an increase of the extraction efficiency, but it is not possible to decrease freely the L/G ratio since, when very large flow rates of the gas stream are used, the liquid is entrained by the gas and flooding occurs determining the failure of the process. In our case, L/G ratio was fixed at 0.1, as a consequence of a previous optimization of the tower fluid dynamics. A CO₂ flow rate of 1.2 kg/h and an emulsion flow rate of 2.3 mL/min were used according to the previous discussion.

X.2.5 Particle characterizations

Emulsions and corresponding suspensions obtained after the SEE process were characterized by particle size distribution (PSD) using dynamic laser scattering (DLS) method using a Nanosizer (NanoZS Malvern Instrument, UK) equipped with a He-Ne laser operating at 4.0 mW and 633 nm, to measure the hydrodynamic diameter of the particles. Data are reported also in terms of mean diameters (MD) and polydispersity index (PDI). Particles were recovered from suspensions by membrane filtration (membrane porosity 0.1 μ m) and dried at air. Particles morphology and approximate composition was observed using field emission-scanning electron microscope (FESEM, mod. LEO 1525, Carl Zeiss SMT AG, Germany),

coupled with an energy dispersive X-ray spectroscopy (EDX, INCA Energy 350, UK). Transmission electron microscopy (TEM....) was also used to characterize nanoparticles. Effective HGNs loading inside PLA nanoparticles was evaluated by inductively coupled plasma mass spectrometry. 20 mg of nanoparticles were digested in 5 mL of aqua regia for 5 days before the analysis.

X.2.6 Rhodamine loading and NIR controlled release

Rhodamine loading was determined by dissolving a known mass (~2–5 mg) of microspheres in 50 μ L dimethylsulfoxide. PBS (500 μ L) was added, and precipitated polymer was removed by centrifugation at 12,000 rpm for 10 min. The concentration of Rhodamine in the supernatant was determined by measuring the absorbance at 550 nm in a multiwall plate spectrophotometer (model Cary 50; Varian, Palo Alto, California).

In vitro release of Rhodamine was determined by resuspending ~20 mg of microspheres encapsulating Rhodamine in 2 mL of phosphate-buffered saline (PBS, pH 7.4) containing 0.5% Tween. Microsphere suspensions were continuously inverted at ~100 revolutions per minute at 37°C. Samples were centrifuged, the supernatant was removed, and the spheres were resuspended in fresh PBS at various time points. Rhodamine concentration was determined by measuring the supernatant absorbance at 550 nm as described above. Rhodamine release was summed with the amounts at each previous time point, and the total divided by the amount of Rhodamine in the microspheres (experimental loading of microspheres), to arrive at the “cumulative percent released.

When NIR laser was applied using laser generator (Model MDL-H-808/2W; Infrared Diode Laser at 808 nm power 2W from Changchun new Industries Optoelectronics Technology Co., Ltd., Changchun, China) samples were incubated at 37°C exposed to NIR irradiation for a period of time between 1 and 5 minutes, then samples were centrifuged, and Rhodamine concentration in the supernatant was analyzed as described above. Temperature profile in the suspension was also measured during irradiation.

X.3 Results and discussion

X.3.1 Photothermally controlled delivery PLA devices production &

characterization

Double emulsion *w-o-w* were prepared for the production of PLA nanoparticles encapsulating Rhodamine (used as a model drug) and HGNs.

Rhodamine was dissolved in the internal water phase, while HGNs were dispersed in the oil phase. SEE process was used to extract ethylacetate from the oil phase of the emulsions. PLA particles produced after SEE process are nanocapsules containing inside small droplets of the water internal phase; HGNs instead are dispersed in the polymer matrix. Four batches of PLA devices, with the same Rhodamine loading (0.5% w/w with respect to the polymer), were produced in this way. One batch of PLA devices was charged only with Rhodamine, while the others were also charged with increasing concentrations of HGNs. All the data related to the samples are reported in **Table X. 1**.

Table X. 1 PSD of samples produced after SEE process. Emulsions were obtained: S/O: sonicating at 40% for 1 minute (repeated until stabilization of the suspension); W₁/O sonicating at 40% of the power for 1 minute; W₁/O/W₂ 7000 rpm for 6 min and 60% sonication for 30 seconds, repeated twice. SEE operative conditions were fixed: 80 bar, 38°C, liquid/gas ratio (L/G) 0.1.

	Theoretical HGN loading (w/w %)	MD (nm)	PDI
G1	0	208	0.17
G2	0.5	237	0.18
G3	1.0	227	0.22
G4	1.5	269	0.21

In all cases, PLA particles produced have a mean diameter around 200-250 nm. The smallest particles with the narrower PSD were produced when only Rhodamine was charged (G1 sample). Increasing the HGN content in the oil phase a weak increase of MD and PDI can be noted from data in **Table X. 1** and also in **Figure X. 2**, where PSD are reported. About the macroscopic aspect, samples produced have a pink color, for the presence of Rhodamine inside; increasing the HGNs content in the polymer matrix the coloring turns to the dark pink, **Figure X. 2**.

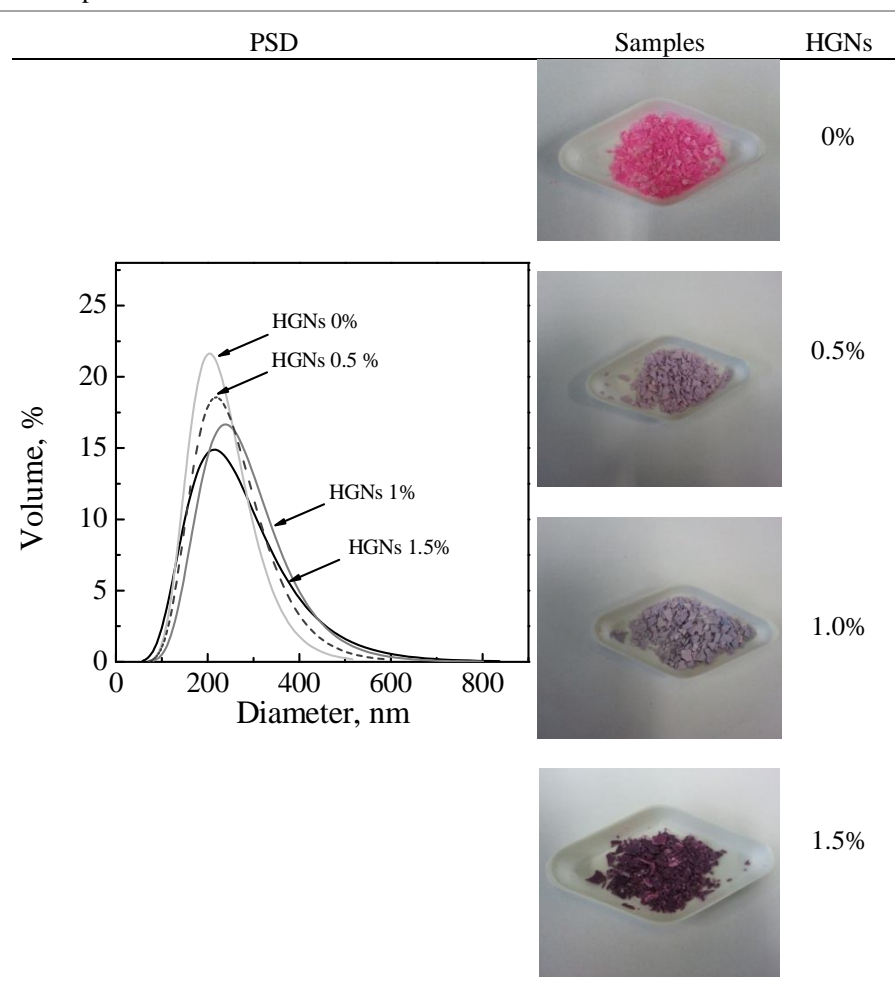


Figure X. 2 Frequency PSD curves of PLA-HGNs nanoparticles encapsulating Rhodamine with different HGN % in the polymer matrix. Photographs of powders obtained are also reported.

SEM images are reported in **Figure X. 3** for all the samples discussed in this section. SEM images show that the SEE technique allows the production of spherical and not aggregated PLA nanoparticles. The yield of the process (gr of particles recovered after the process/ gr of polymer charged in the oil phase) is always >90%. SEM images are reported at the same magnification and it can be noticed that samples have more or less the same mean diameter and polydispersity, that confirms the data obtained from DLS analysis of the

suspensions. The SEE process gives high reproducible results, that are more or less independent from the amount of drug and HGNs charged inside.

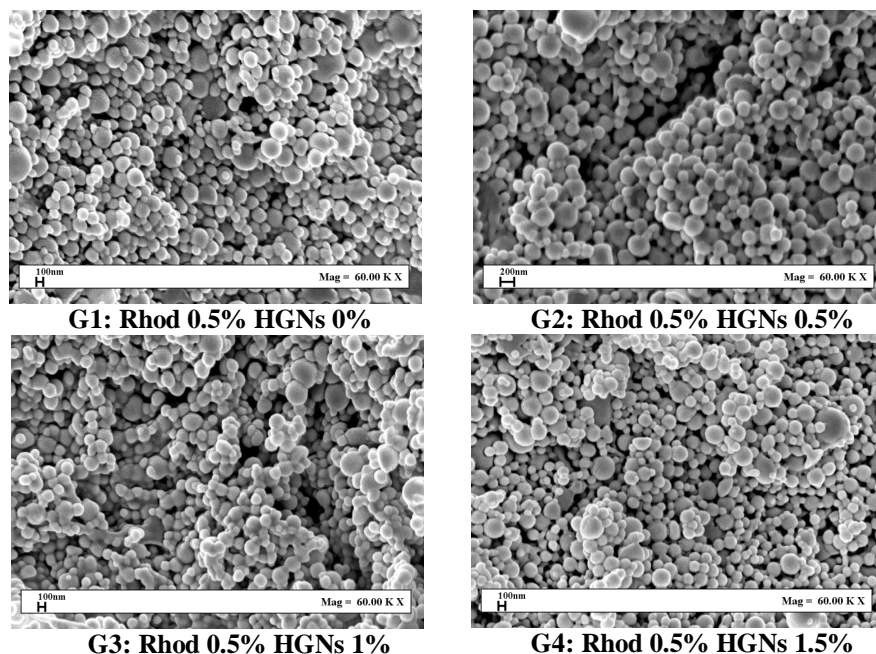


Figure X. 3 SEM images of PLA-HGNs particles encapsulating Rhodamine.

PLA nanoparticles were further characterized to investigate the efficiency of encapsulation of HGNs in the polymer matrix. For this reason a first EDX analysis was conducted, to investigate, if HGNs were encapsulated in nanospheres, results are reported in **Figure X. 4 (b)**, for the experiments with 1.5% theoretical HGN loading obtained. TEM images of the related sample are also reported in the same image, **Figure X. 4 (b)**. From EDX spectra it is evident that HGNs are present in the sample. From this spectra also some impurities of HGNs are detected (as Co or Cl), related to the synthesis of the HGNs process and confirming the presence of HGNs in the nanospheres. From the TEM images HGNs are well visible inside the polymeric spheres, and are homogeneously dispersed.

Quantitative HGNs loadings were evaluated with ICP analysis, confirming that the SEE technique allows high loading efficiency, as also previously demonstrated.

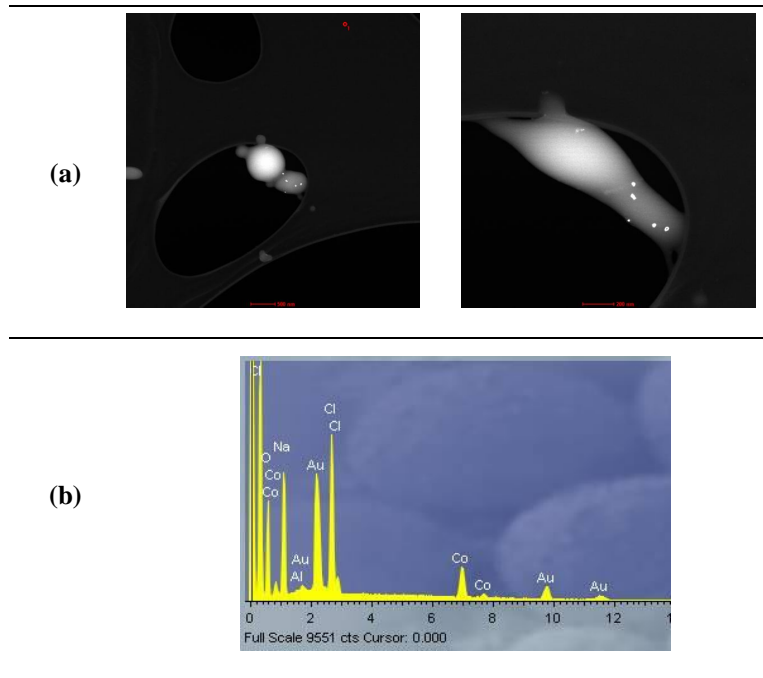


Figure X. 4 TEM mages of PLA/HGN particles encapsulating Rhodamine (a); EDX spectra of related sample (b).

X.3.2 Rhodamine loading and NIR controlled release from PLA particles

Rhodamine encapsulation efficiency was evaluated according to the procedure described in the materials, apparatus and methods section. In all cases Rhodamine encapsulation efficiency was around 80% and was not affected by the HGNs loading.

Regarding the study of NIR controlled Rhodamine delivery from PLA-HGNs devices, first drug release was performed without NIR application for all the samples for comparison purposes with the NIR controlled releases. Rhodamine release in PBS from PLA nanospheres was completed in about 10 days, see **Figure X. 5 (a)**, where Rhodamine release is reported in the case of spheres with no loading of HGNs. A burst initial release is obtained in the first 0.2 days, around 45% of the drug is released immediately. The remaining part of the drug, entrapped in the inner polymer matrix is released slowly consequently with the degradation of the polymer. In the same figure it is also reported the release of Rhodamine form PLA nanocarrier with 1% of HGN loading. The presence of the HGNs does not affect the release when NIR is not applied. SEM images reported in **Figure X. 5** shows particles

after 1 day **(b)** and at the end of the release **(c)**. After one day of release in PBS at 37°C particles maintains their spherical shape while at the end of the release there are only polymer residues.

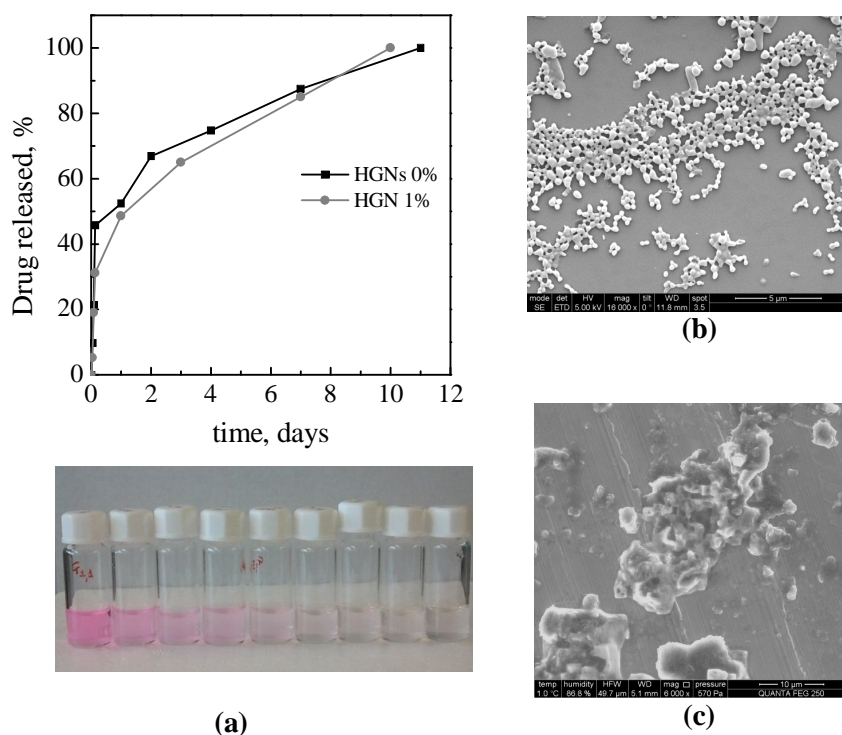


Figure X. 5 Rhodamine release from PLA nanoparticles; Sample G1 and G3 results are compared (a); SEM images of particles after one day of release (b) and at the end of the release (c) are also reported.

When NIR irradiation is applied to the suspension of PLA nanocarriers containing HGNs and encapsulating Rhodamine, what is expected is that HGNs, that are resonant nanomaterials, absorb the radiation and convert it into heat. This heating effect could speed the Rhodamine release rate depending on the power and duration of irradiation and HGN loading.

The heating effect for different power intensity and for different HGN loading in PLA carriers was preliminary studied. Temperature of suspensions of PLA nanocarriers during time was monitored when the suspension were exposed to NIR irradiation for 5 minutes. **Figure X. 6 (a)** reports heating effects generated when NIR irradiation was performed at 80% of the power. Suspensions of PLA carriers with different HGNs loading where tested and also a blank test was performed exposing to NIR irradiation

also pure PBS and suspension of PLA particles without HGNs. With these conditions of irradiation there is a weak increase of temperature in the suspensions used as a blank (from initial 37°C to final temperature of 38.5°C, for pure PBS and sample G1); for the suspension prepared with the sample G2, with the lowest amount of HGNs (0.5%), the heating effect is small considering also the blank test (final temperature reached with 5 minutes of NIR irradiation 39°C); probably the HGN loading is not enough to generate a considerable heating. Increasing the amount of HGNs charged in the PLA nanoparticles an increasing heating effect is recorded. In the case of HGN theoretical loading of 1% (sample G3 in the figure) maximum temperature of 42°C is obtained, while in the case of HGN theoretical loading of 1.5% a maximum temperature of 43.5°C was reached in the suspension. Increasing the power of NIR irradiation, maintaining the exposition time to 5 minutes, an increasing heating effect is obtained **Figure X. 6 (b)**. Final temperature around 45-46°C was obtained in samples loaded with HGNs. In the case of biomedical application the 80% power irradiation is to be preferred because the final temperature reached is compatible with human tissue tissues that can resist to a maximum temperature of 42°C without degeneration (Field S.B. and Morris C.C., 1983). In the same Figure also the temperature decrease in the sample is reported after NIR exposure, to understand how the sample loses the heat after the treatment. Higher is the final temperature reached larger is the time required by the system to lose the heat generated under NIR irradiation. Considering the heating and the subsequent cooling of the sample, exposing the suspension to NIR irradiation for 5 min a period of temperature variation in the sample is generated in the range 15-20 min.

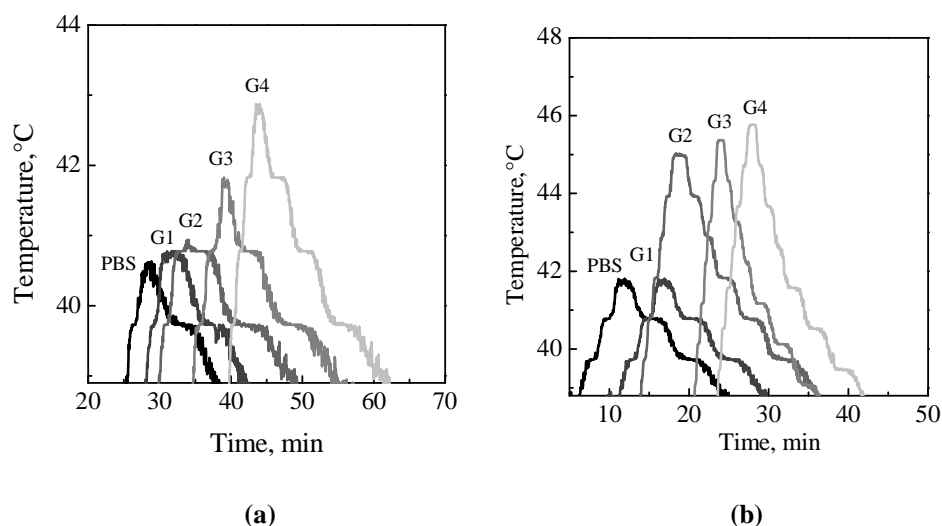


Figure X. 6 Temperature in PLA nanoparticles suspension during NIR irradiation at 80% of the power (a) and 100% of the power (b). NIR irradiation 5 min.

The effect of NIR irradiation condition on Rhodamine release is reported in **Figure X. 7** in the case of sample G3. Drug release without NIR irradiation is also reported for comparison. NIR irradiation was always applied after 0.2 hr of release, when the initial fast diffusion of the drug was completed, in this way it is better appreciated the effect of NIR irradiation. Irradiation were repeated each hour until the complete release of the drug was obtained. Concentration of Rhodamine in the suspension was analyzed before and after the irradiation. In general, from **Figure X. 7**, it is possible to see that PLA carriers produced in this work respond to NIR irradiation; it is possible to control externally the release rate of Rhodamine, changing the NIR irradiation conditions. When NIR is applied Rhodamine release was increased considerably. Complete release of the drug was obtained in less than one day, while without NIR irradiation the release takes 15 days. Slopes of the drug release curves change drastically when NIR was applied (from around 5 day^{-1} without NIR irradiation to several hundred when NIR was applied), indicating that a different release mechanisms are involved in this case. In details, when NIR was applied with the maximum of the power for 5 minutes the fastest release was obtained; just to applications of NIR irradiation were necessary to release all the encapsulated drug. When 80% of irradiation power was used three applications were required to release totally the drug when the duration of application was of 5 minutes. When, instead, shorter applications were used (2 minutes) the complete release is obtained after four NIR irradiations of the suspensions.

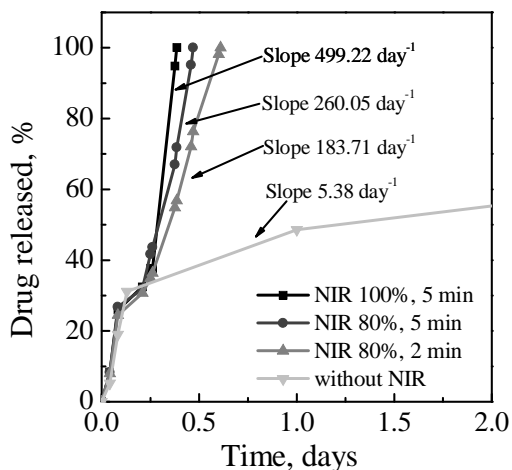


Figure X. 7 NIR controlled Rhodamine release from PLA particles loaded with 1% of HGNs in the polymer matrix (sample G3)

In **Figure X. 8 (a)** a comparison is reported of different Rhodamine release obtained irradiating suspensions of PLA nanoparticles with different HGN loading. 80% of the irradiation power was used and applied for 5 minutes each hour until the complete drug release. From this figure it is possible to notice that an increase of the release rate is obtained with the increase of the theoretical HGN loading in PLA nanoparticles, as also indicated by the slopes of the release curves reported in the same figure. Release rates were also plotted performed at different HGNs contents (reported in **Figure X. 8 (a)**); the release rate plot for the sample G2 is shown in **Figure X. 8 (b)**. When NIR irradiation was applied a peak of the drug concentration in the suspensions was always obtained; for this reason each peak of the release rate represents a different NIR application, therefore, a pulsatile drug delivery is obtained on demand. This is an important results, difficult to achieve otherwise. In the case of PLA nanoparticles suspension with the highest HGN loading (1.5%) the complete release is obtained after 2 irradiation of 5 minutes, as shown in **Figure X. 8 (a)**; in the case of 1% and 0.5% HGN loading 2 and 5 applications of NIR irradiation are respectively necessary to release totally the drug. A progressive increase of the release kinetic was obtained increasing the HGNs loading, probably connected with the larger temperature increase (previously discussed and reported in **Figure X. 6 (a)**).

In **Figure X. 8 (c)** and **(d)** SEM images of sample G4 (PLA nanoparticles encapsulating Rhodamine with 1.5% theoretical HGN loading) after first NIR irradiation, at the end of the release are reported. Polymer particles are partially fused and aggregated; considering all the experimental evidences, the most reasonable mechanism of release seems the softening of the

polymer shell of the PLA carriers due to temperature increase for photothermal effect. Consequently diffusion of water in the polymer matrix is increased and Rhodamine release in the medium accelerates. Thanks to these phenomena induced by NIR application, a pulsatile drug delivery can be obtained and controlled externally.

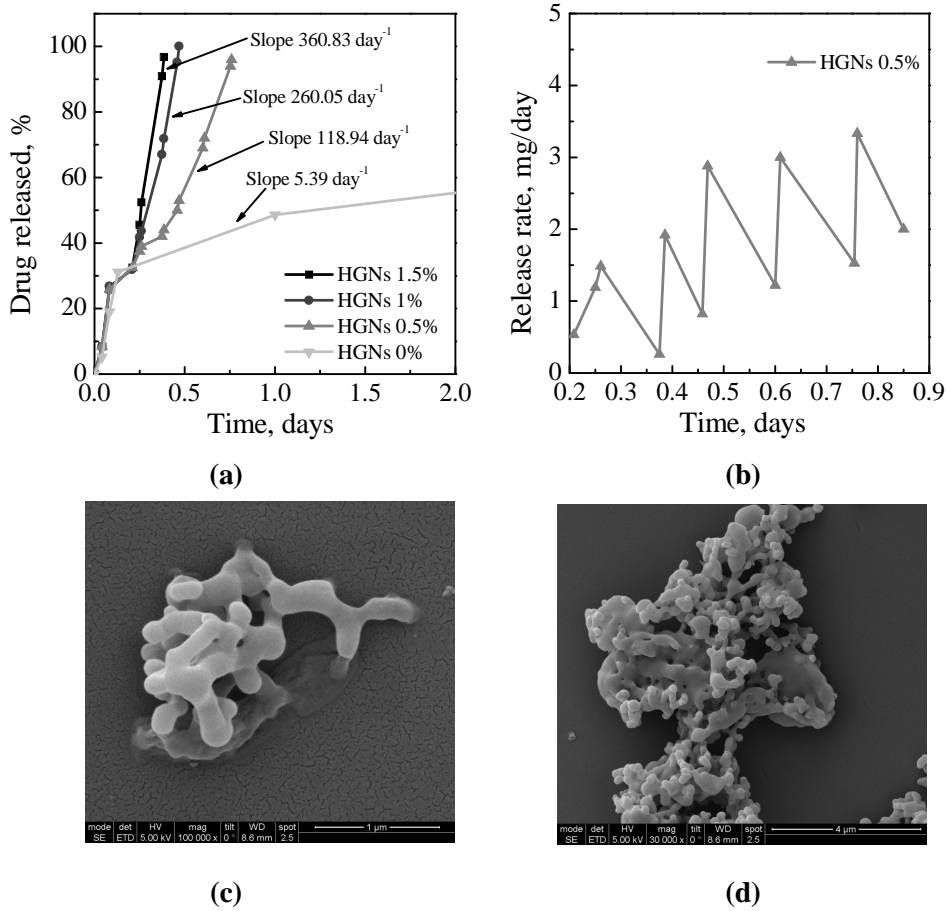


Figure X. 8 (a) NIR controlled release of PLA particles with different HGN loading and related drug release rate (b) NIR conditions: irradiation at 80% of the power for 5 minutes, each application. (c) and (d) SEM pictures of G4 particles at the end of NIR controlled Rhodamine release.

X.4 Conclusions

In this work biocompatible and biodegradable PLA-HGNs nanostructured devices for photothermal induced delivery of Rhodamine

were successfully produced using the SEE technique. Photoactivation of Rhodamine delivery from PLA carriers has been demonstrated successfully under different NIR exposition conditions, obtaining a pulsatile delivery of the drug when NIR is applied. Considering the experimental evidences obtained during this work, the release of the drug during NIR irradiation is probably due to the partial softening of the polymer shell of the PLA caused by temperature local increase for photothermal effect and consequent diffusion of water in the polymer matrix. Thanks to this phenomena, induced by NIR application, drug delivery can be induced on demand with release rate externally controlled.

Chapter XI

Solvent elimination from polymer nanoparticle suspensions by supercritical continuous extraction processing

XI.1 Introduction

According to what previously stated, nanoparticles of polymers, drugs and their co-precipitates are currently investigated to target drugs to specific tissues and to overcome internal membranes that are inaccessible to larger particulate systems (Salata O., 2004).

Several methods have been proposed for nanoparticles formation; they include solvent evaporation/extraction from emulsions (Feng S.S. and Huang G.F., 2001, Li Y.P. et al., 2001, Vila A. et al., 2002), dispersion polymerization (Zhang X. et al., 2008, Lee J.M. et al., 2009), supercritical antisolvent precipitation (Reverchon E. et al., 1998, Reverchon E. et al., 2007, Adami R. et al., 2008), and nanoprecipitation (Barichello J.M. et al., 1999, Govender T. et al., 1999, Peltonen L. et al., 2002, Jin C. et al., 2008). This last method was first developed by Fessi et al. (Fessi H. et al., 1989) and it is a simple and reproducible process. It requires two miscible solvents; the polymer and/or the drug must dissolve in the first one (the solvent) and to be not soluble in the second one (the non-solvent or dispersing phase). Nanoprecipitation occurs instantaneously when the primary polymer solution is added drop wise to the non-solvent phase. The original nanoprecipitation method uses an organic solvent to dissolve the polymer and/or the drug; water or a water solution is used as the non-solvent. A modified nanoprecipitation method has also been developed using two (or more)

organic solvents, as the solvent and the non-solvent; thus extending the application field of the process (Bilati U. et al., 2005b).

Several biopolymers and/or drugs have been processed by nanoprecipitation; among the others, PLGA (Poly-lactic-co-glycolic acid) (Beck-Broichsitter M. et al., 2010), PMMA (Polymethylmetacrylate) (Aubry J. et al., 2009), cellulose acetate (Kulterer M.R. et al., 2011), cyclosporin A, indomethacin, valproic acid, insulin, ketoprofen, vancomycin and phenobarbital nanoprecipitated with PLGA. Some coprecipitates polymer plus drug have also been proposed (Bilati U. et al., 2005a, Zili Z. et al., 2005, Das S. et al., 2010)

In this context, until now only a marginal attention has been given to the problem of the solvent elimination from the non-solvent phase. The classical solvent evaporation technique can fail in the effective removal of solvent residues and can induce thermal or stress solicitations on the nanoparticles system, producing degradation or coalescence of the product.

Supercritical extraction processes allows an effective elimination of the organic solvents from emulsions (Chattopadhyay P. et al., 2006, Della Porta G. et al., 2010). Therefore, the scope of this part of the work was to adapt the supercritical fluid continuous emulsion extraction process (SEE) to solvents removal from nanoparticles suspensions obtained by nanoprecipitation. Suspensions of model biopolymers PCL and PLGA were produced by nanoprecipitation, using solvents like acetone and acetone/ethanol mixtures as solvent phase and processed with the supercritical extraction process. Different nanoprecipitation condition were tested to evaluate the efficiency on the supercritical solvent elimination process.

XI.2 Experimental methods

XI.2.1 Materials

CO₂ (99.9%, SON, Naples, Italy), Polysorbate (Tween 80, Aldrich Chemical Co.), Sorbitan monolaurate (Span 20, Aldrich Chemical Co.) as surfactants, distilled water, Acetone (Ac, purity 99.9%, Aldrich Chemical Co.) as solvent, Ethanol (Et, purity 99.9%, Aldrich Chemical Co.) as cosolvent, Poly(lactic-co-glycolic) acid (PLGA, 75:25 MW: 20000, Resomer RG 752S, Boehringer), Polycaprolactone (PCL, MW 14000, Aldrich Chemical Co.), were used as received.

XI.2.2 Nanoparticles Preparation

The polymer was dissolved in 25 mL of acetone or in acetone/ethanol mixtures used as the organic solvents, at concentrations from 5 to 20 mg/mL to form the solvent phase; this solution was, then, added dropwise to the dispersing phase (50 mL) under magnetic stirring; stirring rate was varied

from 400 to 1500 rpm. The dispersing phase was formed by a liquid, water, in which the polymer is insoluble: the non-solvent. Both the solvent and the non-solvent phase optionally contained a surfactant; in detail, Span 20 and Tween 80 were dissolved in the solvent phase and the non-solvent phase at 0.2%w/w respectively. After the solvent removal, nanoparticles were recovered by filtration with a membrane and dried at air. The above procedure was always used, unless otherwise stated.

XI.2.3 Conventional Evaporation and Supercritical Fluids

Extraction Process

The suspension of nanoparticles prepared according to the illustrated nanoprecipitation method, needs a post-processing to remove the organic solvent. When the solvent was removed by evaporation, the suspension was placed in a 200 mL beaker magnetically stirred at 400 rpm for 2.5 h, at 38°C, at ambient pressure.

When the solvent was removed by supercritical fluid processing, the nanoparticle suspension was fed into a packed column for the continuous counter-current contact with SC-CO₂. A schematic representation of the supercritical process layout is reported in *Figure VII. 1* (pag. 38).

XI.2.4 Nanoparticles morphology, size distributions and zeta

potential determination

Particle size distribution and zeta-potential of the suspensions after the solvent removal were determined by dynamic light scattering (DLS) using a Zetasizer (mod. 5000, Malvern Instruments Ltd). Mean size and distribution was measured three times for each sample. Nanoparticles morphology was analysed by FESEM (mod. LEO 1525, Carl Zeiss SMT AG). Samples were prepared by cutting a piece of membrane and placing it over aluminium stabs. The samples were then coated with a Gold layer (mod.108 A, Agar Scientific).

XI.2.5 Solvent Residue Analysis

Acetone and ethanol residues in the suspensions were measured to determine the efficiency of solvent removal. Solvent residues were measured using a head space sampler (mod. 50 Scan, Hewlett & Packard) coupled to a gas chromatograph interfaced with a flame ionization detector (GC-FID, mod. 6890 Agilent Series, Agilent Technologies Inc). The solvent was separated using a fused-silica capillary column 30 m length, 0.55 mm

internal diameter, 0.1 μm film thickness (mod. DB-WAX). Oven temperature in the GC was set to 45°C for 10 min, then 15°C/min until 150°C. The inlet temperature was set at 250°C, detector at 270°C. Helium was used as carrier gas (5 mL/min), split mode, ratio 1:10. Head space conditions were: vial temperature 95°C, loop temperature 95°C, transfer line temperature 105°C. Head space samples were prepared in 10 mL vials filled with 1 mL of suspension.

XI.3 Results and discussion

XI.3.1 Acetone elimination from PCL water suspensions

The evaporation of solvents from nanoparticle suspensions prepared by nanoprecipitation technique is a very long process and can induce degradation of thermolabile compounds or aggregation of the particles (Li M. et al., 2008); other purification techniques, such as, high speed centrifugation and dialysis can lead to the formation of cakes which are not readily dispersible. In the case of a suspension in an organic solvent, the problem could be even more complex: nanoparticles may give coalescence that occurs during the progressive replacement of the non-solvent, that causes instability of the suspensions. Bilati et al. also reported that flocculation can take place during the washing steps with water.

In this work, we adapted the continuous solvent elimination process previously proposed for emulsions extraction. This technique was used until now to produce microspheres of biopolymers for controlled drug release, starting from emulsions. The process is based on the continuous counter-current contact between two films (liquid and SC-CO₂) in a packed tower; the mixing between the fluids takes place on the extremely high surface area of the packing; thus the extraction is fast and efficient. In this specific work, the tower is used to put in contact the suspension of nanoparticles, freshly formed using the nanoprecipitation method, with SC-CO₂.

The operating conditions, in terms of pressure and temperature, were chosen from high pressure vapor liquid equilibrium diagrams (VLE) to ensure the selective extraction of organic solvents from water based suspensions (Chin H.Y. et al., 2008). Considering the VLE diagram of the solvent/s to be extracted with CO₂, the operating points of the process should be typically located over the mixture critical point (MCP). Temperature was fixed at 38°C, i.e. at a temperature lower than the glass transition temperature of PLGA. Another important operating parameter, to take into account when operating with the continuous extraction tower, is the liquid to gas ratio (L/G). Difficult separations are characterized by very low L/G ratio, it means that high quantities of SC-CO₂ are necessary per unit of liquid, to obtain the desired extraction efficiency. Anyway it is not possible to decrease freely the L/G ratio; at elevated flow rates of the gas stream, the

liquid is entrained by the gas and discharged at the top of the column: this condition does not allow proper working of the tower (flooding) and has to be avoided (Brunner G., 2009). Based on the previous experiments on this process, L/G ratios were varied between 0.05 and 0.2 by weight.

A first set of the results obtained in terms of acetone residues and suspensions stability is reported in **Table XI. 1**, and is referred to PCL nanoparticles in an acetone/water solution. The best results, as expected, have been obtained at a low L/G value (0.1), that, as previously explained, allows the best contact between the two phases and guarantees the contact of a larger quantity of solvent (CO₂) with the organic residue. It is also evident that an increase of CO₂ solvent power, obtained increasing the process pressure improves largely the solvent elimination, that (at L/G=0.1), is reduced from 967 ppm at 80 bar to 74 ppm at 100 bar, i.e. well below the limits imposed for this solvent by current good manufacturing practices (C-GMP) of the pharmaceutical industry (*ICH guidelines for residual solvent*). It is also worth of note that the nanoparticles obtained at the end of the process show a very small SD.

Table XI. 1 Acetone residue after continuous supercritical fluid extraction (SFE). CO₂ flow rate=1.4 Kg/h. An example of traditional solvent evaporation is also reported for comparison (SE). All the suspensions were prepared with 0.5% w/w of PCL and at 800 rpm.

SFE	Pressure [bar]	L/G	MS±SD (nm)	Solvent residue [ppm]
SC1	80	0.2	192±36.5	2700
SC2	90	0.2	184±34.0	2507
SC3	100	0.2	203±48.8	176
SC4	80	0.1	173±32.9	967
SC5	90	0.1	191±42.0	712
SC6	100	0.1	187±43.0	74
SE	Time [h]	Rpm		Solvent residue [ppm]
SE1	2.5	400	178±32.1	>3000

The results are also summarized in *Figure XI. 1*, where it is also possible to observe that, when a pressure of 100 bar is used, the solvent residues for different L/G ratio are very similar: it means that the increase of the CO₂ solvent power overcomes the influence of L/G ratio.

In *Table XI. 1* it is also proposed the solvent residue of a suspension purified by evaporation; this process was performed at 38°C for 2.5 h. A higher solvent residue was found. In addition supercritical process does not modify particle size distribution, as indicated by PSDs data reported in *Table XI. 1* and SEM image of PCL nanoparticles recovered after supercritical fluids extraction in *Figure XI. 2* demonstrates that particles are spherical and not aggregated.

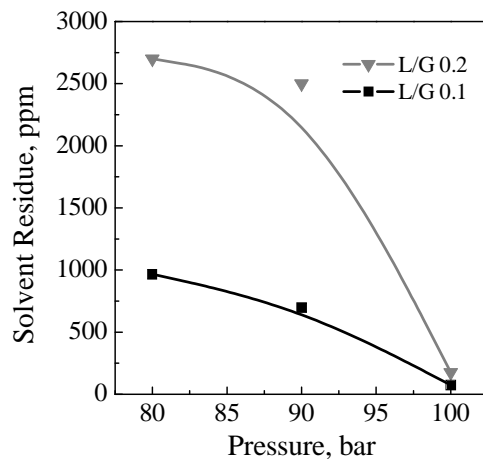


Figure XI. 1 Acetone residue diagram in PCL nanoparticle suspension for different operating pressures and L/G ratios

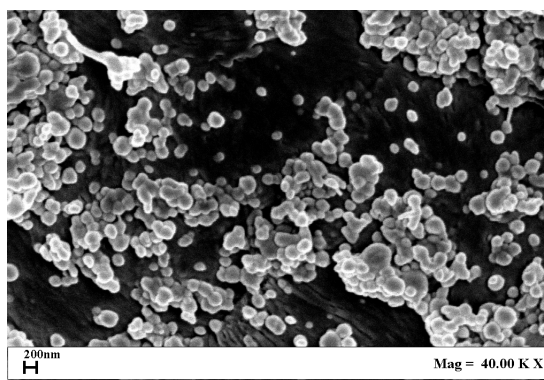


Figure XI. 2 SEM image of PCL nanoparticles recovered after filtration and drying

XI.3.2 Acetone/ethanol elimination from PLGA water suspensions

Another possible nanoprecipitation formulation proposed in the literature (Tsukada Y. et al., 2009) and here applied, is the precipitation of PLGA using a mixture of ethanol plus acetone as the solvent phase. Ethanol is a non-solvent for PLGA therefore, its presence should favour the formation of smaller particles. For this reason, supercritical solvent elimination process conditions have to be optimized also in the case of acetone/ethanol mixtures. The solubility of PLGA in the mixture of solvents decreases increasing the ethanol content. First tests on solvent residues were performed using

suspensions produced with 0.5% of PLGA in 25 ml of acetone/ethanol mixture 50/50 (PLGA does not dissolve in mixtures with higher content of ethanol). The effect of pressure and L/G ratio were measured to reduce the ethanol content below the Pharmacopoeia limit of 5000 ppm.

In the case of mixtures of solvents the optimized operating conditions used for acetone residues (100 bar, 38°C, L/G 0.1) demonstrated to be not useful for elimination (**Table XI. 2**); even if acetone and ethanol are both well miscible in SC-CO₂ and in principle can be completely extracted by the supercritical fluid. Looking at the VLE diagrams of acetone and ethanol with SC-CO₂ at 38°C (Chin H.Y. et al., 2008), reported in **Figure XI. 3**, it is possible to note that although the mixture critical point pressure is below 80 bar and very similar in both cases, the immiscibility region is wider in the case of ethanol. This difference could explain the different results obtained using these two solvents: the larger immiscibility hole in the case of ethanol can be a signal of a lower affinity between this solvent and SC-CO₂.

Table XI. 2 Acetone and ethanol residues after continuous supercritical fluid extraction. CO₂ flow rate=1.4 Kg/h, temperature 38°C. All the suspensions were prepared with 0.5% w/w of PLGA in 25 mL of acetone/ethanol 50/50 and at 400 rpm.

SFE	Pressure [bar]	L/G	Ethanol residue [ppm]	Acetone residue [ppm]	MS±SD (nm)
SC7	100	0.1	>20000	85	167±22
SC8	120	0.1	21680	112	170±31
SC9	130	0.1	11088	55	162±16
SC10	140	0.1	6313	38	158±25
SC11	120	0.05	3862	38	162±28
SC12	130	0.05	2986	38	167±20
SC13	140	0.05	1299	31	163±19

To increase solvent power of SC-CO₂, pressure was varied in the range from 100 and 140 bar. L/G was also reduced to 0.05 reducing liquid flow rate.

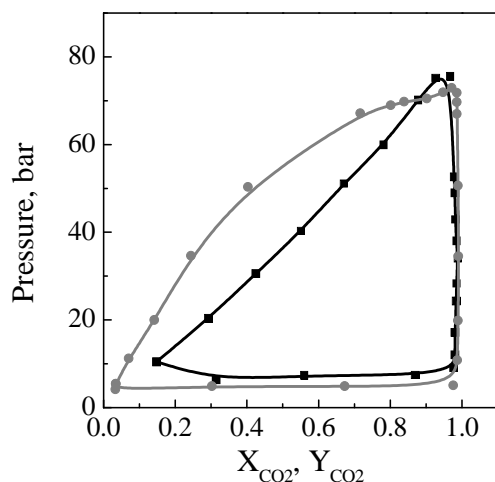


Figure XI. 3 VLE diagram of acetone ■ and ethanol ● with SC-CO₂ at 38°C adapted from Chiu et al. (Chin H.Y. et al., 2008)

From data reported in *Table XI. 2*, and from *Figure XI. 4 a*, it is evident that an increase of CO₂ solvent power, improves largely the solvent elimination. However also at 140 bar ethanol residues is higher than the acceptable limit when operating with L/G ratio of 0.1. But better results were obtained when operating at L/G 0.05. In this case ethanol residues are always below the acceptable limit. At 140 bar 1299 ppm of ethanol residue was obtained, well below the Pharmacopoeia limit.

We measure also solvent residue for acetone at these pressure and L/G and, obviously, acetone residue further reduced (*Table XI. 2, Figure XI. 4 b*) with respect to the tests performed at lower pressure (see *Table XI. 1*).

To verify if the presence of acetone modified ethanol elimination when acetone/ethanol mixtures were tested we also performed experiments on ethanol alone in water; no relevant differences were found.

At this point solvent elimination feasibility has been confirmed; thus, we performed further experiments to verify if the other nanoprecipitation process parameters like the kind of polymer or different solvents or solvent mixtures could influence the solvent elimination. These further results are summarized in *Table XI. 3*

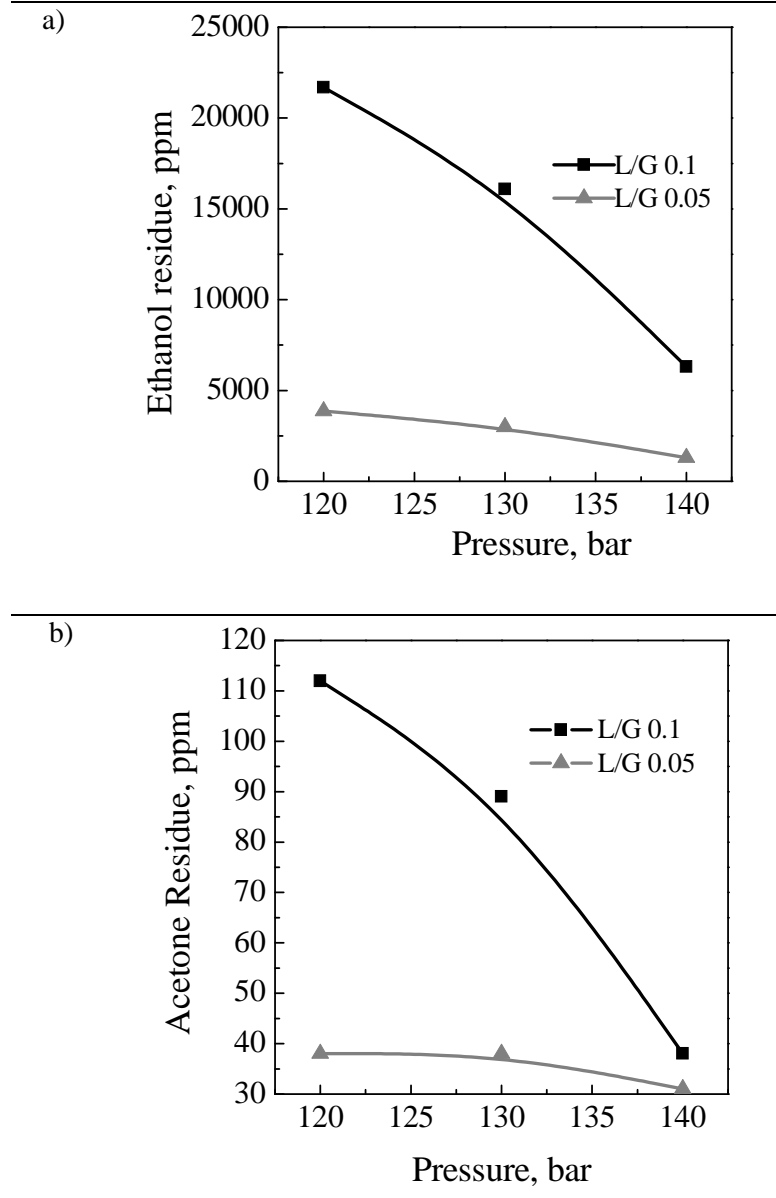


Figure XI. 4 Ethanol and acetone residue in PLGA nanoparticle suspension for different operating pressures and L/G ratios.

XI.3.3 Influence of the nanoprecipitation parameters on the efficiency of the supercritical post processing

The first part of this study has been performed again on PCL dissolved in acetone plus small quantities of Span 20 (0.2% w/w), 0.5-2.0% w/w using water plus Tween 80 (0.2% w/w), as the non-solvent. Nanoparticles with mean size (MS) ranging between about 210 and 360 nm were obtained. Then similar experiments were performed with PLGA using acetone. Again the results are reported in **Table XI. 3** considering also the presence of mixtures acetone/ethanol was considered.

The photo in

Figure XI. 5 shows the macroscopic aspect of the suspensions obtained after the supercritical extraction process, relative to the PCL nanoparticles obtained at three different polymer concentrations 0.5, 1.0 and 2.0% in the solvent phase. The samples show the characteristic opalescence formed by nanoparticle suspensions, the colour of the suspensions varies from lightly opalescent to whitish with the increase of PCL content.



Figure XI. 5 Macroscopic aspect of nanoparticle suspensions obtained with different PCL content. The polymer percentage in solvent phase is 0.5, 1.0, 2.0 from the left to the right of the image

SEM images reported in

Figure XI. 6, show the microscopic aspect of the PLGA particles: they have a regular spherical shape and their diameters substantially confirm the measurements performed using the DLS technique. It is also evident the enlargement of the PSD passing from 0.5% to 2.0% w/w concentration.

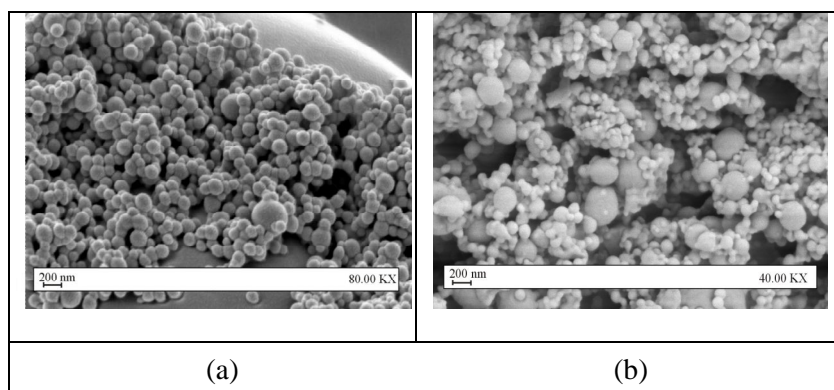


Figure XI. 6 SEM images of nanoparticles recovered after filtration and drying. (a): PLGA 0.5%; (b): PLGA 2%

Looking at **Table XI. 3**, it is possible to observe that acetone residue is not affected by the kind of polymer processed or by its concentration and ranges around 50 ppm, as expected from the previous optimization of the supercritical extraction process. This value is well reproducible and always lower than pharmacopeia limits. Also when the mixtures of solvents are used an efficient solvents removal was confirmed.

Zeta potential values of the processed suspensions (**Table XI. 3**) ranged between about -18 and -7.84 mV; the suspensions before supercritical processing show approximately the same values, showing that the process proposed does not compromise the stability of nanoparticles. The smallest nanoparticles were observed for PLGA using 50/50 ethanol/acetone (167 nm) and the sharpest distribution with a PDI of 0.04 was observed for ethanol/acetone 20/80 (**Table XI. 3**). The supercritical processing successfully contributed in preserving the nanoparticles identity.

Table XI. 3 Nanoprecipitation conditions of the experiment performed with different stirring rate and with different PCL and PLGA content using acetone and ethanol/ acetone mixtures as solvent phase and 50 mL of water as non-solvent phase. Solvent residue values were measured at the optimized processing conditions: 140 bar, 38°C, L/G 0.05.

	(% w/w)	Solvent (mL)	rpm	MS \pm SD (nm)	PDI	[mV]	[ppm]
SC14	PCL 0.5%	25 mL Ac	400	255 \pm 23.5	0.09	-7.67	50
			800	210 \pm 25.2	0.12	-19.9	
			1500	230 \pm 29.9	0.13	-11.1	
SC15	PCL 1.0%	25 mL Ac	400	284 \pm 25.6	0.09	-11.8	58
			800	273 \pm 32.8	0.12	-18.4	
			1500	280 \pm 56	0.2	-15	
SC16	PCL 2.0%	25 mL Ac	400	362 \pm 54	0.16	-17.2	52
			800	317 \pm 57	0.18	-11.8	
			1500	320 \pm 70.4	0.22	-10.1	
SC17	PCL 0.5%	25 mL Ac	400	215 \pm 23.6	0.11	-9.97	50
SC18	PCL 1.0%			248 \pm 19.8	0.08	-9.21	55
SC19	PCL 2.0%			340 \pm 57.8	0.17	-7.84	55
SC20	PLGA 0.5%	25 mL Ac/Et 80/20	400	207 \pm 7.9	0.04	-11.1	Ac 42 Et Y
SC21	PLGA 0.5%	25 mL Ac/Et 60/40	400	196 \pm 17.6	0.09	-12.7	Ac 38 Et 1241
SC22	PLGA 0.5%	25 mL Ac/Et 50/50	400	167 \pm 20	0.12	-11.6	Ac 31 Et 1300

XI.4 Conclusions and perspectives

A new post processing technology was proposed and successfully applied for the removal of the solvents from water based nanoparticle suspensions; it takes advantage of the enhanced mass transfer between supercritical CO₂ and the organic solvents and their mixtures tested were rapidly removed with continuous process. Polymer nanoparticles were successfully processed changing nanoprecipitation solvent and process condition.

Chapter XI

The next part of the thesis work is related to encapsulation of drugs, proteins and metal oxides for the production of multifunctional carriers, the SEE technique was used for this scope because it allows the highest encapsulation efficiency preserving the compounds integrity.

Chapter XII

Supercritical Assisted Injection in Liquid Antisolvent (SAILA)

XII.1 Introduction

There are several of ways to fabricate the nanomaterials. The various processes that have been proposed to obtain nanomaterials follow two main approaches: “top down” and “bottom up”. Top-down is characterized by the production of nanoproducts departing from normal size materials; i.e., reducing the dimensions of the original material; for example, using special size reduction techniques. The bottom-up approach is related to the “synthesis” of nanosized materials, starting from the molecular scale; for example, the formation of particles by precipitation from a fluid phase. The “widely known” methods to obtain nanomaterials are sol-gel synthesis, inert gas condensation, mechanical alloying or high-energy ball milling, high pressure homogenization, plasma synthesis, and electrodeposition.

All these processes synthesize nanomaterials to varying degrees of commercially quantities.

Thermal methods of making nanoparticles involve the hydrolysis of compounds in an oxygen-hydrogen gas flame, but these methods can sometimes be undesirable because of the extremely high temperatures required for processing (approximately 2000 °C). A much more widely used and popular method of manufacturing nanoparticles is the sol-gel processing technique. With this technique particles are precipitated using two main methods but both involve hydrolysis and then subsequent condensation using solvents. Recently, other authors synthesized nanoparticles by directing a high-temperature plasma jet of an inert gas onto a particles-containing compound, thereby forming vapor and condensing the vapor to form nanoparticles (Schultz S. et al., 2002, Schultz S. et al., 2004).

Mainly, these processes are involved in the production of inorganic nanoparticles. However, nanoparticles are also receiving considerable attention for the delivery of therapeutic drugs or nutraceutical compounds.

The literature emphasizes the advantages of nanoparticles over microparticles. The submicron size of nanoparticles offers a number of distinct advantages over microparticles, including relatively higher intracellular uptake compared with microparticles. Other advantages are high stability, high carrier capacity, the feasibility of incorporation of both hydrophilic and hydrophobic substances, and the feasibility of variable routes of administration, including oral application and inhalation. Nanoparticles can also be designed to allow controlled (sustained) drug release from the matrix. These properties of nanoparticles enable the improvement of drug bioavailability, the reduction of side effects and of the problem related to the dosing frequency. This kind of nanoparticles is usually produced by techniques such as emulsification-solvent evaporation micronization, high-pressure homogenization, solubilization using co-solvents (Tomasko D.L. et al., 2003).

The above described processes are well established and widely studied but suffer from some drawbacks that, depending on the cases, range from the control of particle size distribution to the processing of thermolabile compounds. In this prospective, supercritical fluids may provide a way to overcome the above-mentioned disadvantages, via innovative processing conditions and methods. Indeed, in recent years, the huge interest in nanomaterials has also involved supercritical fluid technologies and because of the supercritical fluid properties, the use of CO₂ may well provide a very promising alternative strategy in nanoparticle production (Reverchon E. and Adami R., 2006).

Several supercritical based techniques have been proposed in the literature for the production of micro and nanomaterials, since several processes can operate in the micronic or in the nanometric domain depending on the operating conditions and on the process arrangement.

Particularly useful for the introduction of the innovative process developed during this work, the Rapid Expansion of Supercritical Solutions (RESS) process consists of the saturation of the supercritical fluid with a solid substrate; then, the depressurization of the solution through a heated nozzle into a low pressure chamber produces a rapid nucleation of the substrate in the form of very small particles which are collected from the gaseous stream. Turk et al. used the RESS process to produce β -sitosterol (an anticholesteremic) nanoparticles of about 200 nm mean diameter. They also used this process for the production of griseofulvin (an antibiotic) nanoparticles using supercritical CHF₃ (Turk M. et al., 2002). Sane et al. used RESS to produce fluorinated tetraphenylporphyrin (a photosensitizer for photodynamic therapy) spherical, agglomerated nanoparticles with average particle sizes from 60 to 80 nm, at different pre-expansion temperatures (Sane A. et al., 2003).

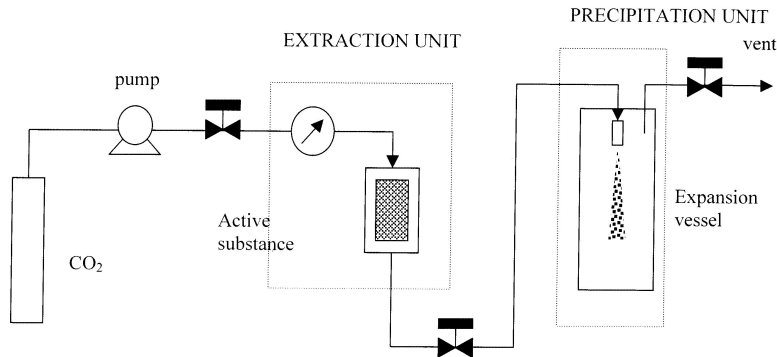


Figure XII. 1 RESS equipment concept (Jung J. and Perrut M., 2001)

The results from RESS experiments suggest that the RESS process generally produces micron- or submicron-sized particles (Helfgen B. et al., 2000, Kröber H. et al., 2000). For nano-sized particles, it has been made a simple but significant modification to the traditional RESS by using a liquid solvent or solution at the receiving end of the supercritical solution expansion, named the Rapid Expansion of a Supercritical Solution into a Liquid Solvent (RESOLV). The RESOLV process produces exclusively nanoparticles from a variety of materials. For example, cadmium sulfide (CdS) nanoparticles of ~3 nm in average diameter were prepared by means of RESOLV by rapidly expanding a supercritical ammonia solution of $\text{Cd}(\text{NO}_3)_2$ into a room-temperature solution of Na_2S in water or ethanol (Sun Y.-P. and Rollins H.W., 1998). The nanoparticles produced in the process could be prevented from aggregating by the presence of a polymeric or other protection agent in the receiving solution. It should be noted that there was a precipitation reaction accompanying the rapid expansion process in the formation of CdS nanoparticles. The same RESOLV process with a similar reaction scheme has been applied to the production of many other semiconductor and metal nanoparticles. These nanoparticles are all small, on average less than 10 nm in diameter, and are protected to form stable suspensions (Sun Y.-P. et al., 2001).

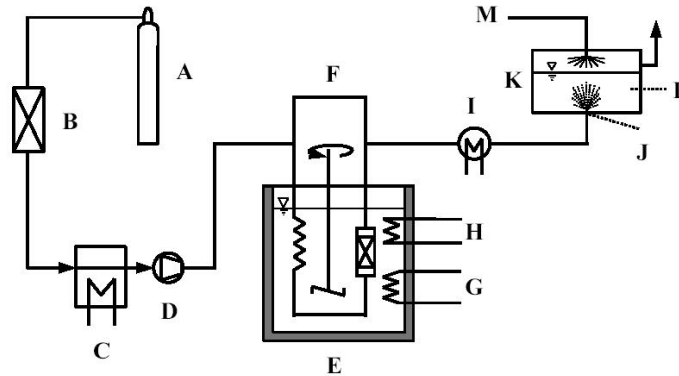


Figure XII. 2 Schematic RESOLV experimental apparatus (Turk M. and Lietzow R., 2004)

The traditional RESS process has been also particularly popular in the processing of polymeric materials. Particle formation in RESS from a large number of polymeric materials has been reported (Mishima K. et al., 2000). For example, Smith and co-workers used RESS to prepare a variety of micron-sized polymer particles, including polystyrene, polypropylene, poly(carbosilane), poly(phenyl sulfone), poly(methyl methacrylate), and cellulose acetate. However, formation of nano-sized particles has apparently not been a focus of the community. Instead, much effort has been on an understanding of the RESS process for different products, particles versus fibers.

The rapid expansion in both RESS and RESOLV should probably produce nanoscale particles in the absence of any secondary processes. Theoretical modeling of the traditional RESS process has predicted the formation of sub-50 nm particles upstream of the Mach disk in the supersonic free jet region and that the typically observed micron-sized particles are from the particle growth processes of condensation and coagulation that occur downstream of the Mach disk in the transonic and subsonic free jet regions. A similar conclusion was reached according to the computational fluid dynamics calculation for the RESS processing of a perfluoropolyether diamide oil, though the final product was a liquid instead of solid particles (Franklin R.K. et al., 2001). In this context, the use of a liquid at the receiving end of the rapid expansion in RESOLV probably inhibits or disrupts the condensation and coagulation in the expansion jet, thus effectively quenching the rapid particle growth processes. In

highlighting the RESOLV production of nanoscale polymeric particles.

The production of polymeric nanoparticles through RESOLV may conceptually be divided into two somewhat related processes. One is the initial formation of nanoparticles in the rapid expansion, and the other is the stabilization of the suspended nanoparticles. Evidently, the protection of initially formed polymeric nanoparticles represents a different set of technical challenges, which are largely independent of the rapid expansion process itself, especially if the protection agent is added immediately after the expansion. The good news is that many methods for stabilizing nanoparticle suspensions are already available in the literature, some of which have shown promise in use with RESOLV.

One common limitation of the RESS and RESS-derived technique is the limited solubility of most the compounds of interest in the SCFs. All these techniques share a solubilisation step in a SCF; but many compounds of industrial interest show very limited or negligible solubility in SC-CO₂, even at high pressure. Therefore, the applicability of these techniques is limited and/or their productivity is small. One possibility to overcome these limitations is to use an expanded liquid; i.e., to form a solution between a liquid solvent and a gas. For example, SC-CO₂ shows a relevant affinity with almost all the organic solvents: the corresponding pressure-composition (p-x) diagrams are characterized by a miscibility hole (two phase system), but also by regions of the diagram in which large quantities of CO₂ can be mixed with the liquid to form a single phase mixture (Reverchon E. and De Marco I., 2011). In this conditions large quantity of solute can be solubilised in the expanded liquid solution. The basic idea of the new process we have proposed with this thesis, is the continuous injection of an expanded ternary solution (SC-CO₂-Solvent-Solute), by depressurization through a nozzle, directly into a second solvent (in which a surfactant can be added) where the solute is not soluble and the organic solvent of the expanded liquid is completely miscible; therefore, the receiving solution works as a liquid antisolvent. Operating in this manner, nanoparticles can be generated.

The proposal of SAILA process takes origin from the following general considerations: liquid-liquid antisolvent precipitation is obtained when the processed compound is soluble in the solvent and not soluble in the antisolvent; the particles size of the precipitates depends on the efficiency of the micromixing between the two liquids

that, in turn, is related to their surface tension (Umemura A. and Wakashima Y., 2002). Therefore, the continuous injection of an expanded liquid solution should be more effective than the mixing with an ordinary liquid. Indeed, expanded liquid are characterized by a reduced surface tension that at high gas molar fractions is near to zero (Brunner G., 1994); this characteristic should improve the micromixing with the antisolvent and produce smaller particles.

The process developed and proposed with this thesis is named Supercritical Assisted Injection in Liquid Antisolvent (SAILA); from the review of the state of the art of the supercritical based technique for the production of micro and nanoparticles reported in this introduction it is clear that the process developed is completely new and brings several conceptual innovations to the RESS and RESS-derived technique, from which it takes inspiration. First of all the use of an expanded liquid solution instead of a supercritical solution used in the RESS technique, which allows to solubilise larger quantity of solute, that in principle can also be completely non-soluble in SC-CO₂, thus enlarging the range of applicability of this process to many class of compound not soluble in SC-CO₂; second the principle of nanoparticles formation is completely different; indeed, it does not evolve from the sovrasaturation and precipitation of particles produced during expansion of the supercritical solution, as in the RESS technique, but sovrasaturation is produced thanks to the solvent-antisolvent effect that takes place at the exit of the nozzle. Furthermore, liquid-liquid antisolvent precipitation is improved by the reduced surface tension of the expanded liquid that enhance the micromixing promoting the fast precipitation of particles. If rapid precipitation conditions are achieved during SAILA process, compact crystalline structures cannot be formed due to insufficient time available for crystal growth. This results in formation of amorphous particles (Li X.-S. et al., 2007). Transforming the physical state of drug to highly disordered amorphous state increases the dissolution rates (Pathak P. et al., 2004, Won D.H. et al., 2005).

In view of all these innovations of our idea a considerable afford has been done to the construction of the most appropriate process layout to convert in practice this innovative idea, with the realization a new experimental apparatus, for the concept validation. Than a wide experimental plane has been done on several different compounds to demonstrate the feasibility of the process, to understand the influence of the process parameters on particles size distributions and to develop a first mechanical model about particle formation process.

XII.2 Experimental SAILA apparatus description

A schematic representation of the SAILA process layout is reported in *Figure XII. 3* and in *Figure XII. 4* a detail of the precipitator is presented.

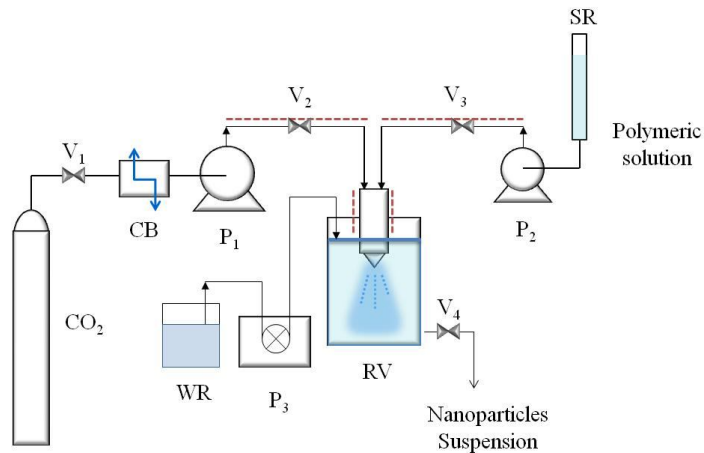


Figure XII. 3 Schematic representation of the SAILA process layout. CO_2 : Carbon Dioxide reservoir; V_1 , V_2 , V_3 , V_4 : on-off valves; CB : cooling bath, P_1 : CO_2 pump; P_2 : liquid pump; P_3 : peristaltic pump SR : solvent reservoir; WR : water reservoir; RV receiving vessel

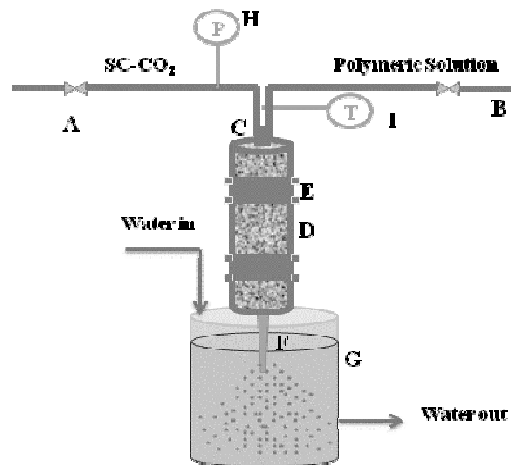


Figure XII. 4 Detail of the saturation-injection of the SAILA process apparatus. A : $SC-CO_2$ feeding line; B : Liquid Solution feeding line; C : Saturator; D : packing elements; E : heating elements; F : injector; G : non-solvent receiving phase; H : manometer; I : thermocouple.

It mainly consists of two feed lines, used to deliver the compressed CO₂ (A) and the liquid solvent (B) to a mixing vessel (saturator, C). Carbon dioxide is cooled, pumped (P1), preheated and delivered to the saturator (C). The liquid mixture formed by the solvent (in which a solid solute is dissolved), is delivered to the saturator by a membrane pump (P2) and is preheated before the inlet to saturator. The saturator is a high-pressure vessel with an internal volume of 0.15 dm³, heated by thin band heaters (E) and packed with stainless steel perforated saddles with a high specific surface area (D). It provides a large contacting surface and an adequate residence time (3-5 min, depending on the flow rates) for the liquid-gas mixing. Therefore, an efficient, continuous solubilisation of SC-CO₂ in the liquid solution is obtained. As a result, the two fluids form an expanded liquid, whose position in the vapor-liquid equilibrium diagram (VLE) of the system CO₂-organic solvent depends on the conditions of temperature, pressure and on gas to liquid ratio (GLR, here expressed as weight ratio). The solution at the exit of the mixer is injected into the receiving water phase using an orifice that has a diameter of 80 µm and a length to diameter ratio of 6.67. The water phase is continuously taken from a reservoir (WR) and pumped with a peristaltic pump (P₃) in the receiving vessel (RV); the suspension is continuously recovered through a regulation valve (V4), that is also used to maintain a constant liquid level in the vessel.

The CAD project of the plant is also reported in *Figure XII. 5*.

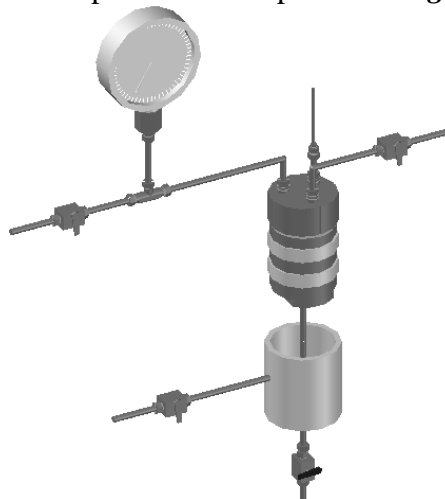


Figure XII. 5 CAD project of the SAILA plant

Specifically, the liquid solution is prepared dissolving a known amount of solute in acetone. The receiving phase is formed by a water solution containing Tween 80 (0.2% w/w), used as surfactant.

XII.3 SAILA process description and mechanism of particles

formations

In the SAILA process particles are mainly produced due to the achievement of instantaneous supersaturation thanks to the micromixing of solvent and antisolvent obtained with the injection of the expanded liquid in the antisolvent solution.

XII.3.1 Role of the antisolvent

The precipitation of nanoparticles proceeds in steps of mixing of expanded liquid solution and antisolvent, generation of supersaturation, nucleation, and growth by coagulation and condensation, followed by agglomeration in case of uncontrolled growth as shown in *Figure XII. 6*. The main driving force for precipitation is rapid and high supersaturation. The crucial particle properties such as size, morphology and purity are significantly dependent on the rate, magnitude and uniformity of supersaturation generated during the process of precipitation (Mayrhofer B. and Nyvlt J., 1988, Jones A.G. and Mullin J.W., 1974). The supersaturation, according to crystallization theory, for one-component in liquids is defined as

$$S = \frac{c}{c^*} \quad 1)$$

where c is the actual concentration of solute in the solution (mol/L) and c^* is the equilibrium solubility (mol/L) of the solute in a mixture of organic solvent and antisolvent.

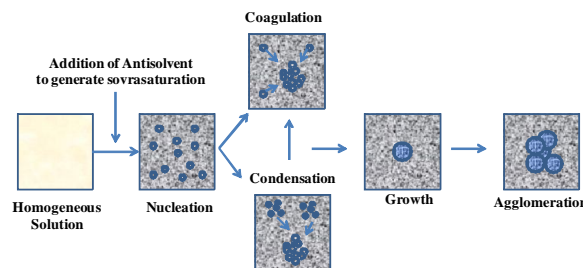


Figure XII. 6 Schematic of particle precipitation process

The energy barrier for particle precipitation from saturated solution depends on the metastable zone width. The metastable zone is the concentration range where no precipitation is observed within given time. Guo et al. (Guo Z. et al., 2005) reported that when metastable zone is wide, inducing nucleation is difficult and therefore in order to achieve higher nucleation rates, metastable zone width should be shorter. Another important parameter is induction time (Granberg R.A. et al., 2001). Induction time is the time elapsed between supersaturation of a solution and appearance of detectable crystals (Mahajan A.J. and Kirwan D.J., 1993). Higher nucleation rates result in precipitation of nanoparticles, as in such a case, supersaturation is mainly consumed by nucleation and not for growth of particles. Therefore, to obtain nanoparticles with narrow size distribution it is necessary to,

- (a) create a high degree of supersaturation,
- (b) uniform spatial concentration distributions in solutions, and
- (c) the negligible growth of all crystals (Dalvi S.V. and Dave R.N., 2009).

The nucleation and growth of particles occur simultaneously and both compete for consumption of supersaturation (Thybo P. et al., 2008). Once nucleation occurs particles grow by condensation (τ_{cond}), (as molecules diffuse to the particle surface and become incorporated into the solid phase), and by coagulation (τ_{coag}). Condensation competes with nucleation by decreasing supersaturation. Coagulation can reduce the rate of condensation by reducing the total number of particles and therefore the surface area (Staff S. and Sun Y.P., 2002). As particles grow, they start agglomerating too. The agglomeration process depends on the population density. It has been reported that higher the population density higher is the agglomeration rate.

Thus, there are several parameters such as, metastable zone width, induction time, interfacial surface energy and supersaturation which control the precipitation of particles from supersaturated solutions. Particle engineering therefore, requires fine-tuning of these variables to obtain desired particle characteristics.

XII.3.2 Role of Mixing

In liquid antisolvent precipitation process, mixing generates supersaturation which is followed by, nucleation and growth. Accordingly, there are two main time scales associated with the process of particle formation, namely mixing time (τ_{mix}) and the precipitation or induction time ($\tau_{\text{precipitation}}$) (Johnson B.K. and Prud'homme R.K., 2003). Mixing time (τ_{mix}) comprises of the time required for macromixing, mesomixing, and micromixing. Mixing occurring on a macroscale scale is termed as macromixing. Mesomixing consists of the large-scale mass transfer of a

solution which is also known as turbulent mixing (Shekunov B.Y. et al., 2001). Molecular diffusion of different solvent composition region below Kolmogorow microscale is termed as micromixing (Baldyga J. et al., 1997). $\tau_{\text{precipitation}}$ is composed of nucleation time ($\tau_{\text{nucleation}}$) and growth time (τ_{growth}) (Matteucci M.E. et al., 2006). The dimensionless Damkohler number (Da) is the ratio of τ_{mix} to $\tau_{\text{precipitation}}$. The particle formation process is controlled by mixing when Da is greater than 1. In this situation, the mixing process is slower than precipitation process and supersaturation is attained at a slower rate. This results in dominance of particle growth leading to large crystals. On the other hand when Da is less than 1, τ_{mix} is reduced relative to $\tau_{\text{precipitation}}$, up to certain threshold where supersaturation is attained rapidly, solution is mixed uniformly at the micro-level and nucleation takes place rapidly. The process of mixing is faster than precipitation and precipitation step controls overall particle formation. In this situation nucleation dominates in the precipitation process. This leads to a large number of nuclei and precipitation of ultrafine particles. Under such a situation longer time is required for condensation and coagulation, which leads to reduction in particle size. Thus, it is necessary to decrease τ_{mix} and increase $\tau_{\text{precipitation}}$ in order to keep $Da < 1$, for production of nanoparticles with narrower size distribution. To decrease τ_{mix} below $\tau_{\text{precipitation}}$, mixing rate has to be increased.

In the experimental apparatus we have developed the expanded liquid is directly injected through a nozzle in to the antisolvent solution. Different jet behavior can be obtained, but to maximize the mixing efficacy atomization regime is the preferred one.

There is an extended literature on the atomization of liquids into gases at room pressure and jets in liquid-liquid systems; but, little is known about the characteristic features of the atomization occurring in high pressure conditions near the critical value of the injected liquid. It is easy to suppose that hydrodynamic contributions to liquid breakup will become more important as surface tension is small, when the surface of a liquid jet approaches the critical mixing state at high pressure (Umemura A. and Wakashima Y., 2002). Thanks to the reduced surface tension of the expanded liquid, the turbulent atomization regime can emerge at lower jet speeds, and can maximize the intermixing of the two phases with the creation of a large surface area which leads to an enhanced mass transfer.

XII.3.3 Stability of nanoparticle suspensions

Stabilization of nanoparticles suspensions is critical to ensure their usability in various drug formulations. Decrease in particle size to nanometer scale increases surface area to volume ratio. This large increase in surface area increases excessive surface energy, which is thermodynamically unfavorable (Lee J. et al., 2005, Liu Y. et al., 2007). An increase in surface

energy accelerates agglomeration of particles in order to minimize excessive surface energy. During agglomeration, two smaller particles condense and form agglomerates of larger size. Agglomeration affects the overall stability of nanoparticles formulation. Apart from agglomeration there are several other mechanisms such as, secondary crystallization, and Ostwald ripening which destabilize the nanoparticles formulation. In secondary crystallization, crystal growth takes place over the initially formed crystals in mother liquor, whereas in Ostwald ripening the small particles shrink/dissolve, due to enhanced solubility arising from their high curvature. The solute thus dissolving diffuses towards the surface of larger particles causing them to grow. The interaction of nanometer sized particles is dependent on interfacial forces such as attractive, repulsive forces, and steric forces. Such interactions between two colloidal particles are collectively referred as colloidal interactions and stability of nanoparticles is strongly influenced by these colloidal interactions (Kind M., 2002). Therefore, nanoparticles stabilization is done by minimizing these colloidal interactions. There are two approaches, namely thermodynamic approach and kinetic approach (Liu R. and Liu R., 2008). Thermodynamic approach uses stabilizers to stabilize nanoparticles. The stabilizer-coated nanoparticles are considerably more stable than the bare nanoparticles. The stabilizer molecules actually preclude or minimize the surface functional groups available on particle surface and thus reduce particle-particle interaction (Maity D. and Agrawal D.C., 2007). Various surfactants, block co-polymers, cellulose based derivatives have been used for the stabilization of nanoparticles (Rasenack N. and Muller B.W., 2002, Dong Y.C. et al., 2009).

On the other hand, kinetic approach uses the energy input to compensate excess surface energy. The high mixing rate provides a high density energy dissipation, which increases the kinetic energy of nanoparticles. The stabilization is achieved due to the inhibition of agglomeration to some degree by increased kinetic energy of nanoparticles (Zhu Z.X. et al., 2010). The kinetic energy in the form of ultrasonic waves or high jet velocities generated by rapid mixing devices can be used for particle stabilization (Gindy M.E. et al., 2008).

Precipitation of particles and formation of protective stabilizer layer on the particle surface simultaneously, leads to controlled growth and agglomeration and hence, formation of nanoparticles. The stabilizers can be added either in solvent or antisolvent (Matteucci M.E. et al., 2006). The strength of adsorption of stabilizer molecules on the drug surface depends on the nature of the stabilizer and drug surface and is usually based on simple rules namely, i) the quantity of the stabilizer adsorbed on the surface is inversely proportional to its solubility in liquid phase, ii) the quantity of stabilizer adsorbed is directly proportional to the strength of stabilizer-particle interaction and inversely proportional to the strength of stabilizer-solution (liquid phase) interactions (Ross S. and Morrison I.D., 1988, Duro

R. et al., 1999). Two main mechanisms of thermodynamic stabilization, i.e. steric stabilization and electrostatic repulsion are discussed in the following.

In steric stabilization, non ionic polymers, and amphiphilic block copolymers are usually used. Polymer molecules start adsorbing on the hydrophobic drug surface through nonspecific interactions between hydrophobic group of the drug and polymer. Adsorption of polymer molecules on the drug particle surface reduces interfacial tension at the solid-liquid interface. This results in increase in nucleation rates and hence decreases the size of the precipitated particles.

A stabilizer monolayer is then formed on drug surface. Depending on its structural interactions with drug surface functional groups, a stabilizer molecule does not lie flat and adopts various conformations. Depending on conformation and interactions of stabilizer with particle surface, stabilizer provides complete or partial coverage of drug nanoparticles. This affects the stability and therefore it is important to take into consideration conformations of a stabilizer molecule at the solid-liquid interface (Rozenberg B.A. and Tenne R., 2008). Polymer molecules adsorbed on particle surface generally form a structure of tail-train loop. The portion adsorbed on the particle surface is called as *train*, while parts of polymer chain with both ends in contact with particle surface are called as *loops*. The portion which extends away from surface is called as *tail* (Scheutjens J.M.H.M. and Fleer G.J., 1980). The portions of polymer chain extending in solution provide steric protection depending on the molecular weight of polymer (Heller W. et al., 1960). The size and molecular weight of stabilizer are thus important for stabilization effect. Apart from size and molecular weight, the concentration of polymer is a very crucial parameter. When concentrations above critical flocculation concentration (CFC) of polymer is used, polymer molecules initiate depletion or bridging flocculation of the particles in suspension as shown schematically in **Figure XII. 7**. Also, at increased concentration of polymer, increase in osmotic pressure leads to increased attraction among colloidal particles leading to agglomeration. The larger size stabilizer molecules provide the good particle surface coverage and higher excluded volume because of their bigger size. Therefore, lower concentration of larger size stabilizers is required for stabilization as compared to the smaller size stabilizers (Verma S. et al., 2011)

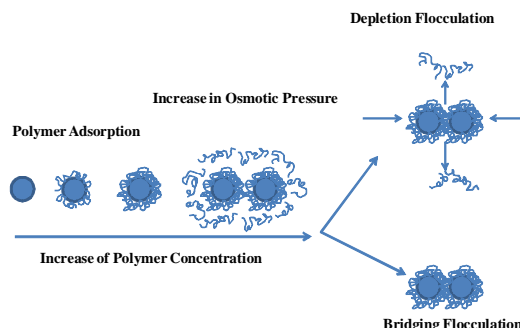


Figure XII. 7 Schematic of polymer-particle interaction in aqueous suspension with an increase in polymer concentration

In electrostatic stabilization, the most effective procedure for stabilization of nanoparticles dispersions is to use ionic surfactants and ionic polymers. These ionic surfactants and ionic polymers adsorb very strongly on the particle surface which is attributed to the strong van der Waals interaction between the surface and the numerous repeating monomer units of the polymer chain (Napper D.H., 1983). Surfactants can provide stabilization at concentrations below critical micelle concentration (CMC), as the concentration above CMC causes micelle formation leaving the particles unprotected as shown schematically in *Figure XII. 8* (Hillgren A. et al., 2002).

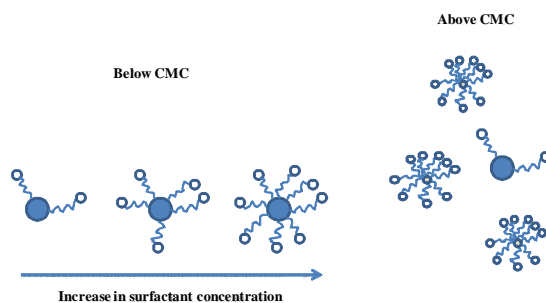


Figure XII. 8 The schematic of particle-surfactant interaction in the aqueous solution with an increase in surfactant concentration.

The schematic shown in *Figure XII. 8* is applicable for a situation where $\tau_{\text{precipitation of drug}}$ is lower than $\tau_{\text{micellization of the surfactant}}$. In case of polyelectrolytes, the charged nature of polyelectrolyte forms a strong double layer around hydrophobic drug particle and, if polyelectrolyte adsorbs loosely, the extending polymer loops provide the steric stabilization. In electrostatic stabilization mechanism, charged stabilizers cause repulsion between approaching particles due to similar charges on particle surface;

which leads to prevention of agglomeration. The electrostatic stabilization depends on repulsive electrostatic forces and attractive van der Waals forces. Due to the charge on particle surface, there exists a double layer surrounding the particle surface. This double layer is referred as electric double layer (Grahame D.C., 1947) . There exists a potential difference between bulk of solution and the outer layer of double layer which is called as zeta potential. The zeta potential is a measure of the stabilization provided by electrostatic stabilization. As a thumb rule, zeta potential higher than $\pm 30\text{mV}$ provides good suspension stability (Wu L.B. et al., 2011).

XII.4 Process parameters

As a preliminary study we have focused the attention to the relevant process parameters influencing the efficiency of the precipitation process, the particle size (PS) and particle size distribution (PSD). These parameters are:

- the mass flow ratio (GLR) between CO_2 and liquid solution,
- the operating pressure (P_{mix}) and temperature (T_{mix}) in the saturator,
- the solute concentration in the liquid solution (C_{sol}),
- concentration of the surfactant in the antisolvent solution,
- the ratio solvent/antisolvent.

P_{mix} , T_{mix} , GLR and C_{sol} influence the thermodynamics of the process. Although vapour-liquid equilibrium (VLE) data are available for many solvent/ CO_2 binary systems, quantitative data at high pressure on multiple (ternary and quaternary) systems is still missing and difficult to determine. For this reason, we usually consider the binary solvent/ CO_2 system involved at fixed process conditions (T_{mix}) as the starting point to choose the operating conditions that assure the complete system miscibility, and the formation of the expanded liquid mixture in the saturator. An empirical study of the effects of GLR and C_{sol} on VLE and PSD is, then, necessary to optimize the process conditions. The presence of the third component could significantly modify the VLE respect to the binary one. This modification often consists of the shifting of the mixture critical point towards higher pressures and it is the more pronounced the higher is C_{sol} (**Figure XII. 9**).

When P_{mix} and T_{mix} are fixed, the mass flow ratio GLR corresponds to a given operating point into the VLE diagram of the system considered. A change of the molar fractions of system components produces a modification of GLR, and if GLR increases, the operating point shifts towards a phase richer in CO_2 (**Figure XII. 9**). Since an efficient atomization process occurs when the operating point falls in the expanded liquid phase, the choice of opportune GLR-values is fundamental to the optimization of the process.

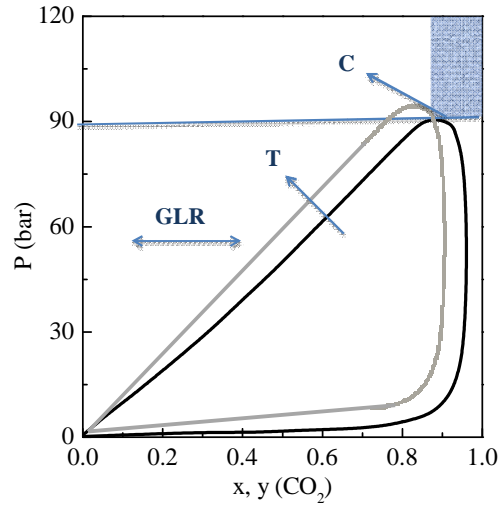


Figure XII. 9 Effect of the process parameter on the miscibility hole. The continuous line refers to the binary system Acetone- CO_2

The solvent antisolvent ratio and the concentration of the solute could have effect on the generation of supersaturation, thus affecting the PS and PSD.

The effect of all these parameters have been the objective of the study reported in the following chapter.

Chapter XIII

Nanoparticle Precipitation by Supercritical Assisted Injection in a Liquid Antisolvent

XIII.1 Introduction

Supercritical fluid (SCF) based literature has proposed some processes aimed at the production of nanoparticles of organic compounds, that can be used in several industrial fields (Adami R. et al., 2008, Reverchon E. and Adami R., 2006, Reverchon E. and De Marco I., 2011, Wang Q. et al., 2010, Mayo A.S. et al., 2010). These processes try to take advantage of the possibility to modulate the SCF mass transport, solubilisation properties and the intrinsic non toxicity and environmental friendly nature of supercritical carbon dioxide (SC-CO₂), that is the supercritical fluid of election in the applications involving the use of thermolabile and or organic compounds (Reverchon E. et al., 2009). More specifically, nanoparticle suspensions techniques assisted by SCFs derive mainly from RESS (Rapid Expansion of Supercritical Solution), in which a supercritical solution formed by SC-CO₂ plus a dissolved solid compound is depressurized inside a precipitation vessel. The solid released can precipitate as micro or submicro-nanoparticles (Turk M. et al., 2002). The main limitation of the RESS technique is the limited solubility of many compounds in the SC-CO₂.

One possibility to overcome this limitation is to use an expanded liquid; i.e., to form a solution between a liquid solvent and a gas. Expanded liquid solution have been proposed in some SC-CO₂ assisted processes: Particle Generation from Gas Saturated Solution (PGSS) (Martin A. and Weidner E., 2010), Depressurization of an Expanded Liquid Organic Solution (DELOS) (Ventosa N. et al., 2001) and Supercritical Assisted Atomization (SAA) (Reverchon E., 2002); though these processes were aimed at different

targets. PGSS can produce micrometric polymer particles by solidification of the ELS (Pemsel M. et al., 2010); DELOS can produce microcrystals by fast cooling crystallization of the solute contained in the ELS; SAA can produce micro and sub-microparticles by atomization and drying of the expanded liquid solution (Adami R. et al., 2009).

In this thesis, we propose the adoption of a new technique, called Supercritical Assisted Injection in Liquid Antisolvent (SAILA), in which an expanded liquid (a ternary mixture acetone-CO₂-solute) is directly injected in a liquid antisolvent, water, causing nanoparticle fast precipitation. The aims of this chapter will be the demonstration of the feasibility of the SAILA process and its application to Polycaprolactone (PCL), as a model biopolymer. The analysis of the influence of process parameters on nanoparticle size and a first attempt at explaining the mechanisms that induce nanoparticle formation will be also performed.

XIII.2 Materials & Methods

XIII.2.1 Materials

CO₂ (99.9%, SON, Naples, Italy), Polysorbate (Tween 80, Aldrich Chemical Co.), Sorbitan monolaurate (Span 20, Aldrich Chemical Co.), Acetone (AC, purity 99.9%, Aldrich Chemical Co.), distilled water, Polycaprolactone (PCL, MW 14.000 Aldrich Chemical Co.).

XIII.2.2 Nanoparticle morphology, size distributions and solvent

residue analysis

Particle size distribution (PSD) of the produced suspensions were determined by dynamic light scattering (DLS) (Zetasizer, mod. 5000, Malvern Instruments Ltd). Mean size and particle size distribution were measured three times for each sample. Nanoparticle morphology was analysed by FESEM (LEO 1525, Carl Zeiss SMT AG). Samples were prepared by spreading concentrated nanoparticle dispersions over aluminium stubs and drying them at air. Then, the samples were coated with a Gold layer, thickness 250 Å (mod.108 Å, Agar Scientific).

Acetone was removed from SAILA produced suspensions using the *Supercritical Fluids Extraction Process* described in section 3.4. Solvent residues in the suspensions was measured by a headspace (HS) sampler (model 7694E, Hewlett Packard) coupled to a gas chromatograph (GC) interfaced with a flame ionization detector (GC-FID, model 6890 GC-SYSTEM, Hewlett Packard). Acetone was separated using a fused-silica capillary column (model Carbowax EASYSEP, Stepbios) connected to the detector, 30 m length, 0.53 mm i.d., 1 µm film thickness. GC conditions

were: oven temperature from 45 to 210 °C for 15 min. The injector was maintained at 135 °C (split mode, ratio 4:1) and helium was used as carrier gas (5 mL/min). Head space conditions were: equilibration time, 30 min at 95 °C; pressurization time, 0.15 min and loop fill time, 0.15 min. Head space samples were prepared in 20 mL vials filled with 3 mL of the suspension.

XIII.3 Results and Discussion

XIII.3.1 Feasibility tests

The proposal of SAILA process takes origin from the following general considerations: liquid-liquid antisolvent precipitation is obtained when the processed compound is soluble in the solvent and not soluble in the antisolvent; the particles size of the precipitates depends on the efficiency of the micromixing between the two liquids that, in turn, is related to their surface tension (Umemura A. and Wakashima Y., 2002). Therefore, the continuous injection of an expanded liquid solution should be more effective than the mixing with an ordinary liquid. Indeed, expanded liquid are characterized by a reduced surface tension that at high gas molar fractions is near to zero (Brunner G., 1994); this characteristic should improve the micromixing with the antisolvent and produce smaller particles.

The first set of experiments was performed setting the temperature in the saturator at 80°C, CO₂ flow rate at 7 gr/min and varying the acetone solution flow rate. Operating in this way, different gas to liquid ratio (GLR) were produced and, correspondingly, expanded liquid mixtures with different CO₂ molar fractions were obtained. The polymeric solution used in the experiments discussed in this paragraph was prepared dissolving PCL in acetone at a concentration of 5 mg/mL. The ratio between the solvent (acetone) and the antisolvent (water) flow rates (S/NS) was fixed at 0.25. Small quantities of surfactant were added to water and to the organic solvent solution to try to control particles coalescence and stability. Tween 80, an hydrophilic surfactant, was added to water since it is approved in pharmaceutical formulations and it has been frequently used to control particles coalescence. Span 20 was added, as a cosurfactant, to the acetone PCL solution, since it is reported in literature that the addition of this lipophilic surfactant can improve suspension stability against sedimentation, flocculation and coalescence (Cho Y.H. et al., 2008). A final consideration is required for the use of a continuous flow of water in the precipitator; this process feature allows to operate at steady state conditions from the point of view of the concentration of the nanoparticles in water, that can influence possible effects of coalescence. Therefore, continuous operation is obtained instead of a semi-batch process and reproducibility problems are avoided.

In *Table XIII. 1* data related to preliminary experiments are reported; the decrease of GLR can also produce a lowering of the pressure in the saturator.

The representation of the vapour-liquid equilibria (VLEs) of the system acetone-SCCO₂ is reported in **Figure XIII. 1**, adapted from literature. The operating points related to the experiments reported in Table 1 are also represented in this figure. Mean diameter (MD), standard deviation (SD) and polydispersity index (PI) of the produced nanosuspensions were calculate by DLS measurements and are also reported in the same table.

Table XIII. 1 Mean diameter (MD), standard deviation (SD) and Polidispersity index (PI) of PCL nanoparticles at 5 mg/mL in acetone. Saturator temperature was set at 80°C.

	GLR	P (bar)	XCO ₂	MD (nm)±SD	PI
SAILA-1	4.0	120	0.84	171±63	0.37
SAILA-2	2.7	100	0.78	174±50	0.29
SAILA-3	1.4	90	0.65	171±66	0.39
SAILA-4	0.8	80	0.52	178±49	0.28
SAILA-5	0.6	75	0.38	206±39	0.19
SAILA-6	0.4	70	0.34	222±67	0.30

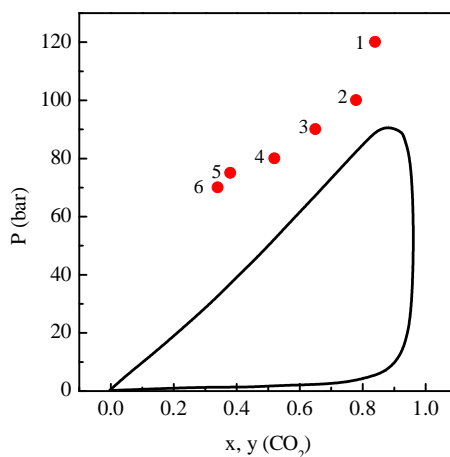


Figure XIII. 1 Representation of the high pressure VLE of the system acetone-SCCO₂ at 80°C, adapted from Sato et al. (Sato Y. et al., 2010). The operating point of the experiments reported in Table 10 is also represented.

These results show that SAILA technique was successful in the production of PCL nanoparticles at all process conditions tested. Examples of corresponding SEM images are reported in **Figure XIII. 2** and show that nanoparticles were approximately spherical, with a smooth surface and were not aggregated. The images were taken at two different enlargements, to better appreciate the uniformity (lower enlargement) and the shape (higher

enlargement) of the processed materials. The results of this series of experiments are also graphically reported in **Figure XIII. 3**. Particle diameter depends asymptotically on X_{CO_2} ; the asymptotic value is at about 170 nm. It is also worth to note that the mean particle size largely increases at X_{CO_2} smaller than about 0.5. **Figure XIII. 4** reports a comparison of the volumetric particle size distributions obtained in the experiments performed at the maximum and minimum value of GLR explored. The tail of the size distributions ends at about 600 nm in the case of GLR 0.4; the presence of larger particles is reduced in the case of GLR 4, in which the PSD ends at about 530 nm. The differences are enhanced by the use of volumetric percentages, that are more sensible to the dimension of the largest particles.

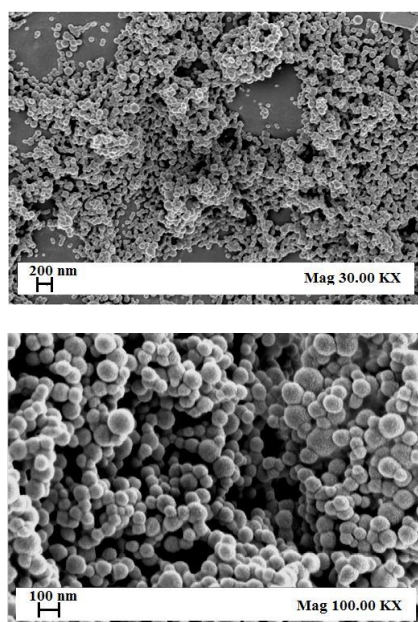


Figure XIII. 2 FESEM images of PCL nanoparticles produced by SAILA-1 ($MD 171 \pm 63$ nm). Process conditions are reported in Table 10.

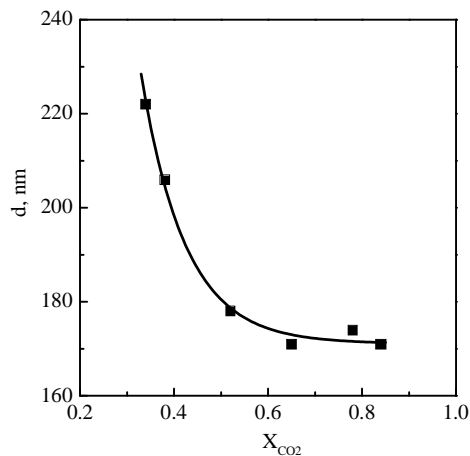


Figure XIII. 3 Effect of CO_2 mole fraction on the mean diameter of PCL nanoparticles

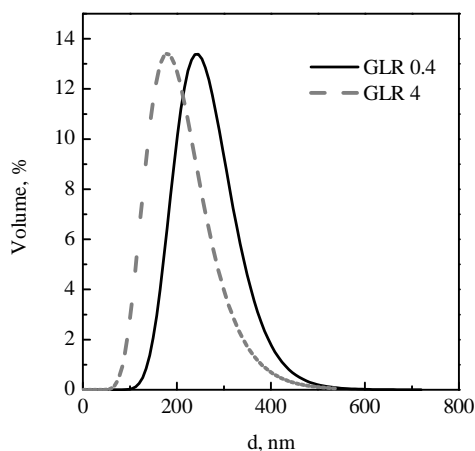


Figure XIII. 4 PSD of PCL nanoparticles obtained by SAILA at GLR 4.0 and 0.4

The results produced until now show a marked influence of the surface tension of the expanded liquid (whose dependence on X_{CO_2} we have previously discussed) on particle size. The fact that at $X_{CO_2} > 0.5$ there is no further variation of the mean diameter of the nanoparticles can be explained observing the behaviour of the surface tension for CO_2 -solvent mixtures: it decreases almost linearly for X_{CO_2} up to 0.6-0.7, then a plateau is reached at

a near zero value (Thorat A.A. and Dalvi S.V., 2012). This property also depends on temperature: the higher is the temperature, the lower is the value of the CO₂ molar fraction at which the plateau is obtained. This concept should also be expressed as: the higher is the temperature, the sharper is the decrease of the surface tension of the expanded solution with the increase of X_{CO₂}.

The second possible consideration is that an increase of X_{CO₂}, leaving all the other process parameters constant, produces also higher pressures in the SAILA saturator. As a consequence, a higher turbulence can be produced in the liquid put in the precipitator. Can an increase of the pneumatic effect also explain the results reported in *Table XIII. 1*? It is in principle possible that an increase of turbulence can produce smaller particles. In this hypothesis, the diameter of the nanoparticles should continuously decrease, increasing GLR; i.e., increasing the pressure in the saturator. There is an extended literature on the atomization of liquids into gases at room pressure and jets in liquid-liquid systems; but, little is known about the characteristic features of the atomization occurring in high pressure conditions near the critical value of the injected liquid. However, diameter and shape of the nanoparticles (irregularly spherical) are in favour of a formation mechanism that does not evolve through the formation of liquid droplets and subsequent drying. In conclusion, the results in *Table XIII. 1* and *Figure XIII. 3* suggest that the interpretation based on nanoparticle formation guided by almost instantaneous nanomixing plus nucleation and growth of nanoparticles is the most probable. The presence of the two surfactants in the expanded liquid and in the water receiving solution blocks particles coalescence.

XIII.3.2 Temperature effect

As discussed in the previous chapter, the surface tension of the expanded liquid is also a function of temperature: increasing the temperature, surface tension of the liquid mixtures containing SC-CO₂ decreases. Therefore, if the previous considerations developed about the SAILA precipitation mechanism are correct, increasing the temperature in the saturator, a reduction in nanoparticle diameters is expected. Thus, the effect of temperature was investigated and experiments were performed at two further temperatures: 60°C and 100°C; the results were compared with the set of experiments performed at 80°C. These experiments at different temperatures were performed at GLR values between 0.4 and 1.8. *Table XIII. 2* summarizes the results obtained that are also graphically organized in *Figure XIII. 5*.

Increasing the saturator temperature smaller nanoparticles were systematically produced, from a maximum mean diameter of 268 nm at 60°C, to a minimum of 165 nm at 100°C. However, looking at the overall effect of the saturator temperature, the effect of temperature is more evident

at lower X_{CO_2} (see **Figure XIII. 5**). These results also confirm the indications obtained in the previous chapter: for X_{CO_2} larger than about 0.5, the diameter of PCL nanoparticles produced by SAILA is no more sensitive to X_{CO_2} and to saturator temperature. The possible explanation for this evidence is the same given to explain the GLR effect: at larger X_{CO_2} the surface tension of the expanded liquid is near to zero.

Table XIII. 2 Mean diameter (MD), standard deviation (SD) and Polidispersity index (PI) of PCL nanoparticles produced at different saturator temperatures and at different GLR. PCL concentration = 5 mg/mL, S/N/S = 1/4., P 70 bar

	T (°C)	GLR	X_{CO_2}	MD (nm)±SD	PI
SAILA_7	100	1.80	0.65	170±34	0.20
SAILA_8	60	1.80	0.65	198±49	0.25
SAILA_9	100	0.92	0.52	165±56	0.34
SAILA_10	60	0.92	0.52	200±54	0.27
SAILA_11	100	0.60	0.38	190±51	0.27
SAILA_12	60	0.60	0.38	236±78	0.33
SAILA_13	100	0.36	0.35	206±62	0.30
SAILA_14	60	0.36	0.35	268±112	0.42

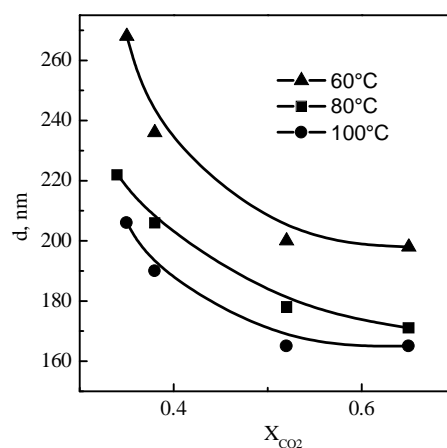


Figure XIII. 5 Effect of temperature on PCL particles mean diameter ($\blacktriangle=60^\circ\text{C}$, $\blacksquare=80^\circ\text{C}$, $\bullet=100^\circ\text{C}$) at different X_{CO_2} values

XIII.3.3 Effect of solvent/non-solvent ratio and polymer**concentration**

The effect of solvent/non-solvent ratio (S/NS) and polymer concentration were investigated in this set of experiments, performed fixing GLR at 1.8, saturator temperature at 100°C and pressure at 70 bar. The results obtained are summarized in **Table XIII. 3**. They show that increasing the dilution in water, smaller particles are obtained; indeed, S/NS ratio represents the quantity by volume of the solvent in water; therefore, for a given PCL quantity in the organic solvent, it is connected the concentration of solute (at steady state conditions) in the liquid suspension. These results can be explained considering that a larger driving force for the nanomixing of the two liquids is expressed at lower concentrations of the organic solvent in water. It is also possible that decreasing S/NS value the possible interactions among nanoparticles in the suspensions are reduced. Particles with a mean diameter of 169 nm were obtained in the case of S/NS ratio 1/4; whereas reducing S/NS at 1/16 smaller particles with a MD of 118 nm were produced.

In **Table XIII. 3** the effect of the PCL concentration in acetone is also reported. Reducing the polymer concentration, fixed all the other SAILA parameters (GLR=1.8, T=100°C, P=70 bar, S/NS=1/16), smaller particles were obtained. During these experiments the smallest PCL nanoparticles were produced, down to a mean diameter of 64 nm, that represent the best result obtained in this work from the point of view of nanoparticles diameters. The results obtained at 2.5 and 1 mg/mL are reported in **Figure XIII. 6** and show that also sharper PSDs were obtained, with a maximum particles diameter of about 140 nm.

This result can be explained considering the nucleation process and its dependence on the concentration of the solute: a higher supersaturation favors particles growth; therefore, increasing the solute concentration, larger particles are obtained.

Table XIII. 3 Mean diameter (MD), standard deviation (SD) and Polidispersity index (PI) of PCL nanoparticles obtained at different solvent/non solvent (S/NS) ratios and at PCL concentrations ranging from 1 to 5 mg/mL. GLR=1.8, T=100°C and p=70 bar

	mg/mL	S/NS	MD (nm)±SD	PI
SAILA_7	5	1/4	169±34	0.20
SAILA_15	5	1/8	168±58	0.35
SAILA_16	5	1/16	118±28	0.24
SAILA_17	2.5	1/16	98±29	0.30
SAILA_18	1.0	1/16	64±22	0.35

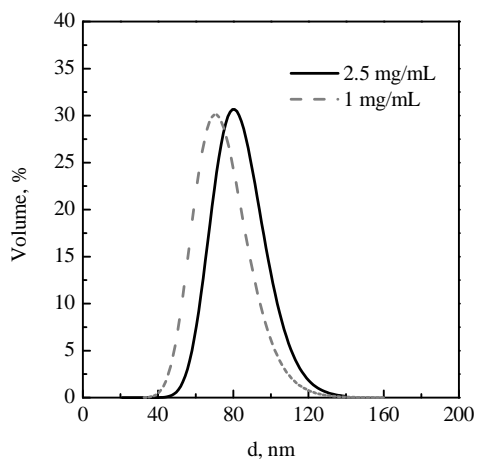


Figure XIII. 6 PSD of the smallest particles obtained in the experiments SAILA_17 and SAILA_18

XIII.4 Conclusions and perspectives

A novel supercritical assisted process for the production of nanoparticles of organic compound has been proposed and successfully demonstrated for PCL. Non coalescing nanoparticles down to 64 nm mean diameter were produced; this result is particularly interesting since 100 nm diameter represents a benchmark that is very difficult to overcome when organic compounds are processed. One possible question could be: is it the process applicable to other compounds? Some SAILA preliminary experiments performed on poorly water soluble drugs and are shown in the following chapter.

Chapter XIV

Preparation of stable aqueous nanodispersions of poorly water soluble drugs by supercritical assisted injection in a liquid antisolvent

XIV.1 Introduction

The bioavailability of poorly water soluble drugs is limited due to their low solubility and dissolution rate. Various drug formulation development strategies have been extensively studied to improve the dissolution rate of these drugs over the past two decades. One of the newest formulation strategies is to prepare nanoparticles/microparticles of these drugs. Decrease in particle size increases the surface area to volume ratio which increases the dissolution rate of poorly water soluble molecules and hence bioavailability (Merisko-Liversidge E.M. and Liversidge G.G., 2008).

The nanoparticles can be produced by either top-down methods or bottom-up methods. The top-down methods start with larger solid particles and break them mechanically down to nano/microparticles. However breaking drug particles to nanoparticles with size below 100 nm is extremely difficult with the top-down methods. The bottom-up methods on the other hand, produce fine particles starting at the atomic level. These methods give, in general, better control over particles properties, such as, size, morphology and crystallinity. However, also these processes have some disadvantages, such as, low yields, degradation of heat sensitive drugs,

difficulties to scale up and low reproducibility, since they are batch processes (Reverchon E. and Adami R., 2006).

SAILA process reveals to be an efficient process for the production of stable PCL water suspensions. For this reason, we propose the adoption of a new technique called the Supercritical Assisted Injection in Liquid Antisolvent (SAILA), for the production of poorly water soluble drug nanoparticles suspensions.

Several different compounds were tested (β -carotene, ketoprofene, beclomethasone, budesonide, triclazadol). Acetone was selected as the organic solvent for the expanded liquid preparation, whereas water was used as the antisolvent. A systematic study of the effect of the operating parameters was conducted in the case of two selected compounds: β -carotene and ketoprofene.

XIV.2 Materials & Methods

XIV.2.1 Materials

CO₂ (99.9%, SON, Naples, Italy), Polysorbate (Tween 80), Acetone (AC, purity 99.9%), β -carotene (β -C), ketoprofene, beclomethasone, budesonide, triclazadol, were all bought from Aldrich Chemical Co. and were used as received.

XIV.2.2 Nanoparticle morphology, size distributions and solvent

residue analysis

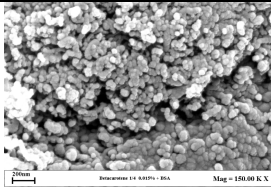
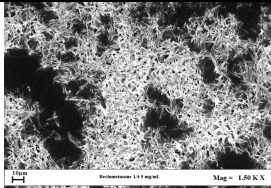
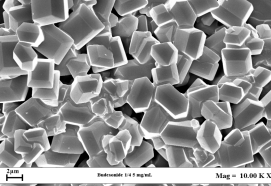
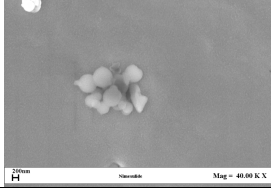
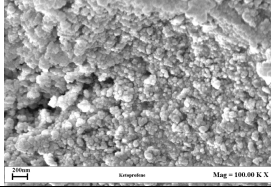
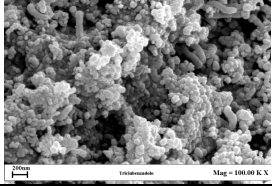
Nanoparticle morphology was analysed by FESEM (LEO 1525, Carl Zeiss SMT AG). Samples were prepared by spreading concentrated nanoparticle dispersions over aluminium stubs and drying them at air. Then, the samples were coated with a gold layer, thickness 250 Å (mod.108 Å, Agar Scientific). Particle size (PS) and particle size distribution (PSD) were measured from SEM photomicrographs using the Sigma Scan Pro Software (release 5.0, Aspire Software International Ashburn, VA). Approximately 1000 particles were measured for each particle size distribution calculation. Histograms, representing the particle size distribution, were fitted using Microcal Origin Software (release 8.0, Microcal Software, Inc., Northampton, MA).

XIV.3 Results and Discussion

XIV.3.1 Feasibility test

Several different poorly soluble drugs were tested with the SAILA process, in order to investigate the applicability of this process to different class of compounds. SAILA process conditions were fixed: saturator pressure 80 bar, saturator temperature 80°C, GLR 1.8, solvent/antisolvent ratio ¼. All the suspensions produced were characterized in terms of morphology. With the same process conditions different morphology were obtained depending on the compound used, as shown in **Table XIV. 1**. In many cases spherical amorphous particles were obtained. In some other cases different morphologies were obtained such as cubic or hexagonal crystals or fibers, see **Table XIV. 1**.

Table XIV. 1 SAILA feasibility tests for the production of nanosuspensions of different compound poorly water soluble

Drug (concentration in solvent phase)	Morphology	FESEM image
β -Carotene (0.3 mg/mL)	spherical	
Beclometasone (5 mg/mL)	Fiber	
Budesonide (5 mg/mL)	Hexagonal	
Nimesulide (5 mg/mL)	spherical	
Ketoprofene (5 mg/mL)	spherical	
Triclabendazol (5 mg/mL)	spherical	

A possible explanation of the different morphologies obtained using the same process conditions, can be found in the different crystallization width of the metastable zone. Indeed, if the metastable zone is crossed quickly

nucleation rate is high and determines the formations many nuclei, thus sovrasaturation is manly consumed by nucleation; spherical amouphus nanoparticles are obtained. Whereas, if the metastable zone is crossed slowly, slow nucleation rate are obtained and sovrasaturation is consumed mainly by growth of crystals formed. Crystalline particles are thus formed.

In the following a systematic study of the effect of the operating parameters is reported in the case of two selected compounds: β -carotene and ketoprofene.

XIV.3.2 Production of β -carotene nanoparticles suspensions

The experiments were performed setting the temperature in the saturator at 80°C, CO₂ flow rate at 10 gr/min and varying the acetone solution flow rate. Operating in this way, different gas to liquid ratio (GLR) were produced and, correspondingly, expanded liquid mixtures with different CO₂ molar fractions were obtained. The β -C solution used in the experiments for the study of GLR effect was prepared dissolving β -C in acetone at a concentration of 0.03 mg/mL. The ratio between the solvent (acetone) and the antisolvent (water) flow rates (S/NS) was fixed at 0.25. Small quantities of surfactant were added to water solution to control particles stability. Tween 80, an hydrophilic surfactant, was added to water since it is approved in pharmaceutical formulations and it has been frequently used to control particles coalescence (Turk M. and Lietzow R., 2004)¹. A consideration is required for the use of a continuous flow of water in the precipitator: this process feature allows to operate at steady state conditions from the point of view of the concentration of the nanoparticles in water, that can influence possible effects of coalescence. Therefore, continuous operation is obtained instead of a semi-batch process and reproducibility problems are avoided.

In **Table XIV. 2** data related to the experiments are reported; the decrease of GLR can also produce a lowering of the pressure in the saturator. The representation of the vapour-liquid equilibria (VLEs) of the system acetone-SCCO₂ is reported in **Figure XIV. 1**, adapted from literature. The operating points related to the experiments reported in Table 1 are also reported in this figure. Mean diameter (MD), standard deviation (SD) and polydispersity index (PI) of the produced nanosuspensions were calculate by DLS measurements and are reported in the same table.

Table XIV. 2 Mean diameter (*MD*), standard deviation (*SD*) and Polidispersity index (*PI*) of β -C nanoparticles obtained from a 0.03 mg/mL β -C solution in acetone. Saturator temperature was set at 80°C

	GLR	P (bar)	XCO ₂	B-C (mg/mL)	MD (nm)±SD	PI
P1	1.58	90	0.68	0.03	37±5	0.13
P2	1.48	80	0.66	0.03	40±5	0.12
P3	1.16	75	0.60	0.03	48±6	0.13
P4	0.81	70	0.52	0.03	56±7	0.12
P5	0.81	70	0.52	0.1	71±8	0.15
P6	0.81	70	0.52	0.2	90±14	0.16

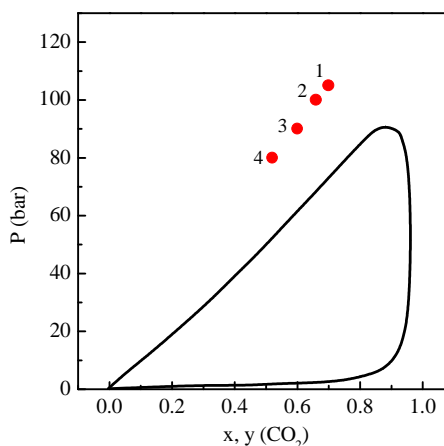


Figure XIV. 1 Representation of the high pressure VLE of the system acetone-SCCO₂ at 80°C, adapted from Sato et al. [14]. The operating points of the experiments reported in Table 1 are also represented.

These results show that SAILA technique was successful in the production of β -C nanoparticle suspension at all GLR tested, moreover the suspensions produced were stable. The macroscopic aspect of the produced suspensions is reported in **Figure XIV. 2**. Suspensions were stable with zeta potential mean value of about -20 mV. Stability of suspensions was also monitored over time: they maintain stability over months. Examples of corresponding SEM images are reported in **Figure XIV. 3** and show that nanoparticles were approximately spherical, with a smooth surface and were not aggregated. To obtain this kind of SEM image a nanoparticles dilute dispersion was produced and high contrast images were taken.



Figure XIV. 2 Macroscopic aspect of β -C nanoparticles suspensions produced by SAILA with variation of GLR. Process conditions are reported in Table 14.

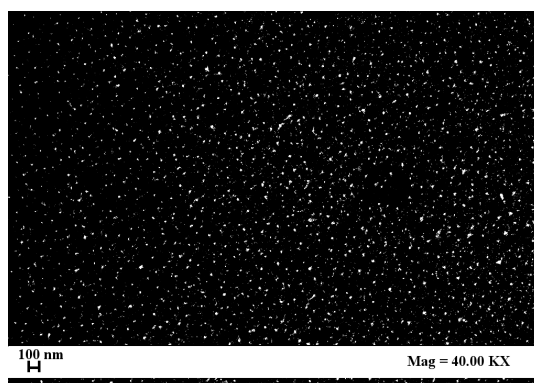


Figure XIV. 3 FESEM image of β -C nanoparticles produced by SAILA (P4). Process conditions are reported in Table 14.

Figure XIV. 4 reports a comparison of the volumetric particle size distributions obtained in the experiments performed at the maximum and minimum value of GLR explored. The PSD of the obtained suspensions demonstrated that there is a sensible effect of X_{CO_2} on particle diameters, that is particle size decreases with the increase of GLR and consequently the increase of X_{CO_2} . This result is related to the fact that antisolvent precipitation is obtained when the processed compound is soluble in the solvent and not soluble in the antisolvent. The particle size of the precipitates depends on the efficiency of the micromixing between the two liquids that, in turn, is related to their surface tension. Expanded liquid are characterized by a reduced surface tension that at high gas molar fractions is near to zero.

Therefore, the continuous injection of an expanded liquid solution is more effective than the mixing with an ordinary liquid. This characteristic should improve the micromixing with the antisolvent and produce smaller particles increasing the X_{CO_2} , i.e. reducing the surface tension of the expanded liquid. From **Figure XIV. 4** it is also possible to see that D100 is below 100 nm in all the cases explored.

The smallest β -C nanoparticles produced showed a mean diameter of 56 nm.

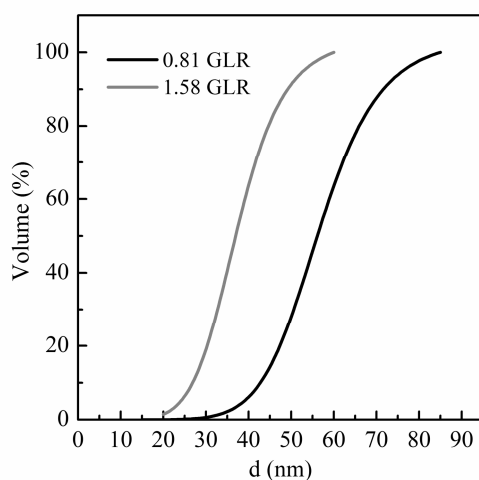


Figure XIV. 4 PSD of β -C nanoparticles suspensions obtained by SAILA at GLR 0.81 and 1.58

The effect of β -C concentration in the acetone solution was also investigated; experiments were performed fixing GLR at 0.81, saturator temperature at 100°C and pressure at 70 bar. The results obtained are summarized in **Table XIV. 2**. Stable suspensions were obtained also with higher concentrations of β -C. A considerable effect on particles MD was observed, as shown in **Table XIV. 2**. This result can be explained considering the nucleation process and its dependence on the concentration of the solute: a higher supersaturation favors particles growth; therefore, increasing the solute concentration, larger particles are obtained. FESEM image of nanoparticles obtained at 0.2 mg/mL concentration is reported in **Figure XIV. 5**. Particles are spherical also in this case and non coalescing with a mean diameter of about 90 nm. **Figure XIV. 6** reports PSD of nanoparticles obtained at minimum and maximum concentration of β -C.

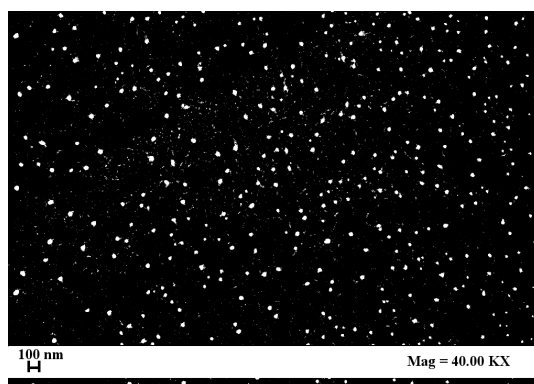


Figure XIV. 5 FESEM image of β -C nanoparticles obtained by SAILA obtained from a solution at 0.2 mg/mL of β -C

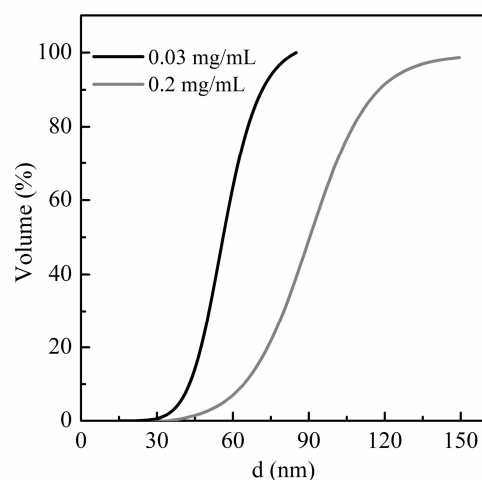


Figure XIV. 6 PSD of β -C nanoparticles suspensions obtained by SAILA operating GLR 0.81.

From *Figure XIV. 5* and from *Figure XIV. 6* it is possible to see that in the case of higher concentration larger particles are obtained with D_{100} located at 150 nm, whereas at a concentration of β -C of 0.03 mg/mL PSD is all below 100 nm, with D_{100} at 86 nm.

XIV.3.3 Production of ketoprofene nanoparticles suspensions

The experiments for the production of ketoprofene nanoparticles were conducted fixing the temperature in the saturator at 80°C, CO₂ flow rate at 10 gr/min, and solvent flow rate at 14 mL/min, obtaining a GLR of 0.85. The

effect of ketoprofene concentration in acetone solution was evaluated, 20 g/mL and 30 g/mL, as shown in Table 15. Solvent/antisolvent ratio was fixed at 0.25. Water solution of Tween 80 at 0.2% w/w was used as antisolvent.

Table XIV. 3 Mean diameter (MD), and Polidispersity index (PI) of ketoprofene nanoparticles obtained from a 20 and 30 mg/mL ketoprofene solution in acetone. Saturator temperature was set at 80°C, GLR 0.85.

	GLR	P (bar)	XCO ₂	Kp (mg/mL)	MD (nm)	PI
K1	0.85	70	0.7	20	200	0.077
K2	0.85	70	0.7	30	1250	0.061

The case of ketoprofene is particularly relevant to highlight a possible phenomena that can be verified precipitating drugs. Indeed in the case of ketoprofene nanoparticles are formed with spherical shape, as in the case of betacarotene, see **Figure XIV. 7(a)** and **(b)**; the effect of concentration on mean size is evident from **Table XIV. 3** and **Figure XIV. 7 (a)** and **(b)**, an increase of mean size is observed increasing the drug concentration in the expanded liquid. Nevertheless the suspensions were not stable, because during time a phenomena of recrystallization led to the formation of big crystal, as shown in **Figure XIV. 7 (c)** and **(d)**. This phenomena is probably due to the partial of the small particles that dissolve, due to enhanced solubility arising from their high curvature. The solute thus dissolving diffuses towards the surface of larger particles causing them to grow.

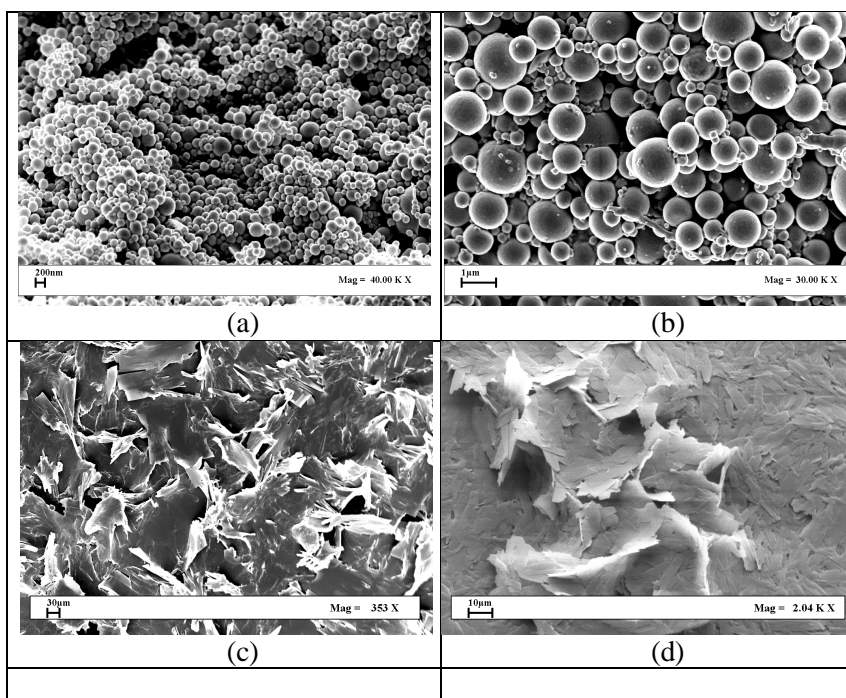


Figure XIV. 7 SEM images of ketoprofen nanoparticles obtained with the SAILA technique at concentration of 20 mg/mL (a) and 30 mg/mL (b). SEM images of crystals formed after 1 day are also reported I figure (c) for the case of 20 mg/mL and (d) for the case of 30 mg/mL

To improve the stability of nanoparticles suspensions a steric stabilization should be tried.

XIV.4 Conclusions

SAILA, the novel supercritical assisted process for the production of nanoparticles of organic compounds, has been successfully demonstrated for many different drugs, improving poorly hydrophilic drugs dispersability in water solutions. Non coalescing spherical nanoparticles down to 100 nm mean diameter were produced in some cases; nanoparticle diameters can be modulated varying two main conditions: GLR and drug concentration in the solvent, with the possibility to produce particles with diameters in the micro and nano range. Different morphologies were also obtained depending of the crystallization rate of the specific compound. When very fast precipitation is obtained very small amorphous nanospheres were produced.

Chapter XV

Conclusions

The aim of this thesis was the development of supercritical assisted processes for the production of micro and nanoparticles for biomedical and pharmaceutical applications.

In this work SEE continuous technology has been applied successfully to the production of sub-micro and nanoparticles. SEE process conditions have been optimized in order to obtain nanoparticles production. Operating in this way nanoparticles in the range 150-400 nm have been obtained using both single and double emulsions. Particles were also loaded with a model drug, metal nanoparticles, proteins and peptides. Indeed, exploiting the possibility to work with multiple emulsions it was possible to produce successfully multifunctional nanocarriers. Fruitful collaboration with specialized foreign center confirmed that the SEE process can be applied successfully to the production of multifunctional nanocarriers for pharmaceutical and biomedical applications.

The development of a completely new supercritical based process, SAILA, has been done, with the aim of improving the existing processes in the field of supercritical fluids techniques. The feasibility of this new process has been demonstrated for polymers and drugs. Nanoparticles aqueous suspensions were successfully produced, nanoparticles with mean diameters down to 100 nm were produced. This dimension is an important benchmark that is really difficult to overcome. It has also been demonstrated that the SAILA process is applicable successfully to several compounds.

References

- Adami R., Osseo L.S. & Reverchon E. (2009). Micronization of Lysozyme by Supercritical Assisted Atomization. *Biotechnology and Bioengineering*, 104, 1162-1170.
- Adami R., Reverchon E., Jarvenpaa E. & Huopalahti R. (2008). Supercritical AntiSolvent micronization of nalmefene HCl on laboratory and pilot scale. *Powder Technol*, 182, 105-112.
- Amass W., Amass A. & Tighe B. (1998). A review of biodegradable polymers: uses, current developments in the synthesis and characterization of biodegradable polyesters, blends of biodegradable polymers and recent advances in biodegradation studies. *Polymer International*, 47, 89-144.
- Aubry J., Ganachaud F., Addad J.P.C. & Cabane B. (2009). Nanoprecipitation of Polymethylmethacrylate by Solvent Shifting: 1. Boundaries. *Langmuir*, 25, 1970-1979.
- Bahl Y. & Sah H. (2000). Dynamic changes in size distribution of emulsion droplets during ethyl acetate-based microencapsulation process. *AAPS PharmSciTech*, 1, 41-49.
- Bałdyga J., Bourne J.R. & Hearn S.J. (1997). Interaction between chemical reactions and mixing on various scales. *Chem Eng Sci*, 52, 457-466.
- Barichello J.M., Morishita M., Takayama K. & Nagai T. (1999). Encapsulation of Hydrophilic and Lipophilic Drugs in PLGA Nanoparticles by the Nanoprecipitation Method. *Drug Dev Ind Pharm*, 25, 471-476.
- Barrett C. & Mermut O. (2005). Polymer multilayer films with azobenzene for photoactive biosurfaces. *Abstr Pap Am Chem S*, 229, U1107-U1107.
- Beck-Broichsitter M., Rytting E., Lehardt T., Wang X. & Kissel T. (2010). Preparation of nanoparticles by solvent displacement for drug delivery: A shift in the "ouzo region" upon drug loading. *Eur J Pharm Sci*, 41, 244-253.
- Berchane N.S., Jebrail F.F., Carson K.H., Rice-Ficht A.C. & Andrews M.J. (2006). About mean diameter and size distributions of poly(lactide-co-glycolide) (PLG) microspheres. *J Microencapsul*, 23, 539-552.
- Bernkop-Schnurch A. & Walker G. (2001). Multifunctional matrices for oral peptide delivery. *Crit Rev Ther Drug*, 18, 459-501.
- Bilati U., Allemann E. & Doelker E. (2005a). Nanoprecipitation versus emulsion-based techniques for the encapsulation of proteins into biodegradable nanoparticles and process-related stability issues. *Aaps Pharmscitech*, 6.
- Bilati U., Allémann E. & Doelker E. (2003). Sonication Parameters for the Preparation of Biodegradable Nanocapsules of Controlled Size by the

References

- Double Emulsion Method. *Pharmaceutical Development and Technology*, 8, 1-9.
- Bilati U., Allémann E. & Doelker E. (2005b). Development of a nanoprecipitation method intended for the entrapment of hydrophilic drugs into nanoparticles. *Eur J Pharm Sci*, 24, 67-75.
- Brunner G. (1994). *Gas extraction*, New York.
- Brunner G. (2009). Counter-current separations. *J Supercrit Fluid*, 47, 574-582.
- Byrappa K. & Yoshimura M. 2001. 1 - Hydrothermal Technology—Principles and Applications. *Handbook of Hydrothermal Technology*. Norwich, NY: William Andrew Publishing.
- Cai R.X., Kubota Y., Shuin T., Sakai H., Hashimoto K. & Fujishima A. (1992). Induction of Cytotoxicity by Photoexcited TiO₂ Particles. *Cancer Res*, 52, 2346-2348.
- Chattopadhyay P. & Gupta R.B. (2003). Supercritical CO₂-based formation of silica nanoparticles using water-in-oil microemulsions. *Ind Eng Chem Res*, 42, 465-472.
- Chattopadhyay P., Huff R. & Shekunov B.Y. (2006). Drug encapsulation using supercritical fluid extraction of emulsions. *J Pharm Sci-US*, 95, 667-679.
- Chattopadhyay P., Shekunov B.Y., Yim D., Cipolla D., Boyd B. & Farr S. (2007). Production of solid lipid nanoparticle suspensions using supercritical fluid extraction of emulsions (SFEE) for pulmonary delivery using the AERx system. *Adv Drug Deliver Rev*, 59, 444-453.
- Chin H.Y., Lee M.J. & Lin H.M. (2008). Vapor-Liquid Phase Boundaries of Binary Mixtures of Carbon Dioxide with Ethanol and Acetone. *J Chem Eng Data*, 53, 2393-2402.
- Cho Y.H., Kim S., Bae E.K., Mok C.K. & Park J. (2008). Formulation of a cosurfactant-free O/W microemulsion using nonionic surfactant mixtures. *J Food Sci*, 73, E115-E121.
- Chowdhury D., Paul A. & Chattopadhyay A. (2005). Photocatalytic polypyrrole-TiO₂-nanoparticles composite thin film generated at the air-water interface. *Langmuir*, 21, 4123-8.
- Dalvi S.V. & Dave R.N. (2009). Controlling Particle Size of a Poorly Water-Soluble Drug Using Ultrasound and Stabilizers in Antisolvent Precipitation. *Ind Eng Chem Res*, 48, 7581-7593.
- Das S., Suresh P.K. & Desmukh R. (2010). Design of Eudragit RL 100 nanoparticles by nanoprecipitation method for ocular drug delivery. *Nanomed-Nanotechnol*, 6, 318-323.
- De Jong W.H. & Borm P.J.A. (2008). Drug delivery and nanoparticles: Applications and hazards. *Int J Nanomed*, 3, 133-149.
- De Oliveira A.M., Da Silva M.L.C.P., Alves G.M., De Oliveira P.C. & Dos Santos A.M. (2005). Encapsulation of TiO₂ by emulsion

- polymerization with methyl metacrylate (MMA). *Polym Bull*, 55, 477-484.
- Dehghani F. & Foster N.R. (2003). Dense gas anti-solvent processes for pharmaceutical formulation. *Curr Opin Solid St M*, 7, 363-369.
- Della Porta G., Campardelli R., Falco N. & Reverchon E. (2011a). PLGA Microdevices for Retinoids Sustained Release Produced by Supercritical Emulsion Extraction: Continuous Versus Batch Operation Layouts. *J Pharm Sci-US*, 100, 4357-4367.
- Della Porta G., Falco N. & Reverchon E. (2010). NSAID Drugs Release from Injectable Microspheres Produced by Supercritical Fluid Emulsion Extraction. *J Pharm Sci-US*, 99, 1484-1499.
- Della Porta G., Falco N. & Reverchon E. (2011b). Continuous Supercritical Emulsions Extraction: A New Technology for Biopolymer Microparticles Production. *Biotechnology and Bioengineering*, 108, 676-686.
- Della Porta G. & Reverchon E. (2008). Nanostructured microspheres produced by supercritical fluid extraction of emulsions. *Biotechnology and Bioengineering*, 100, 1020-1033.
- Determan A.S., Trewyn B.G., Lin V.S.Y., Nilsen-Hamilton M. & Narasimhan B. (2004). Encapsulation, stabilization, and release of BSA-FITC from polyanhydride microspheres. *J Control Release*, 100, 97-109.
- Dong Y.C., Ng W.K., Shen S.C., Kim S. & Tan R.B.H. (2009). Preparation and characterization of spironolactone nanoparticles by antisolvent precipitation. *Int J Pharmaceut*, 375, 84-88.
- Donnelly R.F., Mccarron P.A. & Woolfson A.D. (2005). Drug Delivery of Aminolevulinic Acid from Topical Formulations Intended for Photodynamic Therapy. *Photochemistry and Photobiology*, 81, 750-767.
- Duro R., Souto C., Gomez-Amoza J.L., Martinez-Pacheco R. & Concheiro A. (1999). Interfacial adsorption of polymers and surfactants: Implications for the properties of disperse systems of pharmaceutical interest. *Drug Dev Ind Pharm*, 25, 817-829.
- Fages J., Lochard H., Letourneau J.J., Sauceau M. & Rodier E. (2004). Particle generation for pharmaceutical applications using supercritical fluid technology. *Powder Technol*, 141, 219-226.
- Falco N. (2012). Continuous supercritical emulsion extraction: process characterization and optimization of operative conditions to produce biopolymer microspheres.
- Falco N., Reverchon E. & Della Porta G. (2012). Continuous Supercritical Emulsions Extraction: Packed Tower Characterization and Application to Poly(lactic-co-glycolic Acid) plus Insulin Microspheres Production. *Ind Eng Chem Res*, 51, 8616-8623.

References

- Feng S.S. & Huang G.F. (2001). Effects of emulsifiers on the controlled release of paclitaxel (Taxol (R)) from nanospheres of biodegradable polymers. *J Control Release*, 71, 53-69.
- Fessi H., Puisieux F., Devissaguet J.P., Ammoury N. & Benita S. (1989). Nanocapsule formation by interfacial polymer deposition following solvent displacement. *Int J Pharmaceut*, 55, R1-R4.
- Field S.B. & Morris C.C. (1983). The relationship between heating time and temperature: its relevance to clinical hyperthermia. *Radiotherapy and Oncology*, 1, 179-186.
- Franklin R.K., Edwards J.R., Chernyak Y., Gould R.D., Henon F. & Carbonell R.G. (2001). Formation of Perfluoropolyether Coatings by the Rapid Expansion of Supercritical Solutions (RESS) Process. Part 2: Numerical Modeling. *Ind Eng Chem Res*, 40, 6127-6139.
- Freiberg S. & Zhu X. (2004). Polymer microspheres for controlled drug release. *Int J Pharmaceut*, 282, 1-18.
- Freitas S., Merkle H.P. & Gander B. (2005). Microencapsulation by solvent extraction/evaporation: reviewing the state of the art of microsphere preparation process technology. *J Control Release*, 102, 313-332.
- Freytag T., Dashevsky A., Tillman L., Hardee G.E. & Bodmeier R. (2000). Improvement of the encapsulation efficiency of oligonucleotide-containing biodegradable microspheres. *J Control Release*, 69, 197-207.
- Furlan M., Kluge J., Mazzotti M. & Lattuada M. (2010). Preparation of biocompatible magnetite-PLGA composite nanoparticles using supercritical fluid extraction of emulsions. *The Journal of Supercritical Fluids*, 54, 348-356.
- Gasparini G., Kosvintsev S.R., Stillwell M.T. & Holdich R.G. (2008). Preparation and characterization of PLGA particles for subcutaneous controlled drug release by membrane emulsification. *Colloid Surface B*, 61, 199-207.
- Gindy M.E., Ji S.X., Hoyer T.R., Panagiotopoulos A.Z. & Prud'homme R.K. (2008). Preparation of Poly(ethylene glycol) Protected Nanoparticles with Variable Bioconjugate Ligand Density. *Biomacromolecules*, 9, 2705-2711.
- Gouin S. (2004). Microencapsulation: industrial appraisal of existing technologies and trends. *Trends Food Sci Tech*, 15, 330-347.
- Govender T., Stolnik S., Garnett M.C., Illum L. & Davis S.S. (1999). PLGA nanoparticles prepared by nanoprecipitation: drug loading and release studies of a water soluble drug. *J Control Release*, 57, 171-185.
- Grahame D.C. (1947). The electrical double layer and the theory of electrocapillarity. *Chem Rev*, 41, 441-501.

- Granberg R.A., Ducreux C., Gracin S. & Rasmuson A.C. (2001). Primary nucleation of paracetamol in acetone-water mixtures. *Chem Eng Sci*, 56, 2305-2313.
- Gu F., Amsden B. & Neufeld R. (2004). Sustained delivery of vascular endothelial growth factor with alginate beads. *J Control Release*, 96, 463-472.
- Guo Z., Zhang M., Li H., Wang J. & Kougoulos E. (2005). Effect of ultrasound on anti-solvent crystallization process. *J Cryst Growth*, 273, 555-563.
- Harada Y., Ogawa K., Irie Y., Endo H., Feril L.B., Uemura T. & Tachibana K. (2011). Ultrasound activation of TiO₂ in melanoma tumors. *J Control Release*, 149, 190-195.
- Helfgen B., Türk M. & Schaber K. (2000). Theoretical and experimental investigations of the micronization of organic solids by rapid expansion of supercritical solutions. *Powder Technol*, 110, 22-28.
- Heller W., Pugh T.L. & Mi. W.S.U.D. (1960). "steric" Stabilization of Colloidal Solutions by Adsorption of Flexible Macromolecules, Defense Technical Information Center.
- Hillgren A., Lindgren J. & Alden M. (2002). Protection mechanism of Tween 80 during freeze-thawing of a model protein, LDH. *Int J Pharm*, 237, 57-69.
- Hirsch L.R., Stafford R.J., Bankson J.A., Sershen S.R., Rivera B., Price R.E., Hazle J.D., Halas N.J. & West J.L. (2003). Nanoshell-mediated near-infrared thermal therapy of tumors under magnetic resonance guidance. *Proceedings of the National Academy of Sciences*, 100, 13549-13554.
- Ito F. & Makino K. (2004). Preparation and properties of monodispersed rifampicin-loaded poly(lactide-co-glycolide) microspheres. *Colloid Surface B*, 39, 17-21.
- Jiang H.Y., Kelch S. & Lendlein A. (2006). Polymers move in response to light. *Adv Mater*, 18, 1471-1475.
- Jin C., Bai L., Wu H., Teng Z.H., Guo G.Z. & Chen J.Y. (2008). Cellular uptake and radiosensitization of SR-2508 loaded PLGA nanoparticles. *J Nanopart Res*, 10, 1045-1052.
- Johnson B.K. & Prud'homme R.K. (2003). Chemical processing and micromixing in confined impinging jets. *Aiche Journal*, 49, 2264-2282.
- Jones A.G. & Mullin J.W. (1974). Programmed cooling crystallization of potassium sulphate solutions. *Chem Eng Sci*, 29, 105-118.
- Jung J. & Perrut M. (2001). Particle design using supercritical fluids: Literature and patent survey. *J Supercrit Fluid*, 20, 179-219.
- Kaehler T. (1994). Nanotechnology - Basic Concepts and Definitions. *Clin Chem*, 40, 1797-1799.

References

- Kato M., Kodama D., Sato M. & Sugiyama K. (2006). Volumetric behavior and saturated pressure for carbon dioxide plus ethyl acetate at a temperature of 313.15 K. *J Chem Eng Data*, 51, 1031-1034.
- Kim S.S., Park M.S., Jeon O., Choi C.Y. & Kim B.S. (2006). Poly(lactide-co-glycolide)/hydroxyapatite composite scaffolds for bone tissue engineering. *Biomaterials*, 27, 1399-1409.
- Kind M. (2002). Colloidal aspects of precipitation processes. *Chem Eng Sci*, 57, 4287-4293.
- Klohs J., Wunder A. & Licha K. (2008). Near-infrared fluorescent probes for imaging vascular pathophysiology. *Basic Research in Cardiology*, 103, 144-151.
- Kluge J., Fusaro F., Casas N., Mazzotti M. & Muhrer G. (2009a). Production of PLGA micro- and nanocomposites by supercritical fluid extraction of emulsions: I. Encapsulation of lysozyme. *The Journal of Supercritical Fluids*, 50, 327-335.
- Kluge J., Fusaro F., Mazzotti M. & Muhrer G. (2009b). Production of PLGA micro- and nanocomposites by supercritical fluid extraction of emulsions: II. Encapsulation of Ketoprofen. *J Supercrit Fluid*, 50, 336-343.
- Kongsombut B., Tsutsumi A., Suankaew N. & Charinpanitkul T. (2009). Encapsulation of SiO₂ and TiO₂ Fine Powders with Poly(DL-lactico-glycolic acid) by Rapid Expansion of Supercritical CO₂ Incorporated with Ethanol Cosolvent. *Ind Eng Chem Res*, 48, 11230-11235.
- Krüber H., Teipel U. & Krause H. (2000). Manufacture of Submicron Particles via Expansion of Supercritical Fluids. *Chem Eng Technol*, 23, 763-765.
- Kulterer M.R., Reischl M., Reichel V.E., Hribernik S., Wu M., Kostler S., Kargl R. & Ribitsch V. (2011). Nanoprecipitation of cellulose acetate using solvent/nonsolvent mixtures as dispersive media. *Colloid Surface A*, 375, 23-29.
- Lee J., Lee S.J., Choi J.Y., Yoo J.Y. & Ahn C.H. (2005). Amphiphilic amino acid copolymers as stabilizers for the preparation of nanocrystal dispersion. *Eur J Pharm Sci*, 24, 441-449.
- Lee J.M., Kang S.J. & Park S.J. (2009). Synthesis of Polyacrylonitrile Based Nanoparticles via Aqueous Dispersion Polymerization. *Macromol Res*, 17, 817-820.
- Li M., Rouaud O. & Poncelet D. (2008). Microencapsulation by solvent evaporation: State of the art for process engineering approaches. *Int J Pharmaceut*, 363, 26-39.
- Li W.I., Anderson K.W. & Deluca P.P. (1995). Kinetic and thermodynamic modeling of the formation of polymeric microspheres using solvent extraction/evaporation method. *J Control Release*, 37, 187-198.

- Li X.-S., Wang J.-X., Shen Z.-G., Zhang P.-Y., Chen J.-F. & Yun J. (2007). Preparation of uniform prednisolone microcrystals by a controlled microprecipitation method. *Int J Pharmaceut*, 342, 26-32.
- Li Y.P., Pei Y.Y., Zhang X.Y., Gu Z.H., Zhou Z.H., Yuan W.F., Zhou J.J., Zhu J.H. & Gao X.J. (2001). PEGylated PLGA nanoparticles as protein carriers: synthesis, preparation and biodistribution in rats. *J Control Release*, 71, 203-211.
- Lince F., Marchisio D.L. & Barresi A.A. (2008). Strategies to control the particle size distribution of poly- ϵ -caprolactone nanoparticles for pharmaceutical applications. *Journal of Colloid and Interface Science*, 322, 505-515.
- Liu R. & Liu R. (2008). *Water-Insoluble Drug Formulation, Second Edition*, CRC PressINC.
- Liu Y., Kathan K., Saad W. & Prud'homme R.K. (2007). Ostwald ripening of beta-carotene nanoparticles. *Physical review letters*, 98, 036102.
- Luciani A., Coccoli V., Orsi S., Ambrosio L. & Netti P.A. (2008). PCL microspheres based functional scaffolds by bottom-up approach with predefined microstructural properties and release profiles. *Biomaterials*, 29, 4800-4807.
- Mahajan A.J. & Kirwan D.J. (1993). Rapid Precipitation of Biochemicals. *J Phys D Appl Phys*, 26, B176-B180.
- Mahshid S., Sasani Ghamsari M., Askari M., Afshar N. & Lahuti S. (2006). Synthesis of TiO₂ nanoparticles by hydrolysis and peptization of titanium isopropoxide solution. *Semiconductor Physics, Quantum Electronics & Optoelectronics*, 9, 65-68.
- Maity D. & Agrawal D.C. (2007). Synthesis of iron oxide nanoparticles under oxidizing environment and their stabilization in aqueous and non-aqueous media. *J Magn Magn Mater*, 308, 46-55.
- Martin A. & Weidner E. (2010). PGSS-drying: Mechanisms and modeling. *J Supercrit Fluid*, 55, 271-281.
- Matson D.W., Fulton J.L., Petersen R.C. & Smith R.D. (1987). Rapid Expansion of Supercritical Fluid Solutions - Solute Formation of Powders, Thin-Films, and Fibers. *Ind Eng Chem Res*, 26, 2298-2306.
- Matsumoto A., Kitazawa T., Murata J., Horikiri Y. & Yamahara H. (2008). A novel preparation method for PLGA microspheres using non-halogenated solvents. *J Control Release*, 129, 223-227.
- Matteucci M.E., Hotze M.A., Johnston K.P. & Williams R.O. (2006). Drug nanoparticles by antisolvent precipitation: Mixing energy versus surfactant stabilization. *Langmuir*, 22, 8951-8959.
- Mayo A.S., Ambati B.K. & Kompella U.B. (2010). Gene delivery nanoparticles fabricated by supercritical fluid extraction of emulsions. *Int J Pharm*, 387, 278-85.

References

- Mayrhofer B. & Nyvlt J. (1988). Programmed Cooling of Batch Crystallizers. *Chem Eng Process*, 24, 217-220.
- Mccoy C.P., Rooney C., Edwards C.R., Jones D.S. & Gorman S.P. (2007). Light-triggered molecule-scale drug dosing devices. *J Am Chem Soc*, 129, 9572-+.
- Meng F.T., Ma G.H., Liu Y.D., Qiu W. & Su Z.G. (2004). Microencapsulation of bovine hemoglobin with high bio-activity and high entrapment efficiency using a W/O/W double emulsion technique. *Colloids and Surfaces B: Biointerfaces*, 33, 177-183.
- Merisko-Liversidge E.M. & Liversidge G.G. (2008). Drug Nanoparticles: Formulating Poorly Water-Soluble Compounds. *Toxicol Pathol*, 36, 43-48.
- Mestiri M., Puisieux F. & Benoit J.P. (1993). Preparation and characterization of cisplatin-loaded polymethyl methacrylate microspheres. *Int J Pharmaceut*, 89, 229-234.
- Mikos A.G., Bao Y., Cima L.G., Ingber D.E., Vacanti J.P. & Langer R. (1993). Preparation of poly(glycolic acid) bonded fiber structures for cell attachment and transplantation. *Journal of Biomedical Materials Research*, 27, 183-189.
- Mishima K. (2008). Biodegradable particle formation for drug and gene delivery using supercritical fluid and dense gas. *Adv Drug Deliver Rev*, 60, 411-432.
- Mishima K., Matsuyama K., Tanabe D., Yamauchi S., Young T.J. & Johnston K.P. (2000). Microencapsulation of proteins by rapid expansion of supercritical solution with a nonsolvent. *AIChE Journal*, 46, 857-865.
- Mora-Huertas C.E., Fessi H. & Elaissari A. (2010). Polymer-based nanocapsules for drug delivery. *Int J Pharmaceut*, 385, 113-142.
- Murakami H., Kobayashi M., Takeuchi H. & Kawashima Y. (1999). Preparation of poly(dl-lactide-co-glycolide) nanoparticles by modified spontaneous emulsification solvent diffusion method. *Int J Pharmaceut*, 187, 143-152.
- Murphy W.L., Peters M.C., Kohn D.H. & Mooney D.J. (2000). Sustained release of vascular endothelial growth factor from mineralized poly(lactide-co-glycolide) scaffolds for tissue engineering. *Biomaterials*, 21, 2521-2527.
- Nair L.S. & Laurencin C.T. (2006). Polymers as biomaterials for tissue engineering and controlled drug delivery. *Adv Biochem Eng Biot*, 102, 47-90.
- Nakashima T., Shimizu M. & Kukizaki M. (2000). Particle control of emulsion by membrane emulsification and its applications. *Adv Drug Deliver Rev*, 45, 47-56.
- Napper D.H. (1983). *Polymeric stabilization of colloidal dispersions*, Academic Press.

- O'hagan D.T., Jeffery H. & Davis S.S. (1994). The preparation and characterization of poly(lactide-co-glycolide) microparticles: III. Microparticle/polymer degradation rates and the in vitro release of a model protein. *Int J Pharmaceut*, 103, 37-45.
- O'donnell P.B. & McGinity J.W. (1997). Preparation of microspheres by the solvent evaporation technique. *Adv Drug Deliver Rev*, 28, 25-42.
- Pamula E., Dobrzynski P., Bero M. & Paluszkiwicz (2005). Hydrolytic degradation of porous scaffolds for tissue engineering from terpolymer of L-lactide, ϵ -caprolactone and glycolide. *Journal of molecular structure* 744-47, 557-562
- Park H., Temenoff J.S., Holland T.A., Tabata Y. & Mikos A.G. (2005). Delivery of TGF-beta1 and chondrocytes via injectable, biodegradable hydrogels for cartilage tissue engineering applications. *Biomaterials*, 26, 7095-103.
- Park H., Yang J., Seo S., Kim K., Suh J., Kim D., Haam S. & Yoo K.H. (2008). Multifunctional nanoparticles for photothermally controlled drug delivery and magnetic resonance imaging enhancement. *Small*, 4, 192-196.
- Park J.H., Lee M.A., Park B.J. & Choi H.J. (2007). Preparation and electrophoretic response of poly(methyl methacrylate-co-methacrylic acid) coated TiO₂ nanoparticles for electronic paper application. *Curr Appl Phys*, 7, 349-351.
- Pathak P., Meziani M.J., Desai T. & Sun Y.P. (2004). Nanosizing drug particles in supercritical fluid processing. *J Am Chem Soc*, 126, 10842-10843.
- Peltonen L., Koistinen P., Karjalainen M., Häkkinen A. & Hirvonen J. (2002). The effect of cosolvents on the formulation of nanoparticles from low-molecular-weight poly(l)lactide. *AAPS PharmSciTech*, 3, 52-58.
- Pemsel M., Schwab S., Scheurer A., Freitag D., Schatz R. & Schlucker E. (2010). Advanced PGSS process for the encapsulation of the biopesticide *Cydia pomonella* granulovirus. *J Supercrit Fluid*, 53, 174-178.
- Petersen R.C., Matson D.W. & Smith R.D. (1986). Rapid Precipitation of Low Vapor-Pressure Solids from Supercritical Fluid Solutions - the Formation of Thin-Films and Powders. *J Am Chem Soc*, 108, 2100-2102.
- Preciado-Flores S., Wang D., Wheeler D.A., Newhouse R., Hensel J.K., Schwartzberg A., Wang L., Zhu J., Barboza-Flores M. & Zhang J.Z. (2011). Highly reproducible synthesis of hollow gold nanospheres with near infrared surface plasmon absorption using PVP as stabilizing agent. *J Mater Chem*, 21, 2344-2350.
- Quintanar-Guerrero D., Allémann E., Doelker E. & Fessi H. (1997). A mechanistic study of the formation of polymer nanoparticles by the

References

- emulsification-diffusion technique. *Colloid & Polymer Science*, 275, 640-647.
- Quintanar-Guerrero D., Allemann E., Fessi H. & Doelker E. (1998). Preparation techniques and mechanisms of formation of biodegradable nanoparticles from preformed polymers. *Drug Dev Ind Pharm*, 24, 1113-1128.
- Quintanar-Guerrero D., Fessi H., Allémann E. & Doelker E. (1996). Influence of stabilizing agents and preparative variables on the formation of poly(d,l-lactic acid) nanoparticles by an emulsification-diffusion technique. *Int J Pharmaceut*, 143, 133-141.
- Rao B.C.N.R., Govindaraj A. & Vivekchand S.R.C. (2006). Inorganic nanomaterials: current status and future prospects. *Annual Reports Section "A" (Inorganic Chemistry)*, 102, 20-45.
- Rasenack N. & Muller B.W. (2002). Dissolution rate enhancement by in situ micronization of poorly water-soluble drugs. *Pharmaceutical Research*, 19, 1894-1900.
- Reithmeier H., Herrmann J. & Gopferich A. (2001). Lipid microparticles as a parenteral controlled release device for peptides. *J Control Release*, 73, 339-350.
- Reverchon E. (1999). Supercritical antisolvent precipitation of micro- and nano-particles. *J Supercrit Fluid*, 15, 1-21.
- Reverchon E. (2002). Supercritical-Assisted Atomization To Produce Micro-and/or Nanoparticles of Controlled Size and Distribution. *Ind Eng Chem Res*, 41, 2405-2411.
- Reverchon E. & Adami R. (2006). Nanomaterials and supercritical fluids. *J Supercrit Fluid*, 37, 1-22.
- Reverchon E., Adami R. & Caputo G. (2006). Supercritical assisted atomization: Performance comparison between laboratory and pilot scale. *J Supercrit Fluid*, 37, 298-306.
- Reverchon E., Adami R., Cardea S. & Della Porta G. (2009). Supercritical fluids processing of polymers for pharmaceutical and medical applications. *J Supercrit Fluid*, 47, 484-492.
- Reverchon E., Celano C., Della Porta G., Di Trollo A. & Pace S. (1998). Supercritical antisolvent precipitation: A new technique for preparing submicronic yttrium powders to improve YBCO superconductors. *J Mater Res*, 13, 284-289.
- Reverchon E. & De Marco I. (2011). Mechanisms controlling supercritical antisolvent precipitate morphology. *Chemical Engineering Journal*, 169, 358-370.
- Reverchon E., De Marco I. & Della Porta G. (2002). Tailoring of nano- and micro-particles of some superconductor precursors by supercritical antisolvent precipitation. *The Journal of Supercritical Fluids*, 23, 81-87.

- Reverchon E., De Marco I. & Torino E. (2007). Nanoparticles production by supercritical antisolvent precipitation: A general interpretation. *J Supercrit Fluid*, 43, 126-138.
- Reverchon E., Della Porta G. & Torino E. (2010). Production of metal oxide nanoparticles by supercritical emulsion reaction. *The Journal of Supercritical Fluids*, 53, 95-101.
- Reverchon E., Dellaporta G., Taddeo R., Pallado P. & Stassi A. (1995). Solubility and Micronization of Griseofulvin in Supercritical Chf₃. *Ind Eng Chem Res*, 34, 4087-4091.
- Reverchon E. & Spada A. (2004). Crystalline Microparticles of Controlled Size Produced by Supercritical-Assisted Atomization. *Ind Eng Chem Res*, 43, 1460-1465.
- Rong Y., Chen H.-Z., Li H.-Y. & Wang M. (2005a). Encapsulation of titanium dioxide particles by polystyrene via radical polymerization. *Colloids and Surfaces A: Physicochemical and Engineering Aspects*, 253, 193-197.
- Rong Y., Chen H.-Z., Wu G. & Wang M. (2005b). Preparation and characterization of titanium dioxide nanoparticle/polystyrene composites via radical polymerization. *Materials Chemistry and Physics*, 91, 370-374.
- Ross S. & Morrison I.D. (1988). *Colloidal systems and interfaces*, Wiley.
- Rozenberg B.A. & Tenne R. (2008). Polymer-assisted fabrication of nanoparticles and nanocomposites. *Prog Polym Sci*, 33, 40-112.
- Sabirzyanov A.N., Il'in A.P., Akhunov A.R. & Gumerov F.M. (2002). Solubility of Water in Supercritical Carbon Dioxide. *High Temperature*, 40, 203-206.
- Sah H. (2000). Ethyl formate - alternative dispersed solvent useful in preparing PLGA microspheres. *Int J Pharmaceut*, 195, 103-113.
- Salata O. (2004). Applications of nanoparticles in biology and medicine *Journal of Nanobiotechnology*, 3.
- Sane A., Taylor S., Sun Y.P. & Thies M.C. (2003). RESS for the preparation of fluorinated porphyrin nanoparticles. *Chem Commun*, 2720-2721.
- Sato Y., Hosaka N., Yamamoto K. & Inomata H. (2010). Compact apparatus for rapid measurement of high-pressure phase equilibria of carbon dioxide expanded liquids. *Fluid Phase Equilib*, 296, 25-29.
- Scheutjens J.M.H.M. & Fleer G.J. (1980). Statistical theory of the adsorption of interacting chain molecules. 2. Train, loop, and tail size distribution. *The Journal of Physical Chemistry*, 84, 178-190.
- Schultz S., Wagner G. & Ulrich J. (2002). High-pressure homogenization for emulsion formation. *Chem-Ing-Tech*, 74, 901-909.
- Schultz S., Wagner G., Urban K. & Ulrich J. (2004). High-pressure homogenization as a process for emulsion formation. *Chem Eng Technol*, 27, 361-368.

References

- Schwartzberg A.M., Olson T.Y., Talley C.E. & Zhang J.Z. (2006). Synthesis, characterization, and tunable optical properties of hollow gold nanospheres. *The journal of physical chemistry. B*, 110, 19935-44.
- Sershen S.R., Westcott S.L., Halas N.J. & West J.L. (2000). Temperature-sensitive polymer-nanoshell composites for photothermally modulated drug delivery. *Journal of Biomedical Materials Research*, 51, 293-298.
- Shekunov B., Chattopadhyay P., Seitzinger J. & Huff R. (2006). Nanoparticles of Poorly Water-Soluble Drugs Prepared by Supercritical Fluid Extraction of Emulsions. *Pharmaceutical Research*, 23, 196-204.
- Shekunov B.Y., Baldyga J. & York P. (2001). Particle formation by mixing with supercritical antisolvent at high Reynolds numbers. *Chem Eng Sci*, 56, 2421-2433.
- Singh M., Sandhu B., Scurto A., Berkland C. & Detamore M.S. (2010). Microsphere-based scaffolds for cartilage tissue engineering: Using subcritical CO₂ as a sintering agent. *Acta Biomater*, 6, 137-143.
- Sinha V.R. & Trehan A. (2003). Biodegradable microspheres for protein delivery. *J Control Release*, 90, 261-280.
- Slager J. & Domb A.J. (2002). Stereocomplexes based on poly(lactic acid) and insulin: formulation and release studies. *Biomaterials*, 23, 4389-4396.
- Song M., Zhang R.Y., Dai Y.Y., Gao F., Chi H.M., Lv G., Chen B.A. & Wang X.M. (2006). The in vitro inhibition of multidrug resistance by combined nanoparticulate titanium dioxide and UV irradiation. *Biomaterials*, 27, 4230-4238.
- Sosnik A., Carcaboso A.M. & Chiappetta D.A. (2008). Polymeric Nanocarriers: New Endeavors for the Optimization of the Technological Aspects of Drugs. *Recent Patents on Biomedical Engineering*, 1, 43-59.
- Sovova H., Jez J. & Khachatryan M. (1997). Solubility of squalane, dinonyl phthalate and glycerol in supercritical CO₂. *Fluid Phase Equilib*, 137, 185-191.
- Spenlehauer G., Vert M., Benoît J.P., Chabot F. & Veillard M. (1988). Biodegradable cisplatin microspheres prepared by the solvent evaporation method: Morphology and release characteristics. *J Control Release*, 7, 217-229.
- Staff S. & Sun Y.P. (2002). *Supercritical Fluid Technology in Materials Science and Engineering: Synthesis, Properties and Applications*, Marcel Dekker.
- Stallmann H.P., Faber C., Bronckers A.L., Nieuw Amerongen A.V. & Wuisman P.I. (2006). In vitro gentamicin release from commercially available calcium-phosphate bone substitutes influence of carrier

- type on duration of the release profile. *BMC Musculoskelet Disord*, 7, 18-18.
- Sun Y.-P., Atorngitjawat P. & Meziani M.J. (2001). Preparation of Silver Nanoparticles via Rapid Expansion of Water in Carbon Dioxide Microemulsion into Reductant Solution. *Langmuir*, 17, 5707-5710.
- Sun Y.-P. & Rollins H.W. (1998). Preparation of polymer-protected semiconductor nanoparticles through the rapid expansion of supercritical fluid solution. *Chemical Physics Letters*, 288, 585-588.
- Sun Y.P., Guduru R., Lin F. & Whiteside T. (2000). Preparation of nanoscale semiconductors through the rapid expansion of supercritical solution (RESS) into liquid solution. *Ind Eng Chem Res*, 39, 4663-4669.
- Szacilowski K., Macyk W., Drzewiecka-Matuszek A., Brindell M. & Stochel G. (2005). Bioinorganic photochemistry: Frontiers and mechanisms. *Chem Rev*, 105, 2647-2694.
- Takishima J., Onishi H. & Machida Y. (2002). Prolonged Intestinal Absorption of Cephadrine with Chitosan-Coated Ethylcellulose Microparticles in Rats. *Biological and Pharmaceutical Bulletin*, 25, 1498-1502.
- Thorat A.A. & Dalvi S.V. (2012). Liquid antisolvent precipitation and stabilization of nanoparticles of poorly water soluble drugs in aqueous suspensions: Recent developments and future perspective. *Chemical Engineering Journal*, 181, 1-34.
- Thybo P., Hovgaard L., Lindelov J.S., Brask A. & Andersen S.K. (2008). Scaling up the spray drying process from pilot to production scale using an atomized droplet size criterion. *Pharmaceutical Research*, 25, 1610-1620.
- Tomasko D.L., Han X.M., Liu D.H. & Gao W.H. (2003). Supercritical fluid applications in polymer nanocomposites. *Curr Opin Solid St M*, 7, 407-412.
- Torchilin V.P. (2006). Multifunctional nanocarriers. *Adv Drug Deliver Rev*, 58, 1532-1555.
- Tsuang Y.H., Sun J.S., Huang Y.C., Lu C.H., Chang W.H.S. & Wang C.C. (2008). Studies of photokilling of bacteria using titanium dioxide nanoparticles. *Artif Organs*, 32, 167-174.
- Tsukada Y., Hara K., Bando Y., Huang C.C., Kousaka Y., Kawashima Y., Morishita R. & Tsujimoto H. (2009). Particle size control of poly(DL-lactide-co-glycolide) nanospheres for sterile applications. *Int J Pharmaceut*, 370, 196-201.
- Turk M., Hils P., Helfgen B., Schaber K., Martin H.J. & Wahl M.A. (2002). Micronization of pharmaceutical substances by the Rapid Expansion of Supercritical Solutions (RESS): a promising method to improve bioavailability of poorly soluble pharmaceutical agents. *J Supercrit Fluid*, 22, 75-84.

References

- Turk M. & Lietzow R. (2004). Stabilized nanoparticles of phytosterol by rapid expansion from supercritical solution into aqueous solution. *AAPS PharmSciTech*, 5, e56.
- Umemura A. & Wakashima Y. (Year) Published. Atomization regimes of a round liquid jet with near-critical mixing surface at high pressure. *Proceedings of the combustion institute*, 2002. 633-640.
- Van Vlerken L.E. & Amiji M.M. (2006). Multi-functional polymeric nanoparticles for tumour-targeted drug delivery. *Expert Opinion on Drug Delivery*, 3, 205-216.
- Vehring R. (2008). Pharmaceutical particle engineering via spray drying. *Pharmaceutical Research*, 25, 999-1022.
- Vemavarapu C., Mollan M.J., Lodaya M. & Needham T.E. (2005). Design and process aspects of laboratory scale SCF particle formation systems. *Int J Pharmaceut*, 292, 1-16.
- Ventosa N., Sala S., Veciana J., Torres J. & Llibre J. (2001). Depressurization of an expanded liquid organic solution (DELOS): A new procedure for obtaining submicron- or micron-sized crystalline particles. *Cryst Growth Des*, 1, 299-303.
- Verma S., Kumar S., Gokhale R. & Burgess D.J. (2011). Physical stability of nanosuspensions: investigation of the role of stabilizers on Ostwald ripening. *Int J Pharm*, 406, 145-52.
- Vila A., Sanchez A., Tobio M., Calvo P. & Alonso M.J. (2002). Design of biodegradable particles for protein delivery. *J Control Release*, 78, 15-24.
- Vladisavljevic G.T. & Williams R.A. (2005). Recent developments in manufacturing emulsions and particulate products using membranes. *Adv Colloid Interfac*, 113, 1-20.
- Wang Q., Guan Y.-X., Yao S.-J. & Zhu Z.-Q. (2010). Microparticle formation of sodium cellulose sulfate using supercritical fluid assisted atomization introduced by hydrodynamic cavitation mixer. *Chemical Engineering Journal*, 159, 220-229.
- Won D.H., Kim M.S., Lee S., Park J.S. & Hwang S.J. (2005). Improved physicochemical characteristics of felodipine solid dispersion particles by supercritical anti-solvent precipitation process. *Int J Pharmaceut*, 301, 199-208.
- Wu G.H., Milkhaïlovsky A., Khant H.A., Fu C., Chiu W. & Zasadzinski J.A. (2008). Remotely triggered liposome release by near-infrared light absorption via hollow gold nanoshells. *J Am Chem Soc*, 130, 8175-+.
- Wu L.B., Zhang J. & Watanabe W. (2011). Physical and chemical stability of drug nanoparticles. *Adv Drug Deliver Rev*, 63, 456-469.
- Xia Y., Gates B., Yin Y. & Lu Y. (2000). Monodispersed Colloidal Spheres: Old Materials with New Applications. *Adv Mater*, 12, 693-713.

- Yang Y.Y., Chia H.H. & Chung T.S. (2000). Effect of preparation temperature on the characteristics and release profiles of PLGA microspheres containing protein fabricated by double-emulsion solvent extraction/evaporation method. *J Control Release*, 69, 81-96.
- Yang Y.Y., Chung T.S. & Ng N.P. (2001). Morphology, drug distribution, and in vitro release profiles of biodegradable polymeric microspheres containing protein fabricated by double-emulsion solvent extraction/evaporation method. *Biomaterials*, 22, 231-241.
- York P. (1999). Strategies for particle design using supercritical fluid technologies. *Pharmaceutical Science & Technology Today*, 2, 430-440.
- Zhang J. & Noguez C. (2008). Plasmonic Optical Properties and Applications of Metal Nanostructures. *Plasmonics*, 3, 127-150.
- Zhang X., Shen S.H. & Fan L.Y. (2008). Uniform polystyrene particles by dispersion polymerization in different dispersion medium. *Polym Bull*, 61, 19-26.
- Zheng C.-H., Gao J.-Q., Zhang Y.-P. & Liang W.-Q. (2004). A protein delivery system: biodegradable alginate–chitosan–poly(lactic-co-glycolic acid) composite microspheres. *Biochem Bioph Res Co*, 323, 1321-1327.
- Zhu Z.X., Margulis-Goshen K., Magdassi S., Talmon Y. & Macosko C.W. (2010). Polyelectrolyte Stabilized Drug Nanoparticles via Flash Nanoprecipitation: A Model Study With beta-Carotene. *J Pharm Sci-U.S.*, 99, 4295-4306.
- Zili Z., Sfar S. & Fessi H. (2005). Preparation and characterization of poly- ϵ -caprolactone nanoparticles containing griseofulvin. *Int J Pharmaceut*, 294, 261-267.